DISSERTATION

MYCOBACTERIAL ARABINAN BIOSYNTHESIS: CHARACTERIZATION OF AftB AND AftC ARABINOSYLTRANSFERASE ACTIVITY USING SYNTHETIC SUBSTRATES

Submitted by

Shiva kumar Angala

Department of Microbiology, Immunology and Pathology

In partial fulfillment of the requirements

For the Degree of Doctor of Philosophy

Colorado State University

Fort Collins, Colorado

Fall 2011

Doctoral Committee:

Advisor: Delphi Chatterjee
Co-Advisor: Dean C. Crick

Herbert P. Schweizer
Norman P. Curthoys

ABSTRACT

MYCOBACTERIAL ARABINAN BIOSYNTHESIS: CHARACTERIZATION OF AftB AND AftC ARABINOSYLTRANSFERASE ACTIVITY USING SYNTHETIC SUBSTRATES

Tuberculosis (TB) is a chronic infectious disease caused by *M. tuberculosis* (Mtb). Treatment of TB is prolonged, and multidrug resistant (MDR-TB) and extensively drug resistant TB (XDR-TB) cases are ever increasing. Efforts to discover and develop new drugs have increased in recent years so improvement of the existing therapies is urgently needed. The cell wall of Mtb with its unique physiological properties has historically been an important and valid drug target. Mycobacterial arabinosyltransferases are membrane bound glycosyltransferases involved in the biosynthesis of the arabinan portion of two major polysaccharides, arabinogalactan (AG) and lipoarabinomannan (LAM), associated with the cell wall. In this work, *M. smegmatis* was used as a model organism to study arabinosyltransferases and the biosynthesis of cell wall arabinofuran—the main constituent of AG and LAM.

This dissertation addresses the development of a cell free arabinosyltransferase assay for AftB and AftC glycosyltransferases. Since it was not possible to express AftB transmembrane protein, we probed AftB transferase activity from the crude membranes using a synthetic arabinose disaccharide acceptor. In this study, a robust cell free

radioactive arabinosyltransferase assay was developed using a linkage specific synthetic disaccharide acceptor. Relative mobility of the enzymatic product on a thin layer chromatogram and autoradiography clearly demonstrated the enzymatic conversion of the disaccharide acceptor to a trisaccharide. The trisaccharide product was further confirmed by matrix assisted laser desorption ionization- time of flight (MALDI-TOF) or high pH anion exchange chromatography (HPAEC) analysis. GC-MS analysis showed that the additional arabinose added to the enzymatic product was (1→2) linked. This assay is dependent on time and enzyme concentration and the product formation is not sensitive to the action of ethambutol or the absence of the putative arabinosyltransferases encoded by *embA*, *embB* or *embC*. Additionally, further optimal conditions were determined including buffers, pH, divalent cations, detergents, and the effect of alkylating and reducing agents.

In a contiguous study, we wanted to convert this assay into a non-radioactive assay for the screening of compounds. We successfully developed an ELISA based non-radiolabeled arabinosyltransferase assay using CS35-mAb that recognized (1→2) linked enzymatic product. As this method involves several washing steps and time consuming processes, we further modified the substrate with fluorescent labeling, however, we failed to establish a fluorescence based arabinosyltransferase assay.

Unlike AftB, in a parallel study we were successful in expressing, solubilizing and purifying Mtb AftC. We developed an *in vitro* transferase assay using purified recombinant AftC and demonstrated that AftC retains transferase activity only when reconstituted into proteoliposomes. Additionally, we were successful in synthesizing alternate arabinose donors *Z*-nerylphosphoryl D-arabinose (*Z*-NPA), *Z,Z*-

farnesylphosphoryl D-arabinose (*Z*-FPA), *E*,*E*-farnesylphosphoryl D-arabinose (*E*-FPA), and *Z*,*Z*,*Z*,*Z*,*E*,*E*-heptaprenylphosphoryl D-arabinose (*Z*-HPA). Among these lipid donors, Z-FPA demonstrated better solubility in the assay buffer compared to the native donor decaprenyphophoryl D-arabinose (DPA).

This dissertation describes screening of drug candidate compounds using a microtiter plate based whole cell Alamar Blue assay. We have successfully screened nearly three thousand compounds for Mtb growth inhibition.

ACKNOWLEDGEMENTS

I am heartily thankful to my academic mentor, Professor Dr. Delphi Chatterjee, for the opportunity to work under her guidance and her support that she has given during my graduate career. I am also thankful to my all committee members – Drs. Dean Crick, Herbert Schweizer and Norman Curthoys who always gave me intellectual input over the years.

It is my pleasure to thank all my lab members- Anita Amin, Jian Zhang, Shi libin, Wenli Zhang, Somashekar, Kayla, Elyse, Laura, Pradeep, and past work studies for their support and Sakamuri Ramamurthy for his helpful discussions during the course of my graduate studies. I would like to specially thank Anita Amin who has given me the love of a sister. I would like to thank Peter H. Seeberger, Jian Zhang and Li Kai for their help in providing synthetic acceptors for all my studies.

I am very much thankful to MRL and all members of Brennan, Crick, Spencer, Jackson and McNeil labs and BSL-III facility (Jerry Tews and Tom Knee).

Finally, this thesis would not have been possible without the funding from NIH-NIAID AI-37139 and CSU departmental bridge fund.

DEDICATION

I dedicate this dissertation

to almighty for opening my eyes to the world

And to my family, especially…

to my parents Late Mr. Angala Raj Gopal and Mrs. Angala Pushpavathi, for instilling the importance of hard work and higher education;

to my in-laws Late Mr. Somani Venkataiah and Mrs. Somani Vijaya laxmi, for their warm blessings;

to my Grandma Late. Purnima Chatterjee and my Graduate co-ordinator Late Mrs. Marcia Boggs for their encouragement and warm regards;

to my brothers Deva Kumar, Uday Kumar, Praveen Kumar for their encouragement and support;

to my beloved wife Bhanu for her patience and understanding;

Finally, this thesis is dedicated to all those who believe in the richness of learning.

Shiva Kumar Angala.

TABLE OF CONTENTS

LIST OF FIGURES AND TABLES

LIST OF ABBREVIATIONS

Ac	acylated
AftA	arabinosyltransferase A
AftB	arabinosyltransferase B
AftC	arabinosyltransferase C
AftD	arabinosyltransferase D
AG	arabinogalactan
Ara*f*	D-arabinofuranose
AraLAM	uncapped lipoarabinomannam
BCG	bacillus Calmette-Guerin
CF	cord factor
CR	complement receptor
DAG	diacylglycerol
DAP	diaminopimelic acid
DC-SIGN	dendritic cell-specific intracellular grabbing non-integrin
DOTS	directly observed therapy shortcourse
DPA	decaprenyl-monophosphoryl-D-arabinose (C_{50}-p-Ara*f*)
E-FPA	*E*,*E*-farnesylphosphoryl D-arabinose
ELISA	enzyme-linked immunosorbent assay
EMB	ethambutol
f	furanose
Gal*f*	D-galactofuranose

GC	gas chromatography
GC-MS	gas chromatography-mass spectrometry
Glc*N*Ac	*N*-acetyl-glucosamine (2-acetamido-2-deoxy-α-D-glucopyranose)
GT	glycosyltransferase
HPAEC	high pH anion exchange chromatography
INH	isoniazid
LAM	lipoarabinomannan
LM	lipomannan
mAGP	mycolyl-arabinogalactan-peptidoglycan
MALDI-TOF	matrix assisted laser desorption ionization-time of flight
Man*p*	D-mannopyranose
ManLAM	mannose-capped lipoarabinomannan
MDR-TB	multi-drug resistant tuberculosis
MDT	multidrug therapy
MS	mass spectrometry
Mtb	*Mycobacterium tuberculosis*
Mur*N*Ac	*N*-acetylmuramic acid
p	pyranose
PI	phosphatidyl-*myo*-inositol
PIG	phosphatidylinositol glycan
PILAM	phosphatidyl-*myo*-inositol capped lipoarabinomannan
PIM	phosphatidyl-*myo*-inositol mannoside
PG	peptidoglycan
Pol-P	polyprenyl phosphate
pRpp	phospho-ribosyl-pyrophosphate
Rha	rhamnose
RIF	rifampin (rifampicin)

SP-A	human surfactant protein A
TB	tuberculosis
TLC	thin layer chromatography
TNF-α	tumor necrosis factor-α
WHO	world health organization
XRD-TB	extensively drug resistant tuberculosis
Z-FPA	*Z,Z*-farnesylphosphoryl D-arabinose
Z-HPA	*Z,Z,Z,Z,E,E*-heptaprenylphosphoryl D-arabinose
Z-NPA	*Z*-nerylphosphoryl D-arabinose

LIST OF PUBLICATIONS

Publications associated with this dissertation

Zhang, J., **S.K. Angala**, P.K. Pramanik, K. Li, D.C. Crick, A. Liav, A. Jozwiak, E. Swiezewska, M. Jackson, and D. Chatterjee. 2011. Reconstitution of Functional Mycobacterial Arabinosyltransferase AftC Proteoliposome and Assessment of Decaprenylphosphorylarabinose Analogues as Arabinofuranosyl Donors. *ACS chem. biol*. 6:819-828.

Anita G., **S.K. Angala,** D. Chatterjee and D.C. Crick. 2009. Rapid screening of inhibitors of M. tuberculosis growth using tetrazolium salts. *Methods Mol Biol,* 2009. 465: p. 187-201.

Dhiman, R.K., S. Mahapatra, R.A. Slayden, M.E. Boyne, A. Lenaerts, J.C. Hinshaw, **S.K. Angala,** D. Chatterjee, K. Biswas, and P. Narayanasamy, D.C. Crick. 2009. Menaquinone synthesis is critical for maintaining mycobacterial viability during exponential growth and recovery from non replicating persistence. *Mol. Microbiol.* 72:85-97.

Liav, A., **S.K. Angala,** P.J. Brennan, and M. Jackson. 2008. N-D-aldopentofuranosyl-N'-[p-(isoamyloxy)phenyl]-thiourea derivatives: potential anti-TB therapeutic agents. *Bioorg. Med. Chem. Lett.* 18:2649-2651.

CHAPTER 1

LITERATURE REVIEW OF TUBERCULOSIS

1.1 Introduction

Tuberculosis (TB) is an ancient disease present in the human population and it is hypothesized that the genus mycobacterium originated 150 million years ago (Hayman, 1984). This disease is known by several names, Potts disease in Peruvian mummies (Salo et al., 1994), phthisis (consumption) in Greece, white plague (Zumla, 2011), Miliary TB (Kathuria and Ramesh, 2010), Tuberculosis luposa (Lupus vulgaris) (Farina et al., 1995) and Koch's disease (Koch, 1882).

TB is a chronic infectious disease caused by *Mycobacterium tuberculosis* (Mtb). TB is a disease of poverty, killing one-third of the world's population. Every day nearly 4700 people die from the disease and that accounts for approximately 1.7 million deaths in 2009. A major concern with rising TB is HIV co-infection. According to the World Health Organization (WHO) annual report of 2010, (www.who.int/tb) there were an estimated 9.4 million new TB cases including 1.1 million HIV-positive patients (WHO, 2010). Increase in the incidences of new TB cases is seen mostly within developing countries of Russia, Africa, Asia, and Latin America (Figure 1.1).

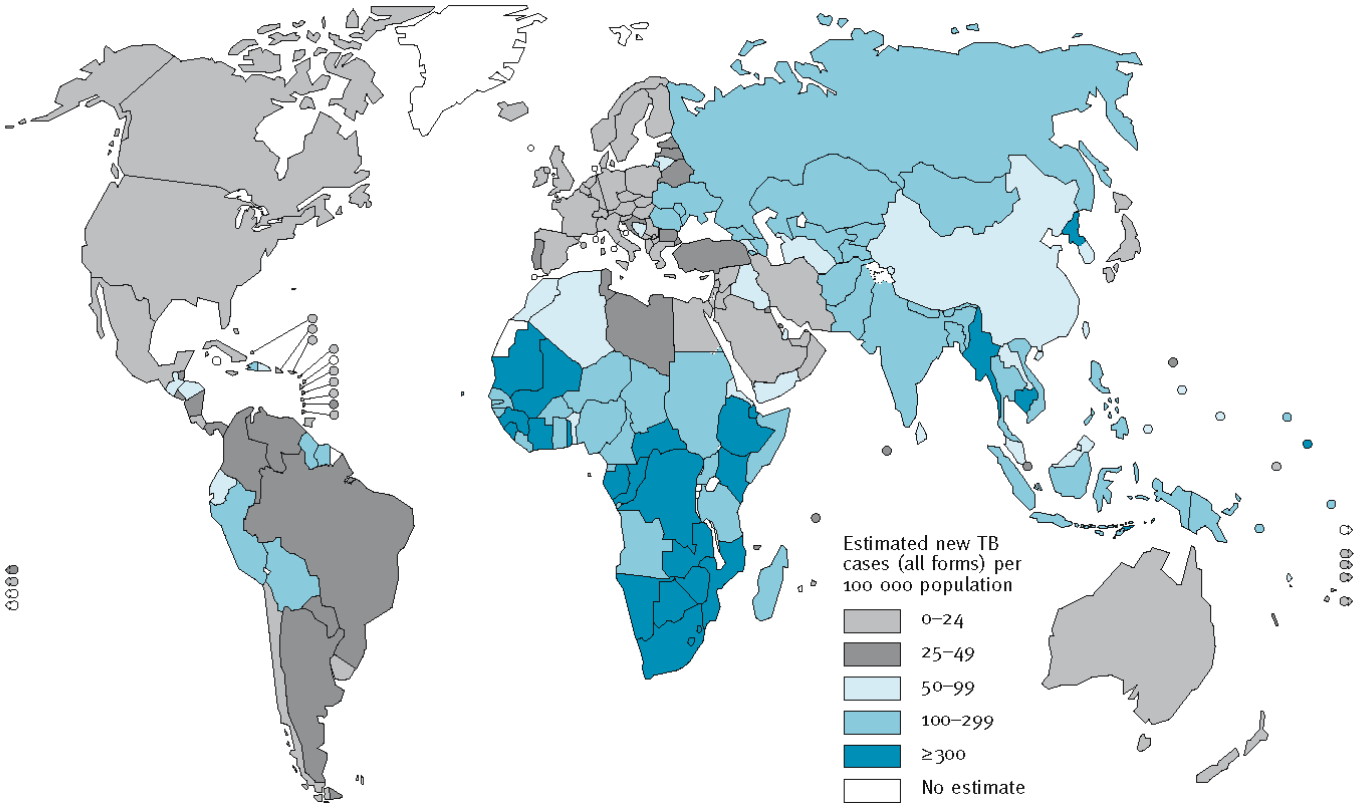

Figure 1.1 Total number of estimated TB rates by country. (WHO annual report- 2010)

The emergence of MDR-TB (multidrug-resistant TB) and XDR-TB (extensive drug resistant TB) are worrisome and are virtually untreatable with existing anti-TB drugs. It has been estimated that 3.3% of all new TB cases are MDR-TB and XDR-TB positive cases as seen in 58 countries (WHO, 2010).

1.2 Pathogenesis of tuberculosis

According to the Linnaeus system of classification, mycobacteria belong to the phylum actinobacteria, order actinomycetales, sub order corynebacterineae, family-mycobacteriaceae, and genus *mycobacterium.*

Mtb is an aerobic, intracellular pathogen transmitted from patients with active disease via respiratory route (Bates, 1980). A thorough understanding of Mtb pathogenesis in humans is still not clear. It is estimated that mean concentration of viable TB bacilli in sputum samples of pulmonary TB patients range from 6.6×10^4 to 3.4×10^7 mL^{-1} (Yeager et al., 1967). Following inhalation of droplets loaded with Mtb, bacilli enter the lung tissue and are phagocytosed by alveolar macrophages. The mechanism of how Mtb crosses walls of alveolar macrophages and gains access to lymphatic and circulatory systems is still not clear. However, complement receptors (CR1, CR2, CR3, CR4) and mannose receptors play an important role in binding of Mtb to macrophages or monocytes (Schlesinger, 1996). Mtb interacts with alveolar macrophages during which mannose-capped lipoarabinomannan (ManLAM) (Maeda et al., 2003; Schlesinger, 1996; Schlesinger et al., 1994) and other unknown factors mediate the interaction in the absence

of opsonins. Phagocytosis of Mtb by human macrophages is enhanced by a pulmonary surfactant protein A (SP-A) (Gaynor et al., 1995).

The presence of a dense cell wall in Mtb provides resistance against microbicidal action of alveolar macrophages. Mtb escapes degradation by intralysosomal acidic hydrolysis by preventing phagolysosomal fusion inside macrophages (Hart et al., 1972).

It is reported that derivatives of multiacylated trehalose 2-sulphate of mycobacteria aids in preventing phagolysosomal fusion (Goren et al., 1976a; Goren et al., 1976b). Later, Mtb interferes with intracellular trafficking which results into immature phagosomal compartment where it replicates during early stages of infection (Stewart et al., 2003). Intracellular Mtb present in the macrophages has the ability to evade many anti-mycobacterial functions mediated by cytokines such as generation of reactive oxygen intermediates (ROI) and reactive nitrogen intermediates (RNI) (Walker and Lowrie, 1981).

Mtb inhibits production of prostaglandin E_2, thereby, inhibiting apoptosis and promotes necrosis of macrophages (Divangahi et al., 2010). Mtb contained in apoptopic vesicles from infected macrophages are taken up by dendritic cells (DCs) which finally stimulates $CD4^+$ and $CD8^+$ T-lymphocytes by major histocompatibility complex (MHC) class I & II respectively.

There are two pathways proposed for antigen presentation. First, direct loading of Mtb secreted degradation products onto MHC-I and secondly, cross-priming in which vesicles carrying mycobacterial antigens are taken by DCs (Kaufmann, 2010). MHC-I & II

efficiently presents to $CD4^+$ and $CD8^+$ T-lymphocytes which further leads to production of inflammatory chemokines such as tumor necrosis factor (TNF)–α, interferon (IFN)-γ and interleukins (IL) and immune system isolates to the site of infection by granuloma formation.

In the tubercular granuloma a central area of necrosis is surrounded by lymphocytes, infected macrophages, foamy giant cells which are sealed off with fibrotic capsule of collagen and other extracellular matrix as the last defense mechanism. This stage of infection is characterized by a closed boundary where TB bacilli remain forever within this granuloma as a characteristic feature of latent TB as shown in Figure 1.2 (Stewart et al., 2003).

In later stages as the host immune system weakens, necrosis leads to caseous granuloma, and persistent TB infection is transformed into active disease. Reactivation of latent/persistent bacilli in immunocompromised individuals (HIV patients) is a high risk factor in TB treatment.

1.3 TB chemotherapy

During 18^{th} and 19^{th} century there were no measures available either for prevention of or resisting TB, and at that time physicians introduced sanatorium care as the first step for the management of TB (Urban et al., 2011).

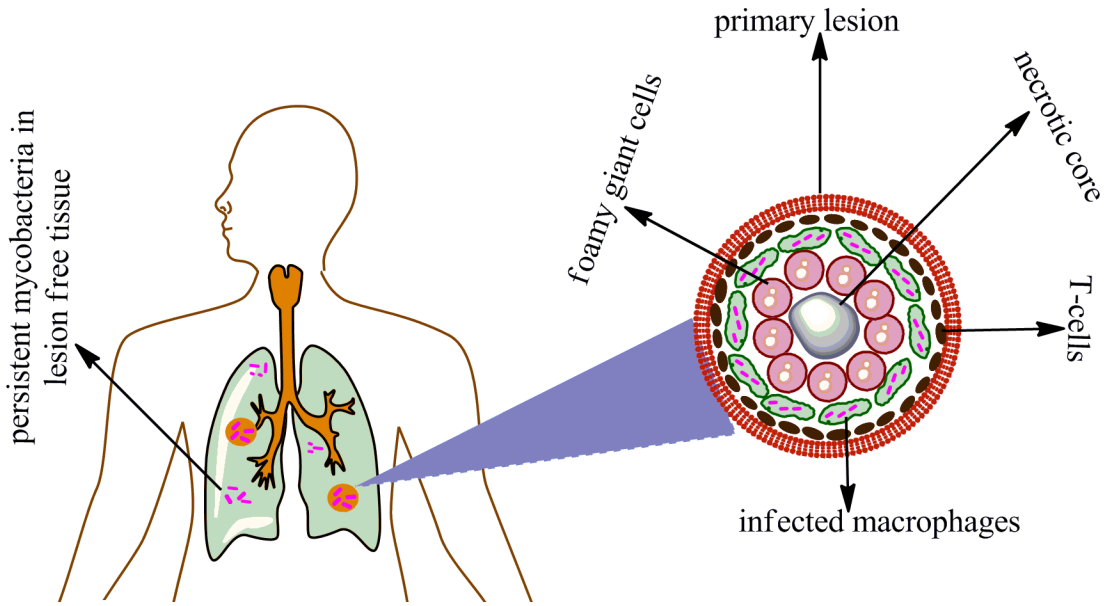

Figure 1.2 The figure shows presence of viable Mtb bacilli in primary lesions showing an aggregation of lymphocytic cells and foamy macrophages with a central necrotic core.

Fresh air, balanced diet, exercise were the important features of the sanatorium treatment, but it was not the ultimate solution to cure TB. Nearly 60% of the patients that recovered during sanatorium treatment died within six years of being discharged (Koul and Arora, 2010).

The first success for treatment of TB came in 1944 with the discovery of streptomycin by Selman A. Waksman. Later *p*-aminosalicyclic acid (1946), isoniazid (1952), pyrazinamide (1954), linezolid (2000) were introduced as anti-TB agents. Most of the anti-TB drugs (first line and second line drugs) were discovered between 1940- 2000 (Figure 1.3) and since then no new drugs have been identified that are in TB treatment.

The regimen for treating drug-susceptible TB involves six month treatment with isoniazid (INH), rifampin(RIF), pyrazinamide (PZA) and ethambutol (EMB) for first 2 months followed by INH and RIF for 4 months (Koul et al., 2011). WHO recommends this regimen as the best therapy for TB patients and it is also known as the DOTS (directly, observed, treatment, short-course) treatment. It is important to find successful treatment regimen for MDR-TB (resistant to at least INH and RIF) and XDR-TB (resistant to INH, RIF and any of second line anti-TB drugs) that is better tolerated, more efficient and inexpensive.

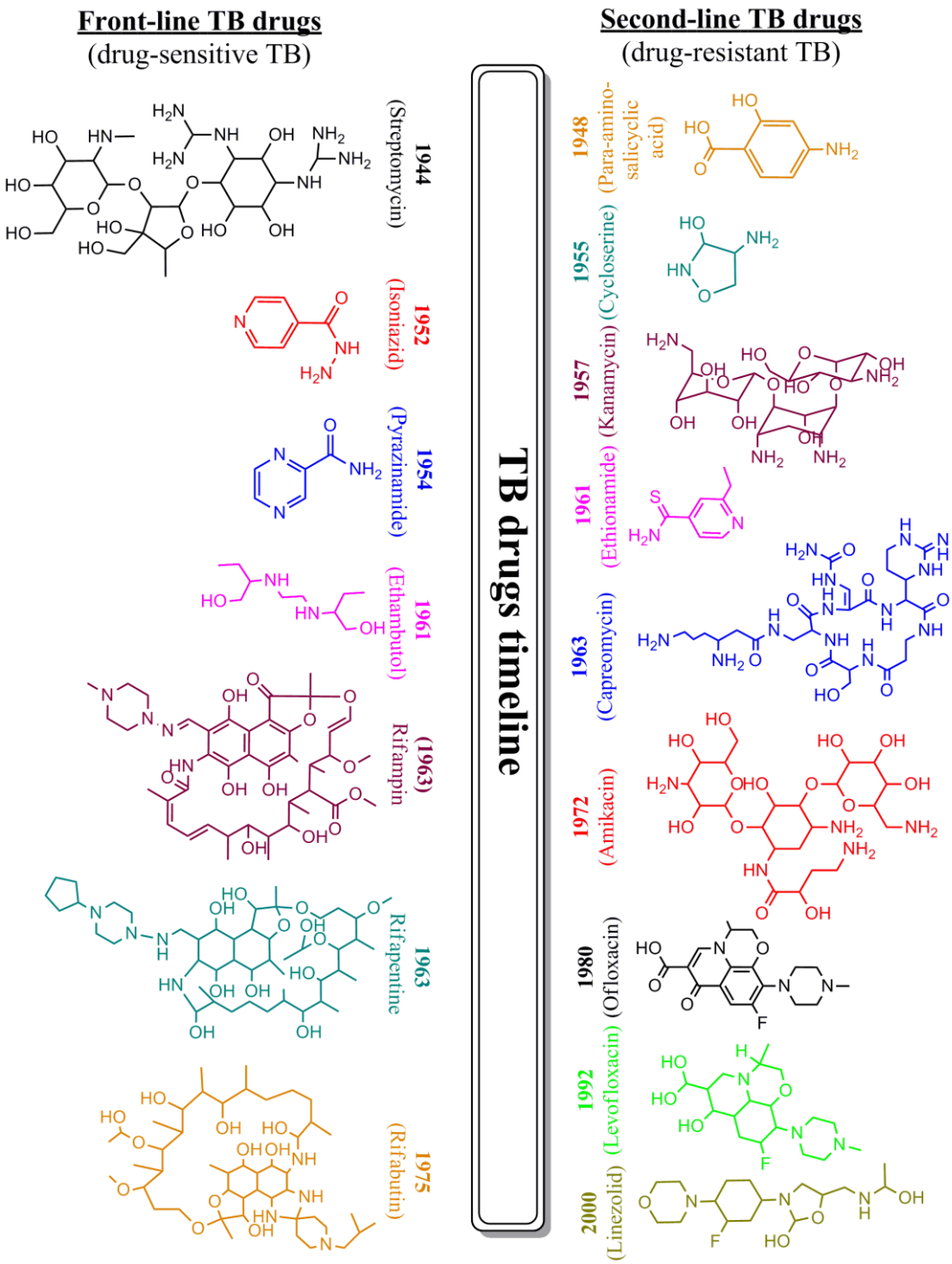

Figure 1.3 Timeline of TB drug discoveries during 1940-2000. First-line TB drugs (left panel) and second-line drugs (right panel).

1.4 Mycobacterial cell envelope

The rigid model of mycobacterial cell envelope is shown in Figure 1.4. The unusual cell envelope of mycobacteria differs significantly from the gram-positive and gram-negative bacterial architecture. In recent years, studies on cell envelope extended the original model proposed by Minnikin (Minnikin, 1982; Minnikin et al., 2002; Zuber et al., 2008). The major components of the mycobacterial cell envelope include the plasma membrane, cell wall core, and capsule (Brennan and Crick, 2007). The major components of the cell wall are mycolic acids, peptidoglycan (PG), arabinogalactan (AG) and lipoarabinomannan (LAM). The cytoplasmic membrane of all mycobacterial species is an asymmetrical phospholipid bilayer (Silva and Macedo, 1983b) and the "extra" thickness of this outer layer of inner membrane is due to the presence of different species of phosphotidylinositol mannosides (PIMs), lipomannan (LM) and LAM (Silva and Macedo, 1983a). Plasma membrane also contains key isoprenyl phosphate glycosyl donors, that are essential for the synthesis and assembly of AG, LAM, LM and PG (Brennan and Crick, 2007). The covalently linked mycolyl-arabinogalactan-peptidoglycan (mAGP) structure is intercalated with numerous glycolipids such as lipoarabinomannan (LAM), the phosphatidylinositol mannosides (PIMs), the pthiocerol-containing phenolic glycolipids (PGLs), trehalose dimycolate (TDM; the so called "cord factor"), trehalose monomycolates (TMM), in the outer membrane. The following section describes more of the structural features of complex mAGP and other non-covalently attached lipoglycans of mycobacterial cell wall.

1.4.1 Structural features of mycolyl-arabinogalactan-peptidglycan (mAGP)

Mycolic acids

Mycolic acids form major permeability barrier with its lipid rich environment in the outer layer, a dominant feature of mycobacterial cell wall. These mycolic acids are composed of α-alkyl branched, β-hydroxy long chain fatty acids with 70-90 carbon atoms (Barry et al., 1998; Minnikin, 1982). In Mtb, mycolic acids are classified into 3 types based on the modification at the distal end of the meromycolate chain. The α-mycolates possess two *cis*-cyclopropane rings, whereas keto and methoxy mycolic acids consist of their respective oxygen functions at the distal position with a proximal cyclopropane ring that is either in *cis*-form or in *trans* orientation. The α-mycolate chain is shorter than its oxygenated mycolates. Methoxy and ketomycolates contain nearly 80-90 carbon residues (Barry et al., 1998) and the non-reducing end of AG terminal and penultimate arabinosyl residues are esterifed with mycolic acids.

Arabinogalactan (AG)

The unique feature of AG is the presence of D-arabinofuranose (D-Ara*f*) and D-galactofuranose (D-Gal*f*) residues in the furanosyl forms. The D-arabinan of AG is known to be responsible for structural integrity and serological activity (Kaur et al., 2002; Misaki et al., 1977). Disruption of AG biosynthesis completely destroys assembly of the mycolyl-AGPG (mAGP) complex which in turn augments susceptibility of mycobacteria to the anti-TB drugs (Brennan and Nikaido, 1995).

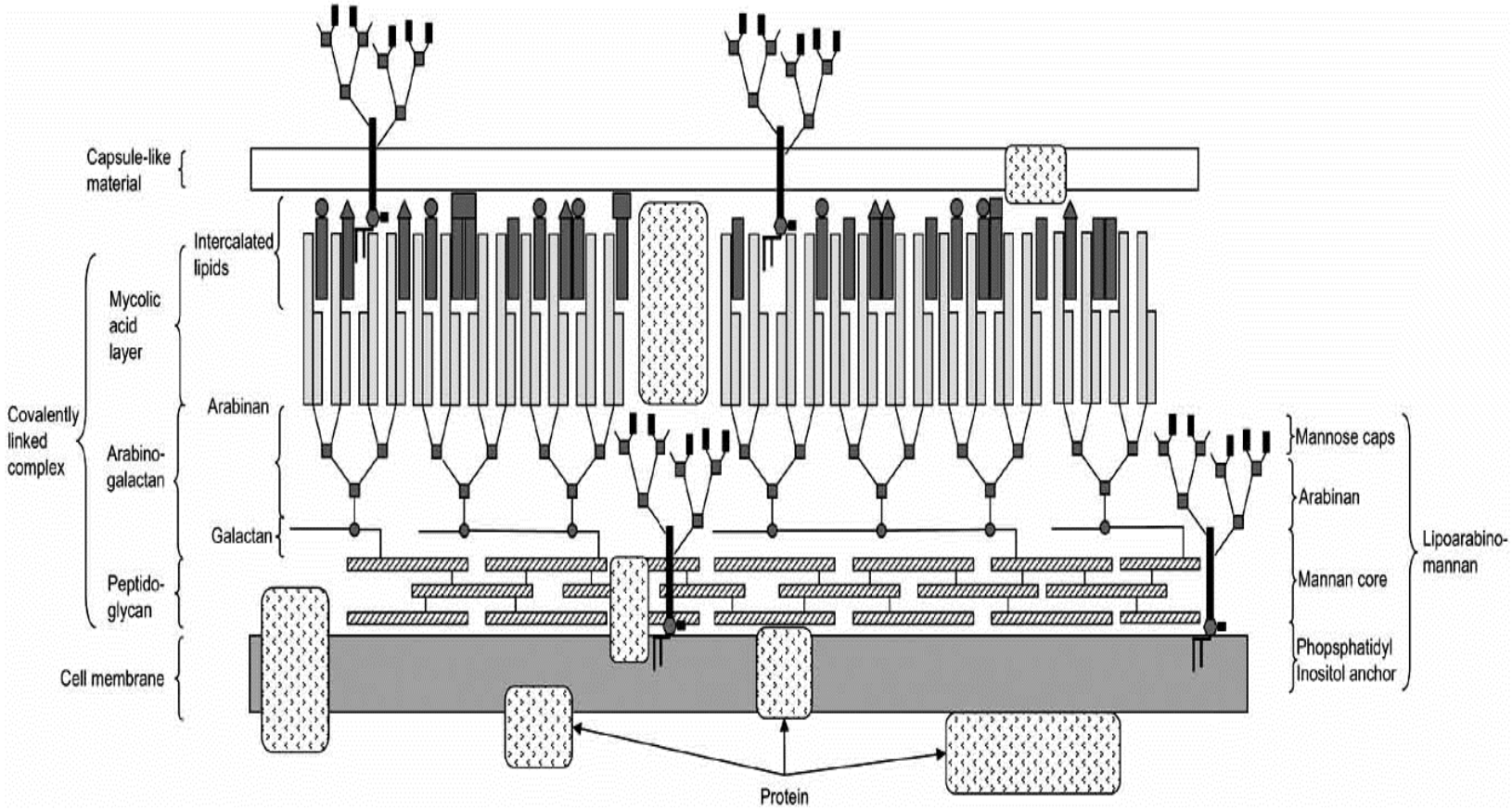

Figure 1.4 A schematic of the cell envelope of mycobacteria (Brennan and Crick, 2007)**.** The figure depicts complex assembly of two major cell wall polysaccharides, Lipoarabinomannan anchored non-covalently into the plasma membrane and mycolylate D-arabinogalactan attached covalently to the peptidoglycan (mAGP complex). Figure taken from (Brennan and Crick, 2007).

Structurally AG has three domains, the reducing end, a galactan backbone and a non-reducing end. Elegant work by McNeil et al., elucidated the structural organization of AG and has shown that, AG is attached to the PG by a linker disaccharide unit α-L-Rha*p*-(1→3)- Glc*N*Ac-(1→PG) (McNeil et al., 1990). There are 23 X 3 Gal*f* residues in AG with linear structure of alternating 5- and 6- linked β-D-Gal*f* residues (Brennan, 2003; Daffe et al., 1990). Three arabinan chains are attached to C-5 of 6-linked Gal*f* of galactan backbone at residues 8, 10 and 12 respectively (Alderwick et al., 2005; Daffe et al., 1990). The D-Ara*f* residues in AG are comprised of 2, 5 and 3, 5 linkages. Non-reducing end of AG terminates with a characteristic structural motif of Ara_6, [β-D-Ara*f*-(1→2)-α-D-Ara*f*-(1→)]$_2$-(3,5)-α-D-Ara*f*-(1→5)-α-D-Ara*f*, in which terminal β-D-Ara*f* and the penultimate 2-α-Ara*f* are esterified with clusters of four mycolic acids. Further, assembly of two such Ara_6 motifs with an extended arabinan chain form a structure of $Ara_{\mathbf{31}}$-mer, largest arabinan unit reported to date (Bhamidi et al., 2008). In mycolylate D-AG (Figure 1.5), $Ara_{\mathbf{31}}$-mer, the O-2 of inner 3,5-linked $Ara_{\mathbf{17}}$ at the non-reducing end is galactosaminylated and there is one $GalNH_2$ per entire AG (Draper et al., 1997). Similarly, the O-2 of inner 3, 5-linked $Ara_{\mathbf{17}}$ of the non-mycolated AG is esterified with succinyl groups (Bhamidi et al., 2008).

Peptidoglycan (PG):

PG (murein) is an essential continuous covalent structural element of mycobacterial cell wall (Ghuysen, 1973). It plays the major role in preserving cell integrity by withstanding osmotic pressure and also in the processes of cell growth and cell division. It also contributes to the defined cell shape and serves as a scaffold for anchoring cell wall

components such as AG (Brennan, 2003) and non-covalently associated proteins (Hirschfield et al., 1990). It is still a matter of debate on two opposing models, parallel vs perpendicular orientation of peptidoglycan with the plasma membrane (Dmitriev et al., 1999; Dmitriev et al., 2000; Ghuysen, 1968; Vollmer and Holtje, 2004). Peptidoglycan is made up of alternating units of *N*-acetlyglucosamine (Glc*N*Ac) and *N*-acetylmuramic acid (Mur*N*Ac) residues linked by β(1→4)linkages. The lactyl group of each Mur*N*Ac is substituted by L-Ala-D-Glu-meso-diaminopimelic acid [DAP]-D-Ala-D-Ala pentapeptide. In mycobacteria, glycan strands cross link in two different ways, where 70% of cross linking occurs between DAP-Ala, while 30% is between DAP-DAP (Adam et al., 1969; Lederer et al., 1975; Wietzerbin et al., 1974). Further, carboxyl groups of D-Glu and DAP are amidated (Lederer et al., 1975). The muramic residue of PG in Mtb is present in two forms, *N*-acetylated and *N*-glycolated, whereas in *M. leprae* it is *N*-acetylated (Lederer et al., 1975; Mahapatra et al., 2008). Mycolated-AG linker disaccharide Glc*N*Ac C-1 carbon further links with muramic acid residues of PG results in formation of complex structure called mycolyl-arabinogalactan-peptidoglycan (mAGP) complex.

1.4.2 Structural features of lipoglycans (PIMs, LM and LAM)

PIMs, LM and LAM are the major glycolipids anchored non-covalently in the plasma membrane and these are also present in the outer envelope where they interact with the CD1-restricted T-cell of the immune system (Ortalo-Magne et al., 1996; Sieling et al., 1995). In 1966, Pangborn and McKinney first reported the multiacylated forms of PIMs, later Ballou and Brennan discovered PIM_2 species in *M. phlei* (Brennan and Ballou, 1968; Pangborn and McKinney, 1966). Several others further identified the presence of

di, tri and tetra acylated forms of PIM_2 (Khuller and Subrahmanyam, 1968). Chatterjee et al., identified the presence of hexa-mannoside PIM_6 species in Mtb. LAM, LM, and PIM biosynthesis proceeds from common precursor phosphotidyl-*myo*-inositol (PI). The two major species of PIMs are Ac_1PIM_2, Ac_2PIM_2 and Ac_1PIM_6, Ac_2PIM_6. The di and hexamannoside species of PIMs possess specificity with attachment of third and fourth fatty acyl chains. The Ac_1PIM_2 and Ac_1PIM_6 are linked with third fatty acid chain to Man*p* which is in turn attached to the C-2 of *myo*-inositiol. The fourth fatty acid chain in Ac_2PIM_2 and Ac_2PIM_6 is attached to the C-3 position of *myo*-inositol. Mannosylation of PIM_2 precursors results in the formation of lipomannan (LM), further glycosylation of LM with arabinose forms lipoarabinomannan (LAM). Structurally, it has been shown that about sixty D-Ara*f* residues and about 30-35 D-Man*p* residues makes a mature LAM (Chatterjee et al., 1992). The mannan backbone in both LM and LAM is composed of 20-25 Man*p* residues with a (1→6) linkages. In all mycobacterial species LM single mannose branching occurs at C-2 position of mannan core except in *M. chelonae* where branching occurs at C-3 position (Guerardel et al., 2002).

In pathogenic mycobacterial species such as Mtb, *M. leprae, M. avium* and *M. kansasii* the terminal arabinan domain is capped with single, di- and tri-mannoside units and hence termed as ManLAM (Chatterjee et al., 1993; Dinadayala et al., 2006). In non-pathogenic mycobacterial species such as *M. smegmatis,* and *M. fortuitum* the terminal arabinan domain is capped with inositol-phosphate and termed PI-LAM. There is no capping observed in *M. chelonae* LAM and it is termed AraLAM (Besra et al., 1994). Structure of LAM also differs based on substitutions on the terminal mannose with succinyl group

(Delmas et al., 1997), 5-deoxy-5-methyhioxylose residue (MTX) and its oxidized form, 5-deoxy-5-methylsulfoxypentofuranosyl (MSP) (Turnbull et al., 2004).

1.5 Genetics and enzymology of arabinan in AG and LAM

1.5.1 Arabinose source in mycobacteria

The only known source of D-arabinofuranosyl residue in mycobacteria is decaprenylphosphoryl-D-Ara*f* (DPA) (Scherman et al., 1995). Radiolabeling experiments with growing cultures of *M. smegmatis* indicated that the D-Ara*f* residues are derived from the pentose phosphate shunt (Scherman et al., 1995; Scherman et al., 1996). The first step in the biosynthesis of DPA via the pentose shunt pathway is the formation of 5'-phosphoribosyl-β-1-monophospho-decaprenol (DPPR), which involves transfer of 5-phospho-α-D-ribofuranose1-pyrophosphate (pRpp) to decaprenylmonophosphate (DP) by decaprenyl transferase UbiA (*Rv3806c*) (Huang et al., 2005). Synthesis of β-D-ribosyl-1-monophophodecaprenol (DPR) is formed by the catalysis of phospholipid phosphatase encoded by non-essential gene *Rv3807*. Finally 2'-epimerization of D-ribofuranosyl residue of DPR results in the formation of β-D-arabinofuranosyl-1-monophosphodecaprenol (DPA) (Mikusova et al., 2005). This reaction possibly involves formation of intermediate decaprenyl-phospho-2'-keto-D-arabinose (DPX) [69].

1.5.2 Arabinosyltransferases involved in the biosynthesis of arabinan in AG and LAM

Extensive studies on mycobacterial arabinosyltransferases in the last decade led to the identification of several key enzymes involved in the polymerization of arabinan in AG and LAM. In spite of this tremendous active research focused on cell wall of

mycobacteria, the complete knowledge of events involved in the assembly of arabinan polymerization either in AG or LAM biosynthesis is still not clear. Arabinan biosynthesis begins with the transfer of a D-Ara from lipid linked arabinose donor (DPA). The structural complexity of AG suggests that it requires a large number of linkage specific arabinosyltransferases for the complete assembly of Ara_{31}-mer on to 8, 10 and 12th residues of the galactan backbone of AG. In AG, six major arabinosyltransferases (Figure 1.5) have been identified AftA (Rv3792) (Alderwick et al., 2006), AftB (Rv3805c) (Seidel et al., 2007), AftC (Rv2673) (Birch et al., 2008), AftD (Rv0236c) (Skovierova et al., 2009) and the Emb proteins, EmbA (Rv3794) and EmbB (Rv3795) (Belanger et al., 1996).

AftA arabinosyltransferase catalyzes the transfer of the first D-Ara*f* from DPA to the galactan chain (Alderwick et al., 2006). Seidel et al., identified AftB arabinosyltransferase and characterized its role in the formation of terminal β-(1→2) linkage at the non-reducing termini of AG biosynthesis in *C. glutamicum* (Seidel et al., 2007; Shi et al., 2008). EmbA and EmbB arabinosyltransferases are shown to be involved in the formation of proper Ara_6 motif at the non-reducing end (Escuyer et al., 2001; Khasnobis et al., 2006). AftC arabinosyltransferase introduces α-(1→3) branch points in the internal region of arabinan in AG biosynthesis (Birch et al., 2008). AftD, another arabinosyltransferase, was reported with similar α-(1→3) branching activity using synthetic acceptors in cell free arabinosyltransferase assays, but the precise role of this protein, either in AG or LAM, was not clearly elucidated (Skovierova et al., 2009).

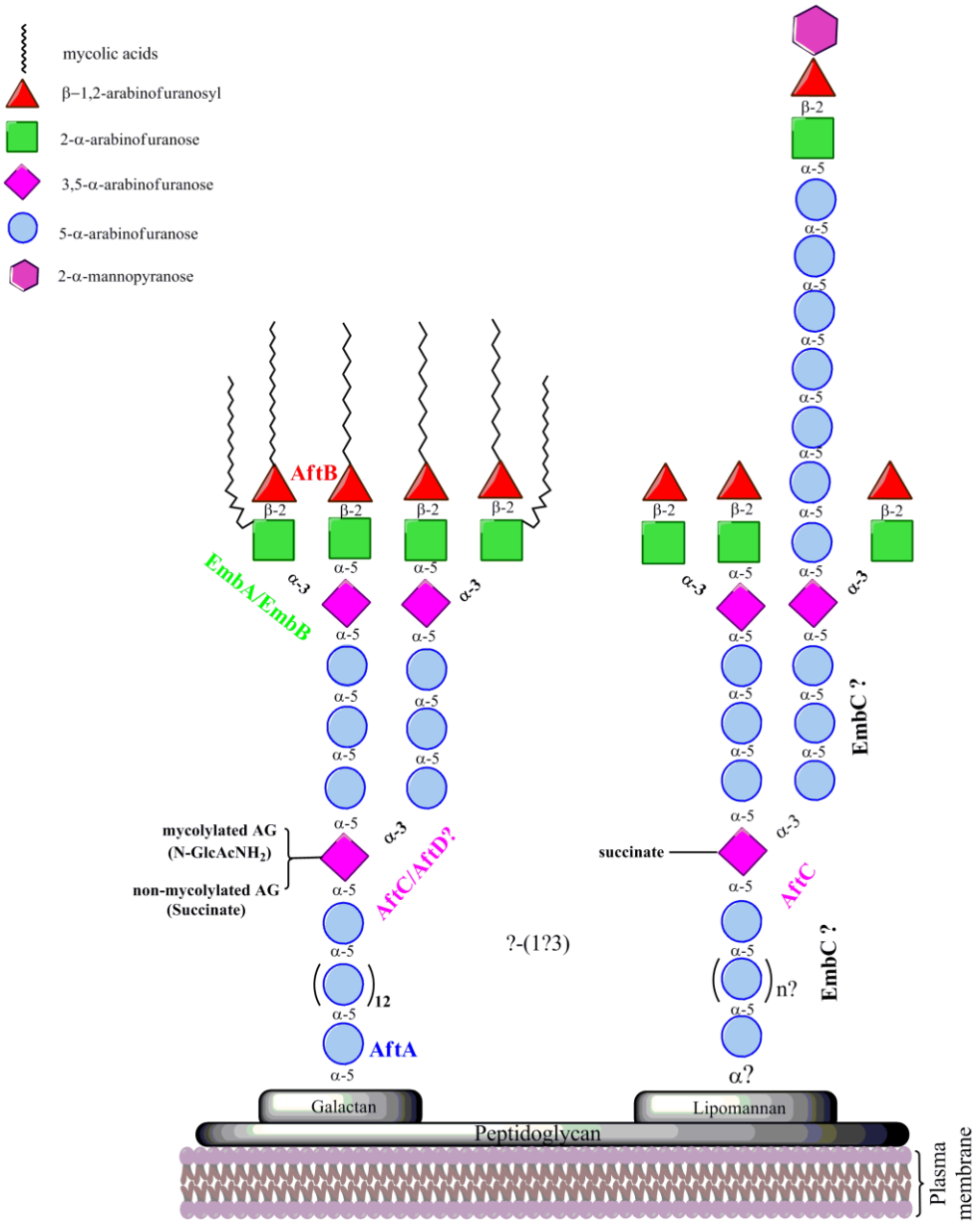

Figure 1.5 Arabinosyltransferases involved in the biosynthesis of AG and LAM. **AftA** (initiates the arabinan biosynthesis with transfer of first arabinose on the galactan backbone of AG), **AftB** (terminates arabinan biosynthesis by introducing β-(1→2) linked capping residues), **AftC** (introduces α-(1→3) internal branch points in both AG and LAM), **AftD** (is also α-(1→3) branching enzyme but is not clear in either AG or LAM), **EmbA** and **EmbB** are involved in the α-(1→3) branching at the terminal Ara_6 motif of AG. **EmbC** is known to be involved in the arabinan biosynthesis of LAM.

There are nearly 31 x 3 Ara*f* residues reported per AG (Bhamidi et al., 2008), and the arabinosyltransferases that have been identified transfer only one specific arabinose in AG biosynthesis. The α-(1→5) arabinosyltransferases that are responsible for synthesis of the major segment of arabinan biosynthesis in AG have not yet been identified.

As shown in Figure 1.5, EmbC and AftC are the only two arabinosyltransferases involved in the extension of mannan core of LM. EmbC protein of *M. smegmatis* is critical for LAM synthesis (Zhang et al., 2003). The presence of one to two Ara*f* residues on the mannan backbone of *embC* knock out mutant indicates the existence of unidentified priming arabinosyltransferase specific for LAM biosynthesis (Zhang et al., 2003).

GT-C motif is essential for the activity of glycosyltransferases, which has been demonstrated using site directed mutagenesis of *embC* GT-C motif resulting in inhibition of LAM biosynthesis (Berg et al., 2005). Truncation of C-terminal sequential aminoacids of *embC*, determine the chain length extension of arabinan in LAM (Shi et al., 2006). This is further supported from recently published data on crystal structure of C-terminal hydrophilic domain of EmbC from Mtb (Alderwick et al., 2011). Co-crystallization of EmbC with the arabinose disaccharide acceptor has shown that the C-terminal domain of EmbC has two separate carbohydrate binding sites called as sub domains I and II (Alderwick et al., 2011).

AftC is identified as an α-(1→3) internal branching arabinosyltransferase and evidence has shown it to be involved in the biosynthesis of both AG and LAM. Thus, AftC seems to be a crucial enzyme. The deletion of *aftC* in *M. smegmatis* led to altered growth, and arabinan of AG was devoid of α-D-Ara*f*-(1→3) branch. In LAM biosynthesis, the mutant

expressed a severely truncated arabinan domain lacking 3,5- linked arabinose residues (Birch et al., 2010).

1.5.3 Arabinan of LAM in pathogenesis

Mycobacterial cell wall arabinan may be an important drug target for anti-mycobacterial drug development. Mycobacterial sugars are involved in key interactions between Mtb and host cells (Ehlers and Daffe, 1998). In fact, the arabinan portion of LAM is a critical virulence factor compared to the biologically inactive LM devoid of arabinan. Immunological activity of sugars substituted/capped on arabinofuranosyl residues present at the non-reducing end of LAM play a vital role in the TB pathogenesis (Oashi, 1970). First, ManLAM formed by capping of mannan residues (mono, di and tri) with α-(1→2) linkages on to the terminal β-(1→2) arabinose residue is seen only in slow growing *M. bovis*. Moreover, ManLAM is a potent anti-inflammatory molecule with the ability to inhibit (i) macrophage activation, (ii) production of IL-12 and TNF-α and (iii) Mtb induced macrophage apoptosis (Nigou et al., 2001). Secondly, AraLAM and ManLAM seem to elicit immediate early gene responses. However, AraLAM also induces TNF-α and lethal TNF-dependent nitric oxide responses (Roach et al., 1993). Third, the presence of 5-deoxy-5-methylthioxylose structure on ManLAM plays a role in TB pathogenesis. The exact biological function of this moiety on LAM is not clearly understood but believed to provide the antioxidative properties (Turnbull et al., 2004). It has, therefore, been speculated that arabinan moiety of LAM indirectly contributes towards many clinical manifestations in Mtb pathogenesis. Finally, the esterification of complex mycolic acids with the terminal and penultimate D-Ara*f* residues in AG provide lipid rich

hydrophobic environment that, in turn, provides resistance to anti-mycobacterial chemotherapy. Apart from the most important arabinosyltransferase EmbC, targeting the other terminal capping arabinosyltransferase AftB, responsible for many substitutions/capping, or AftC, necessary in introducing the branch points in the growing chain of arabinan, are ideal targets for TB drug development.

1.6 Mycobacterial cell envelope as drug target

The following section describes various current anti-TB drugs and drug like molecules that are in clinical trials targeting one or more enzymes of cell wall biosynthesis.

The mycobacterial cell wall is essential for survival and pathogenesis of the bacterium. The Mtb surface complex enriched with a glycolipid environment forms a physical barrier for many drugs [30]. Peptidoglycan protects Mtb against osmotic lysis and serves as the base for a lipid-rich capsule. D-cycloserine (a second-line anti-Tb drug) inhibits a major component of peptidoglycan biosynthesis by targeting alanine racemase (Alr) that catalyzes the racemization of L-Ala into D-Ala (LeMagueres et al., 2005).

Glycosyltransferases, involved in the assembly of complex cell wall carbohydrate moieties, make it an excellent drug choice for inhibiting the cell wall. It is evident from the literature that ethambutol, a front-line anti-TB drug, is known to target cell wall arabinosyltransferases *embA, and embB* of *M. avium* (Belanger et al., 1996). Recently identified ethambutol structural analog SQ109 also shows a similar transcriptional profile as its parent ethambutol (Boshoff et al., 2004) indicating it may also have a similar mode

of action. Ethambutol is the only proven inhibitor of arabinosyltransferase in several mycobacterial species. However, it is still not clear how it inhibits the transferase activity.

Mycolic acid biosynthetic machinery is another key feature of the mycobacterial cell wall which is known to be inhibited by the drugs isoniazid and ethionamide (Johnsson et al., 1995). Both of these prodrugs get converted into their active acyl-radical form by KatG and EtaA enzymes respectively (Zhang et al., 1992). Activated radicals catalyze the NADH-dependent reduction of the acyl-carrier protein, an enzyme that is responsible in the final step of FAS-II biosynthetic pathway of mycolic acids (Wang et al., 2007; Zhang et al., 1992). Currently, the two promising bicyclic nitroimidazole candidates PA-824 and OPC-67683 are known to disrupt mycolic acid formation in the cell envelope (Matsumoto et al., 2006; Stover et al., 2000).

To date, treatment of tuberculosis has been successful using these front-line and second-line drugs that target cell wall biosynthesis, but there is an urgent need for new drugs with different modes of action to treat MDR and XDR-TB cases. The mycobacterial cell wall is essential for the bacterium's growth and survival in the host. Inhibition of cell wall biosynthesis, therefore, is targeted to identify novel drugs for the treatment of MDR and XDR-TB.

1.7 Pipeline of novel anti-TB drug candidates

Advances in TB drug targets have been driven with the availability of mycobacterial genome finding novel strategies for anti-sequences, but unfortunately, genome derived approaches have had little success. At present, the global anti-TB drug development plan shows some promise with new candidates in the pipeline for TB treatment as shown in Table 1.1. The following section describes the anti-TB drug candidates currently in clinical trials. Recently a whole cell screening strategy led to identification of two new anti-TB drug candidates such as diarylquinolines (TMC207) and benzothiazines (BTZ043). Diarylquinoline (TMC207) which is currently in phase II clinical trials is known to inhibit mycobacterial ATP synthase activity and it is effective in treatment of drug susceptible and MDR TB patients (Yew et al., 2011). BTZ043, on the other hand, inhibits cell wall arabinan synthesis with excellent prospects for killing not only TB but also XDR-TB. BTZ043 is currently in pre-clinical trials (Pasca et al., 2010). Pyrrole LL-3858 (sudoterb) structural analog of isoniazid showed higher anti-mycobacterial activity than isoniazid.

Table 1.1 Recently developed new anti-TB candidates in clinical trials with potential novel mechanism of action.

Clinical status	Inhibitors of protein synthesis	Cell wall/ multiple targets	Inhibitors of DNA gyrases	Inhibitors of ATP synthase	Inhibitors with unknown target
Phase I	PNU100480 AZD5847	SQ109			
Phase II		PA824 OPC 67683		TMC207	Pyrrole LL-3858 (Sudoterb)
Phase III			Moxifloxacin Gatifloxacin		

Another emerging strategy in development of new anti-TB drug candidates is the chemical tailoring of old drug classes that were discovered decades ago. Lederle laboratories developed ethambutol (EMB) in 1950's. Structural modification of ethambutol has led to the discovery of a novel compound SQ109 (Lee et al., 2003) which is currently in phase-I clinical trials. The exact target and mode of action of SQ109 is still not clear, but transcriptional profile of Mtb in the presence of SQ109 shows its action to be similar to EMB to a certain extent (Boshoff et al., 2004).

Compounds identified as candidates with structural modifications are shown in Figure 1.6. Oxazolidinones were originally discovered in 1970's at Dupont, and its modified version such as linezolid has led to new structures such as PNU-100480 which is currently in phase-I clinical trials. Linezolids have toxicity issues (Fortun et al., 2005), and structurally modified PNU-100480 is under screening process for its bone marrow toxicity in early phase of clinical trials.

PA-824, which is a structural analog of metronidazole is in phase-II clinical trials, mimics host defense strategy and acts as nitric oxide donor which reacts with cytochromes/cytochromooxidase poisoning respiratory chain. PA-824 and OPC-67683 are prodrugs activated selectively by mycobacterial flavin dependent nitroreductase that are absent in humans (Manjunatha et al., 2009). Gatifloxacin and moxifloxacin which are in phase-III clinical trials are also structural analogs modified from fluoroquinolones class of nalidixic acid. The presence of MDR-TB and XDR-TB strains in HIV-infected patients complicates the selection of appropriate treatment regimen, most importantly, because of toxic side effects caused by drug-drug interaction.

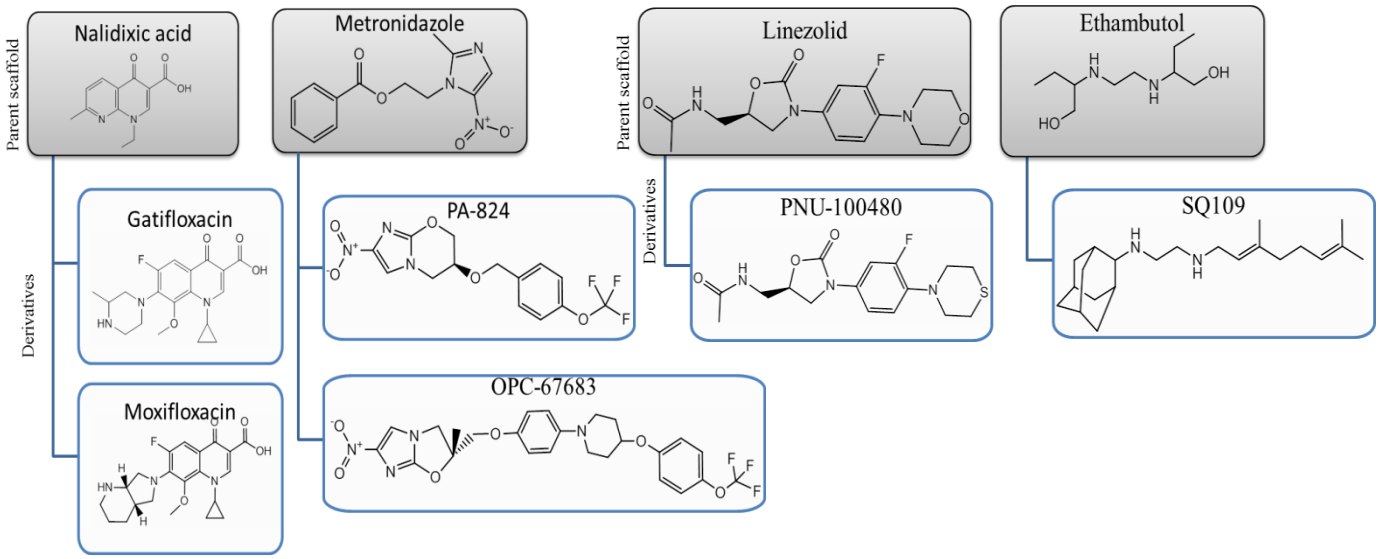

Figure 1.6 Chemical tailoring of existing anti-TB drugs led to the identification of novel candidates that are in clinical trials. Modification of parental scaffold of fluoroquinolones (nalidixic acid), nitroimidazoles (metronidazole), oxazolidinones (linezolid) and 1,2-ethyldiamine (ethambutol).

Treatment of HIV co-infected TB patients with rifampicin results in induction of hepatic cytochrome P450 expression system (Lecluyse et al., 2010). This causes decreased therapeutic concentrations of HIV-protease inhibitor such as ritonavir given as co-medication for HIV patients. There is a definite need for more structural analogs of rifampicin and other second line anti-TB drugs which interacts minimally with drug metabolizing enzymes to treat HIV-infected TB patients.

1.8 Rationale and objectives

The current knowledge regarding the earlier events in cell-wall core synthesis has attracted interest in terms of new anti-TB drug development. The biosynthetic pathways of two major complex polysaccharides AG and LAM of mycobacterial cell envelope offer themselves as potential drug targets. AftB and AftC arabinosyltransferases are known to be involved in both AG and LAM synthesis and are insensitive to action of ethambutol, therefore, we focused on developing a radioactive cell free arabinosyltransferases for AftB and AftC to screen cell wall inhibitors as described in Chapters 2, 3 and 4. In this study, we used synthetic arabinose acceptors as they mimic the native structural domains of AG and LAM. The objectives of my study were as follows

1.8.1 AftB arabinosyltransferase

- Development of cell free radioactive arabinosyltransferase assay using synthetic disaccharide acceptors and characterize the product catalyzed by the specific arabinosyltransferase.

- Conversion of radioactive assay into a non-radioactive plate based format for screening small molecule inhibitors.

1.8.2 AftC arabinosyltransferase

Generate efficient system/tools for developing a platform for screening small molecule inhibitors for AftC.

- Expression and purification of AftC arabinosyltransferase and development of cell free AftC arabinosyltransferase assay and MALDI-TOF analysis of the enzymatic product.
- Assessment of various synthetic donor and acceptor analogs for AftC arabinosyltransferase activity.

1.8.3 Mtb growth inhibition

- An additional objective of this dissertation is to screen small molecule inhibitors against Mtb growth inhibition using plate based microtiter alamar blue assay (MABA) method (Chapter 5)

1.9 References

Adam, A., J. Petit, and P. Wietzerbin-Falszpan. 1969. L'acide N-glycolyl-muramique, constituant des parois de *Mycobacterium smegmatis*: Identification par spectrometrie de masse (The N-glycolyl-muramic, forming the walls of *Mycobacterium smegmatis*: Identification by mass spectrometry). *FEBS Lett.* 4:87-92.

Alderwick, L.J., G.S. Lloyd, H. Ghadbane, J.W. May, A. Bhatt, L. Eggeling, K. Futterer, and G.S. Besra. 2011. The C-terminal domain of the Arabinosyltransferase *Mycobacterium tuberculosis* EmbC is a lectin-like carbohydrate binding module. *PLoS Pathog*. 7:e1001299.

Alderwick, L.J., E. Radmacher, M. Seidel, R. Gande, P.G. Hitchen, H.R. Morris, A. Dell, H. Sahm, L. Eggeling, and G.S. Besra. 2005. Deletion of Cg-emb in corynebacterianeae leads to a novel truncated cell wall arabinogalactan, whereas inactivation of Cg-ubiA results in an arabinan-deficient mutant with a cell wall galactan core. *J. Biol. Chem*. 280:32362-32371.

Alderwick, L.J., M. Seidel, H. Sahm, G.S. Besra, and L. Eggeling. 2006. Identification of a novel arabinofuranosyltransferase (AftA) involved in cell wall arabinan biosynthesis in *Mycobacterium tuberculosis*. *J. Biol. Chem*. 281:15653-15661.

Barry, C.E., 3rd, R.E. Lee, K. Mdluli, A.E. Sampson, B.G. Schroeder, R.A. Slayden, and Y. Yuan. 1998. Mycolic acids: structure, biosynthesis and physiological functions. *Prog. Lipid Res.* 37:143-179.

Bates, J.H. 1980. Transmission and pathogenesis of tuberculosis. *Clin. Chest Med.* 1:167-174.

Belanger, A.E., G.S. Besra, M.E. Ford, K. Mikusova, J.T. Belisle, P.J. Brennan, and J.M. Inamine. 1996. The *embAB* genes of *Mycobacterium avium* encode an arabinosyl transferase involved in cell wall arabinan biosynthesis that is the target for the antimycobacterial drug ethambutol. *Proc. Natl. Acad. Sci. U. S. A.* 93:11919-11924.

Berg, S., J. Starbuck, J.B. Torrelles, V.D. Vissa, D.C. Crick, D. Chatterjee, and P.J. Brennan. 2005. Roles of conserved proline and glycosyltransferase motifs of EmbC in biosynthesis of lipoarabinomannan. *J. Biol. Chem*. 280:5651-5663.

Besra, G.S., D. Chatterjee, and B. Bloom. 1994. Lipids and carbohydrates of *Mycobacterium tuberculosis*. *In* Tuberculosis: Pathogenesis, protection, and control. B.R. Bloom, editor. ASM Press: Washington, DC. 285-306.

Bhamidi, S., M.S. Scherman, C.D. Rithner, J.E. Prenni, D. Chatterjee, K.H. Khoo, and M.R. McNeil. 2008. The identification and location of succinyl residues and the characterization of the interior arabinan region allow for a model of the complete primary structure of *Mycobacterium tuberculosis* mycolyl arabinogalactan. *J. Biol. Chem*. 283:12992-13000.

Birch, H.L., L.J. Alderwick, B.J. Appelmelk, J. Maaskant, A. Bhatt, A. Singh, J. Nigou, L. Eggeling, J. Geurtsen, and G.S. Besra. 2010. A truncated lipoglycan from mycobacteria with altered immunological properties. *Proc. Natl. Acad. Sci. U. S. A.* 107:2634-2639.

Birch, H.L., L.J. Alderwick, A. Bhatt, D. Rittmann, K. Krumbach, A. Singh, Y. Bai, T.L. Lowary, L. Eggeling, and G.S. Besra. 2008. Biosynthesis of mycobacterial arabinogalactan: identification of a novel alpha(1-->3) arabinofuranosyltransferase. *Mol. Microbiol.* 69:1191-1206.

Boshoff, H.I., T.G. Myers, B.R. Copp, M.R. McNeil, M.A. Wilson, and C.E. Barry, 3rd. 2004. The transcriptional responses of *Mycobacterium tuberculosis* to inhibitors of metabolism: novel insights into drug mechanisms of action. *J. Biol. Chem*. 279:40174-40184.

Brennan, P., and C.E. Ballou. 1968. Biosynthesis of mannophosphoinositides by *Mycobacterium phlei*. Enzymatic acylation of the dimannophosphoinositides. *J. Biol. Chem*. 243:2975-2984.

Brennan, P.J. 2003. Structure, function, and biogenesis of the cell wall of *Mycobacterium tuberculosis*. *Tuberculosis (Edinb)*. 83:91-97.

Brennan, P.J., and D.C. Crick. 2007. The cell-wall core of *Mycobacterium tuberculosis* in the context of drug discovery. *Curr. Top. Med. Chem*. 7:475-488.

Brennan, P.J., and H. Nikaido. 1995. The envelope of mycobacteria. *Annu. Rev. Biochem.* 64:29-63.

Chatterjee, D., S.W. Hunter, M. McNeil, and P.J. Brennan. 1992. Lipoarabinomannan. Multiglycosylated form of the mycobacterial mannosylphosphatidylinositols. *J. Biol. Chem*. 267:6228-6233.

Chatterjee, D., K.H. Khoo, M.R. McNeil, A. Dell, H.R. Morris, and P.J. Brennan. 1993. Structural definition of the non-reducing termini of mannose-capped LAM from Mycobacterium tuberculosis through selective enzymatic degradation and fast atom bombardment-mass spectrometry. *Glycobiology*. 3:497.

Daffe, M., P.J. Brennan, and M. McNeil. 1990. Predominant structural features of the cell wall arabinogalactan of *Mycobacterium tuberculosis* as revealed through characterization of oligoglycosyl alditol fragments by gas chromatography/mass spectrometry and by 1H and 13C NMR analyses. *J. Biol. Chem*. 265:6734-6743.

Delmas, C., M. Gilleron, T. Brando, A. Vercellone, M. Gheorghui, M. Riviere, and G. Puzo. 1997. Comparative structural study of the mannosylated-lipoarabinomannans from *Mycobacterium bovis* BCG vaccine strains: characterization and localization of succinates. *Glycobiology*. 7:811-817.

Dinadayala, P., D. Kaur, S. Berg, A.G. Amin, V.D. Vissa, D. Chatterjee, P.J. Brennan, and D.C. Crick. 2006. Genetic basis for the synthesis of the immunomodulatory mannose caps of lipoarabinomannan in *Mycobacterium tuberculosis*. *J. Biol. Chem*. 281:20027-20035.

Divangahi, M., D. Desjardins, C. Nunes-Alves, H.G. Remold, and S.M. Behar. 2010. Eicosanoid pathways regulate adaptive immunity to *Mycobacterium tuberculosis*. *Nat Immunol*. 11:751-758.

Dmitriev, B.A., S. Ehlers, and E.T. Rietschel. 1999. Layered murein revisited: a fundamentally new concept of bacterial cell wall structure, biogenesis and function. *Med. Microbiol. Immunol*. 187:173-181.

Dmitriev, B.A., S. Ehlers, E.T. Rietschel, and P.J. Brennan. 2000. Molecular mechanics of the mycobacterial cell wall: from horizontal layers to vertical scaffolds. *Int. J. Med. Microbiol.* 290:251-258.

Draper, P., K.H. Khoo, D. Chatterjee, A. Dell, and H.R. Morris. 1997. Galactosamine in walls of slow-growing mycobacteria. *Biochem. J.* 327 (Pt 2):519-525.

Ehlers, M.R., and M. Daffe. 1998. Interactions between *Mycobacterium tuberculosis* and host cells: are mycobacterial sugars the key? *Trends. Microbiol.* 6:328-335.

Escuyer, V.E., M.A. Lety, J.B. Torrelles, K.H. Khoo, J.B. Tang, C.D. Rithner, C. Frehel, M.R. McNeil, P.J. Brennan, and D. Chatterjee. 2001. The role of the *embA* and *embB* gene products in the biosynthesis of the terminal hexaarabinofuranosyl motif of *Mycobacterium smegmatis* arabinogalactan. *J. Biol. Chem.* 276:48854-48862.

Farina, M.C., M.I. Gegundez, E. Pique, J. Esteban, L. Martin, L. Requena, A. Barat, and M. Fernandez Guerrero. 1995. Cutaneous tuberculosis: a clinical, histopathologic, and bacteriologic study. *J. Am. Acad. Dermatol.* 33:433-440.

Fortun, J., P. Martin-Davila, E. Navas, M.J. Perez-Elias, J. Cobo, M. Tato, E.G. De la Pedrosa, E. Gomez-Mampaso, and S. Moreno. 2005. Linezolid for the treatment of multidrug-resistant tuberculosis. *J. Antimicrob. Chemother.* 56:180-185.

Gaynor, C.D., F.X. McCormack, D.R. Voelker, S.E. McGowan, and L.S. Schlesinger. 1995. Pulmonary surfactant protein A mediates enhanced phagocytosis of *Mycobacterium tuberculosis* by a direct interaction with human macrophages. *J. Immunol.* 155:5343-5351.

Ghuysen, J.M. 1968. Use of bacteriolytic enzymes in determination of wall structure and their role in cell metabolism. *Bacteriol. Rev.* 32:425-464.

Ghuysen, J.M. 1973. The Bacterial Membranes and Walls: Biosynthesis of peptidoglycan. Vol. 1. L. Leive, editor. Dekker New-York. 37-130.

Goren, M.B., O. Brokl, and B.C. Das. 1976a. Sulfatides of *Mycobacterium tuberculosis*: the structure of the principal sulfatide (SL-I). *Biochemistry (Mosc).* 15:2728-2735.

Goren, M.B., P. D'Arcy Hart, M.R. Young, and J.A. Armstrong. 1976b. Prevention of phagosome-lysosome fusion in cultured macrophages by sulfatides of *Mycobacterium tuberculosis*. *Proc. Natl. Acad. Sci. U. S. A.* 73:2510-2514.

Guerardel, Y., E. Maes, E. Elass, Y. Leroy, P. Timmerman, G.S. Besra, C. Locht, G. Strecker, and L. Kremer. 2002. Structural study of lipomannan and lipoarabinomannan from *Mycobacterium chelonae*. Presence of unusual components with alpha 1,3-mannopyranose side chains. *J. Biol. Chem*. 277:30635-30648.

Hart, P.D., J.A. Armstrong, C.A. Brown, and P. Draper. 1972. Ultrastructural study of the behavior of macrophages toward parasitic mycobacteria. *Infect. Immun.* 5:803-807.

Hayman, J. 1984. *Mycobacterium ulcerans*: an infection from Jurassic time? *Lancet*. 2:1015-1016.

Hirschfield, G.R., M. McNeil, and P.J. Brennan. 1990. Peptidoglycan-associated polypeptides of *Mycobacterium tuberculosis*. *J. Bacteriol*. 172:1005-1013.

Huang, H., M.S. Scherman, W. D'Haeze, D. Vereecke, M. Holsters, D.C. Crick, and M.R. McNeil. 2005. Identification and active expression of the *Mycobacterium tuberculosis* gene encoding 5-phospho-{alpha}-d-ribose-1-diphosphate: decaprenyl-phosphate 5-phosphoribosyltransferase, the first enzyme committed to decaprenylphosphoryl-d-arabinose synthesis. *J. Biol. Chem*. 280:24539-24543.

Johnsson, K., D.S. King, and P.G. Schultz. 1995. Studies on the mechanism of action of isoniazid and ethionamide in the chemotherapy of tuberculosis. *J. Am. Chem. Soc.* 117:5009-5010.

Kathuria, S., and V. Ramesh. 2010. Clinical profile of cutaneous tuberculosis in pediatric age. *G. Ital. Dermatol. Venereol.* 145:289-302.

Kaufmann, S.H. 2010. Future vaccination strategies against tuberculosis: thinking outside the box. *Immunity*. 33:567-577.

Kaur, D., T.L. Lowary, V.D. Vissa, D.C. Crick, and P.J. Brennan. 2002. Characterization of the epitope of anti-lipoarabinomannan antibodies as the terminal hexaarabinofuranosyl motif of mycobacterial arabinans. *Microbiology*. 148:3049-3057.

Khasnobis, S., J. Zhang, S.K. Angala, A.G. Amin, M.R. McNeil, D.C. Crick, and D. Chatterjee. 2006. Characterization of a specific arabinosyltransferase activity involved in mycobacterial arabinan biosynthesis. *Chem. Biol.* 13:787-795.

Khuller, G.K., and D. Subrahmanyam. 1968. On the mannophosphoinositides of *Mycobacterium 607*. *Experientia*. 24:851-852.

Koch, R. 1882 Die Aetiologie der tuberkulose. Berl Klin Wschr. 19::221-230.

Koul, A., E. Arnoult, N. Lounis, J. Guillemont, and K. Andries. 2011. The challenge of new drug discovery for tuberculosis. *Nature*. 469:483-490.

Koul, A., and N. Arora. 2010. Celecoxib mitigates cigarette smoke induced oxidative stress in mice. *Indian J. Biochem. Biophys.* 47:285-291.

Lecluyse, E.L., M.W. Sinz, N. Hewitt, S.S. Ferguson, and J. Sahi. 2010. Enzyme Inhibition in Drug Discovery and Development: Cytochrome P450 Induction. John Wiley & Sons, Inc. 265-314.

Lederer, E., A. Adam, R. Ciorbaru, J.F. Petit, and J. Wietzerbin. 1975. Cell walls of Mycobacteria and related organisms; chemistry and immunostimulant properties. *Mol Cell Biochem*. 7:87-104.

Lee, R.E., M. Protopopova, E. Crooks, R.A. Slayden, M. Terrot, and C.E. Barry, 3rd. 2003. Combinatorial lead optimization of [1,2]-diamines based on ethambutol as potential antituberculosis preclinical candidates. *J. Comb. Chem*. 5:172-187.

LeMagueres, P., H. Im, J. Ebalunode, U. Strych, M.J. Benedik, J.M. Briggs, H. Kohn, and K.L. Krause. 2005. The 1.9 A crystal structure of alanine racemase from *Mycobacterium tuberculosis* contains a conserved entryway into the active site. *Biochemistry (Mosc).* 44:1471-1481.

Maeda, N., J. Nigou, J.L. Herrmann, M. Jackson, A. Amara, P.H. Lagrange, G. Puzo, B. Gicquel, and O. Neyrolles. 2003. The cell surface receptor DC-SIGN discriminates between Mycobacterium species through selective recognition of the mannose caps on lipoarabinomannan. *J. Biol. Chem*. 278:5513-5516.

Mahapatra, S., D.C. Crick, M.R. McNeil, and P.J. Brennan. 2008. Unique structural features of the peptidoglycan of *Mycobacterium leprae*. *J. Bacteriol*. 190:655-661.

Manjunatha, U., H.I. Boshoff, and C.E. Barry. 2009. The mechanism of action of PA-824: Novel insights from transcriptional profiling. *Commun. Integr. Biol*. 2:215-218.

Matsumoto, M., H. Hashizume, T. Tomishige, M. Kawasaki, H. Tsubouchi, H. Sasaki, Y. Shimokawa, and M. Komatsu. 2006. OPC-67683, a nitro-dihydro-imidazooxazole derivative with promising action against tuberculosis in vitro and in mice. *PLoS medicine*. 3:e466.

McNeil, M., M. Daffe, and P.J. Brennan. 1990. Evidence for the nature of the link between the arabinogalactan and peptidoglycan of mycobacterial cell walls. *J. Biol. Chem*. 265:18200-18206.

Mikusova, K., H. Huang, T. Yagi, M. Holsters, D. Vereecke, W. D'Haeze, M.S. Scherman, P.J. Brennan, M.R. McNeil, and D.C. Crick. 2005. Decaprenylphosphoryl arabinofuranose, the donor of the D-arabinofuranosyl residues of mycobacterial arabinan, is formed via a two-step epimerization of decaprenylphosphoryl ribose. *J. Bacteriol*. 187:8020-8025.

Minnikin, D.E. 1982. Lipids: complex lipids, their chemistry, biosynthesis and roles. *The biology of the mycobacteria*. 1:95-184.

Minnikin, D.E., L. Kremer, L.G. Dover, and G.S. Besra. 2002. The methyl-branched fortifications of *Mycobacterium tuberculosis*. *Chem. Biol.* 9:545-553.

Misaki, A., I. Azuma, and Y. Yamamura. 1977. Structural and immunochemical studies on D-arabino-D-mannans and D-mannans of *Mycobacterium tuberculosis* and other Mycobacterium species. *J. Biochem*. 82:1759-1770.

Nigou, J., C. Zelle-Rieser, M. Gilleron, M. Thurnher, and G. Puzo. 2001. Mannosylated lipoarabinomannans inhibit IL-12 production by human dendritic cells: evidence for a negative signal delivered through the mannose receptor. *J. Immunol.* 166:7477-7485.

Oashi, M. 1970. Studies on the chemical structure of serologically active arabinomannan from mycobacteria. *Jpn. J. Exp. Med.* 40:1-14.

Ortalo-Magne, A., A. Lemassu, M.A. Laneelle, F. Bardou, G. Silve, P. Gounon, G. Marchal, and M. Daffe. 1996. Identification of the surface-exposed lipids on the cell envelopes of *Mycobacterium tuberculosis* and other mycobacterial species. *J. Bacteriol*. 178:456-461.

Pangborn, M.C., and J.A. McKinney. 1966. Purification of serologically active phosphoinositides of *Mycobacterium tuberculosis*. *J. Lipid Res.* 7:627-633.

Pasca, M.R., G. Degiacomi, A.L. Ribeiro, F. Zara, P. De Mori, B. Heym, M. Mirrione, R. Brerra, L. Pagani, L. Pucillo, P. Troupioti, V. Makarov, S.T. Cole, and G. Riccardi. 2010. Clinical isolates of *Mycobacterium tuberculosis* in four European hospitals are uniformly susceptible to benzothiazinones. *Antimicrob. Agents Chemother.* 54:1616-1618.

Roach, T.I., C.H. Barton, D. Chatterjee, and J.M. Blackwell. 1993. Macrophage activation: lipoarabinomannan from avirulent and virulent strains of *Mycobacterium tuberculosis* differentially induces the early genes c-fos, KC, JE, and tumor necrosis factor-alpha. *J. Immunol.* 150:1886-1896.

Salo, W.L., A.C. Aufderheide, J. Buikstra, and T.A. Holcomb. 1994. Identification of *Mycobacterium tuberculosis* DNA in a pre-Columbian Peruvian mummy. *Proc. Natl. Acad. Sci. U. S. A.* 91:2091-2094.

Scherman, M., A. Weston, K. Duncan, A. Whittington, R. Upton, L. Deng, R. Comber, J.D. Friedrich, and M. McNeil. 1995. Biosynthetic origin of mycobacterial cell wall arabinosyl residues. *J. Bacteriol*. 177:7125-7130.

Scherman, M.S., L. Kalbe-Bournonville, D. Bush, Y. Xin, L. Deng, and M. McNeil. 1996. Polyprenylphosphate-pentoses in mycobacteria are synthesized from 5-phosphoribose pyrophosphate. *J. Biol. Chem*. 271:29652-29658.

Schlesinger, L.S. 1996. Role of mononuclear phagocytes in *Mycobacterium tuberculosis* pathogenesis. *J. Investig. Med.* 44:312-323.

Schlesinger, L.S., S.R. Hull, and T.M. Kaufman. 1994. Binding of the terminal mannosyl units of lipoarabinomannan from a virulent strain of *Mycobacterium tuberculosis* to human macrophages. *J. Immunol.* 152:4070-4079.

Seidel, M., L.J. Alderwick, H.L. Birch, H. Sahm, L. Eggeling, and G.S. Besra. 2007. Identification of a novel arabinofuranosyltransferase AftB involved in a terminal step of cell wall arabinan biosynthesis in Corynebacterianeae, such as *Corynebacterium glutamicum* and *Mycobacterium tuberculosis*. *J. Biol. Chem*. 282:14729-14740.

Shi, L., S. Berg, A. Lee, J.S. Spencer, J. Zhang, V. Vissa, M.R. McNeil, K.H. Khoo, and D. Chatterjee. 2006. The carboxy terminus of EmbC from *Mycobacterium smegmatis* mediates chain length extension of the arabinan in lipoarabinomannan. *J. Biol. Chem*. 281:19512-19526.

Shi, L., R. Zhou, Z. Liu, T.L. Lowary, P.H. Seeberger, B.L. Stocker, D.C. Crick, K.H. Khoo, and D. Chatterjee. 2008. Transfer of the first arabinofuranose residue to galactan is essential for *Mycobacterium smegmatis* viability. *J. Bacteriol*. 190:5248-5255.

Sieling, P.A., D. Chatterjee, S.A. Porcelli, T.I. Prigozy, R.J. Mazzaccaro, T. Soriano, B.R. Bloom, M.B. Brenner, M. Kronenberg, P.J. Brennan, and et al. 1995. CD1-restricted T cell recognition of microbial lipoglycan antigens. *Science*. 269:227-230.

Silva, M., and P. Macedo. 1983a. A comparative ultrastructural-study of the membranes of *Mycobacterium leprae* and of cultivable Mycobacteria. *Biol. Cell*. 47:383-386.

Silva, M.T., and P.M. Macedo. 1983b. The interpretation of the ultrastructure of mycobacterial cells in transmission electron microscopy of ultrathin sections. *Int. J. Lepr. Other Mycobact. Dis*. 51:225-234.

Skovierova, H., G. Larrouy-Maumus, J. Zhang, D. Kaur, N. Barilone, J. Kordulakova, M. Gilleron, S. Guadagnini, M. Belanova, M.C. Prevost, B. Gicquel, G. Puzo, D. Chatterjee, P.J. Brennan, J. Nigou, and M. Jackson. 2009. AftD, a novel essential arabinofuranosyltransferase from mycobacteria. *Glycobiology*. 19:1235-1247.

Stewart, G.R., B.D. Robertson, and D.B. Young. 2003. Tuberculosis: a problem with persistence. *Nat. Rev. Microbiol*. 1:97-105.

Stover, C.K., P. Warrener, D.R. VanDevanter, D.R. Sherman, T.M. Arain, M.H. Langhorne, S.W. Anderson, J.A. Towell, Y. Yuan, D.N. McMurray, B.N. Kreiswirth, C.E. Barry, and W.R. Baker. 2000. A small-molecule nitroimidazopyran drug candidate for the treatment of tuberculosis. *Nature*. 405:962-966.

Turnbull, W.B., K.H. Shimizu, D. Chatterjee, S.W. Homans, and A. Treumann. 2004. Identification of the 5-methylthiopentosyl substituent in *Mycobacterium tuberculosis* lipoarabinomannan. *Angew. Chem. Int. Ed. Engl.* 43:3918-3922.

Urban, C., H. Tiruvury, N. Mariano, R. Colon-Urban, and J.J. Rahal. 2011. Polymyxin-resistant clinical isolates of *Escherichia coli*. *Antimicrob. Agents Chemother.* 55:388-389.

Vollmer, W., and J.V. Holtje. 2004. The architecture of the murein (peptidoglycan) in gram-negative bacteria: vertical scaffold or horizontal layer(s)? *J. Bacteriol*. 186:5978-5987.

Walker, L., and D.B. Lowrie. 1981. Killing of *Mycobacterium microti* by immunologically activated macrophages. *Nature*. 293:69-71.

Wang, F., R. Langley, G. Gulten, L.G. Dover, G.S. Besra, W.R. Jacobs, Jr., and J.C. Sacchettini. 2007. Mechanism of thioamide drug action against tuberculosis and leprosy. *J. Exp. Med.* 204:73-78.

WHO. 2010. World Health Organization (WHO) Global tuberculosis control report. www.who.int/tb.

Wietzerbin, J., B.C. Das, J.F. Petit, E. Lederer, M. Leyh-Bouille, and J.M. Ghuysen. 1974. Occurrence of D-alanyl-(D)-meso-diaminopimelic acid and meso-diaminopimelyl-meso-diaminopimelic acid interpeptide linkages in the peptidoglycan of Mycobacteria. *Biochemistry (Mosc).* 13:3471-3476.

Yeager, H., Jr., J. Lacy, L.R. Smith, and C.A. LeMaistre. 1967. Quantitative studies of mycobacterial populations in sputum and saliva. *Am. Rev. Respir. Dis.* 95:998-1004.

Yew, W.W., C. Lange, and C.C. Leung. 2011. Treatment of tuberculosis: update 2010. *Eur. Respir. J.* 37:441-462.

Zhang, N., J.B. Torrelles, M.R. McNeil, V.E. Escuyer, K.H. Khoo, P.J. Brennan, and D. Chatterjee. 2003. The Emb proteins of mycobacteria direct arabinosylation of lipoarabinomannan and arabinogalactan via an N-terminal recognition region and a C-terminal synthetic region. *Mol. Microbiol.* 50:69-76.

Zhang, Y., B. Heym, B. Allen, D. Young, and S. Cole. 1992. The catalase-peroxidase gene and isoniazid resistance of *Mycobacterium tuberculosis*. *Nature*. 358:591-593.

Zuber, B., M. Chami, C. Houssin, J. Dubochet, G. Griffiths, and M. Daffe. 2008. Direct visualization of the outer membrane of mycobacteria and corynebacteria in their native state. *J. Bacteriol*. 190:5672-5680.

Zumla, A. 2011. The white plague returns to London with a vengeance. *Lancet*. 377:10-11.

CHAPTER 2:

DEVELOPMENT OF CELL FREE ARABINOSYLTRANSFERASE ASSAY USING SPECIFIC SYNTHETIC DISACCHARIDE ACCEPTOR

Shiva K. Angala, Jian Zhang, Dean C. Crick, Mike R. McNeil, Peter H. Seeberger and Delphi Chatterjee, "Probing AftB arabinosyltransferase activity and characterization of its enzymatic product using a disaccharide acceptor" (Manuscript in preparation).

2.1 Précis

In this study, *Mycobacterium smegmatis* mc^2155 (WT) was used as a model organism to study the biosynthesis of essential cell wall arabinofuran and putative arabinosyltransferases. A cell-free arabinosyltransferase assay was developed using a specific synthetic arabinose disaccharide acceptor. In a typical experiment, the disaccharide acceptor was incubated with membrane and cell wall fractions isolated from *M. smegmatis*, as an enzyme source in the presence of phospho[^{14}C]ribose pyrophosphate (p[^{14}C]Rpp to DPA *in situ*) as an indirect arabinose donor. Analysis of the enzymatic product after removal of unincorporated p[^{14}C]Rpp using anion exchange chromatography indicated the formation of a neutral radioactive product absent in control

reactions (without an acceptor). This enzymatic reaction is dependent on time and enzyme concentration. The product formation is not sensitive to the action of ethambutol or the absence of the putative arabinosyltransferases encoded by *embA*, *embB* or *embC*. Characterization of the product by MALDI-TOF or HPAEC after endoarabinanase digestion showed that the product formed was a trisaccharide. In addition, GC-MS analysis depicted that the additional arabinose added to the acceptor was 1→2 linked. Thus, we have identified an arabinosyltransferase (AftB) specific transferase activity not related to the EMB proteins that is insensitive to ethambutol treatment and is likely involved in the formation of terminal arabinofuran in *M. smegmatis*.

2.2 Introduction

The mycobacterial cell envelope contains two complex polysaccharides called arabinogalactan (AG) and lipoarabinomannan (LAM). The presence of unique sugars in the cell wall of mycobacteria, in particular D-arabinofuranose, D-galactofuranose and D-rhamnose, and, their absence in the biosynthetic pathways in the mammalian systems has led to an interest in identifying novel targets for anti-TB drug development (Besra et al., 1994).

Decaprenylphosphoryl-arabinose (DPA) is identified as the only source of D-Ara*f* in the biosynthesis of mycobacterial cell wall arabinan (Wolucka et al., 1994) (Figure 2.1). In mycobacteria, DPA is biosynthesized enzymatically from D-glucose to phosphoribosylpyrophosphate (pRpp) (Scherman et al., 1995). Over the past several years, researchers employed the use of prototype synthetic arabinose acceptors to probe the acceptor dependent activity of mycobacterial arabinosyltransferases (Ayers et al.,

1998; Lee et al., 1997; Pathak et al., 1998; Zhang et al., 2007). This study is focused on the development of a cell free arabinosyltransferase assay and the characterization of its enzymatic product. A synthetic arabinose disaccharide acceptor molecule was used to mimic the native structural domain of mycobacterial arabinan (Figure 2.1). The pentenyl group present on the acceptor molecule renders the product non-polar and helps in the distribution in organic solvents. In this study, radioactive p[^{14}C]Rpp was used as an indirect arabinose donor in the cell free arabinosyltransferase assays. The Figure 2.2 represents cell free arabinosyltransferase assay using disaccharide arabinose acceptor.

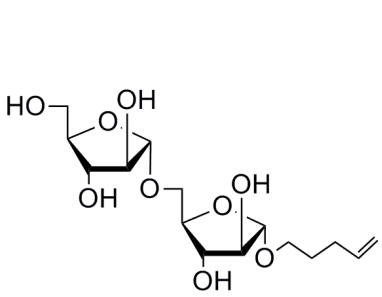

Synthetic disaccharide acceptor
α-D-Ara*f*-(1-5)-α-D-Ara*f*-C_5H_9

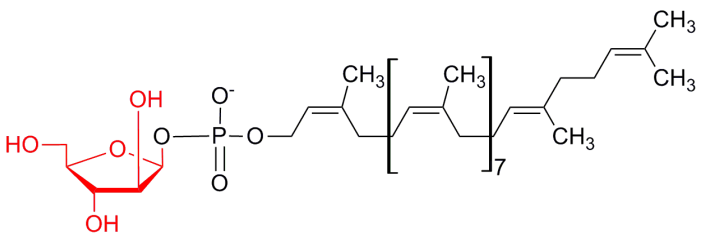

Decaprenylphophoryl-arabinose
DP[^{14}C]A (donor)

Figure 2.1 Structures of acceptor and donor substrates

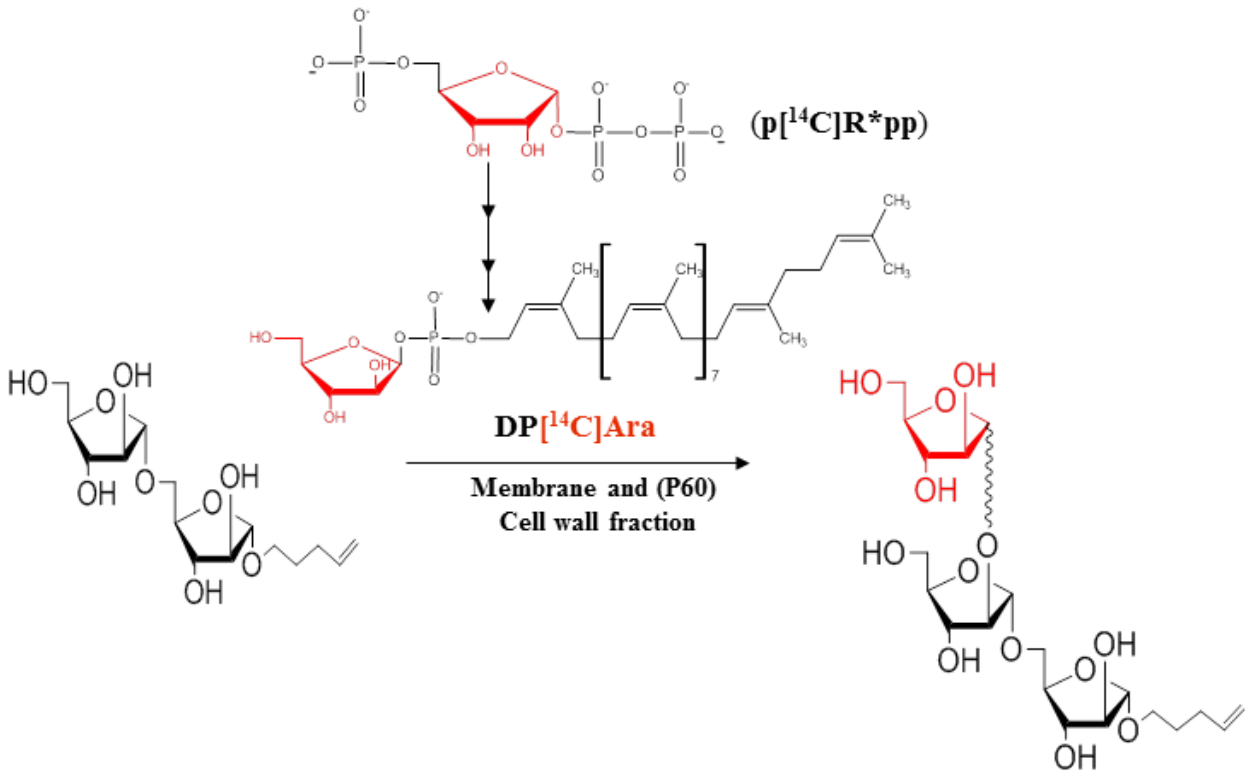

Figure 2.2 Schematic representation of cell free arabinosyltransferase assay using synthetic disaccharide arabinose acceptor, DPA and membranes.

2.3 Materials and Methods

The p[^{14}C]Rpp (300 mCi/mmol) was prepared from uniformly labeled D-[^{14}C]glucose (American Radiolabeled Chemicals). Most of the chemicals and detergents used in this study including MOPS, 2-mercaptoethanol, and ethambutol were purchased from Sigma-Aldrich and were used without further purification. Non-radiolabeled pRpp from Sigma was further purified by HPAEC and the fractions containing pRpp were detected by phenol-H_2SO_4, pooled, and stored at −20°C for further use. ATP (Calbiochem), percoll (sterile) was purchased from Pharmacia. Protein concentrations were determined using the BCA assay (Pierce Biotechnology, Rockford, IL). Thin-layer chromatography (TLC) was performed on silica gel G 60 (EM Science) aluminum-backed plates.

2.3.1 Bacterial strains and growth condition

M. smegmatis mc^{2}155 was obtained from American Type Culture Collection ATCC (Snapper et al., 1990). Individual knockout mutants of *M. smegmatis,* Δ*embA, ΔembB* and Δ*embC,* were constructed in our laboratory (Escuyer et al., 2001). The liquid cultures were grown to mid log phase O.D. 600 nm (0.7–0.8) at 37°C in Luria Bertani (LB) broth medium (Difco) harvested, washed with phosphate buffered saline (PBS), and stored at −80°C until further use.

2.3.2 Preparation of membrane and cell wall enzyme fractions

M. smegmatis cells (10 g wet weight) were washed and resuspended in 30 ml of buffer A (50 mM MOPS pH 8.0 with KOH, 5 mM β-mercaptoethanol and 10 mM $MgCl_2$) and subjected to probe sonication on ice for a total time of 10 min in 60 seconds pulses with

90 seconds cooling intervals between pulses. The cell lysate was then centrifuged at 27,000 × g for 60 min at 4°C. The cell wall pellet was removed and the supernatant was centrifuged at 100,000 × g for an additional 2 hr at 4°C. The supernatant was discarded and the pellet of enzymatically active membranes was gently resuspended in 500 µl of buffer A with homogenization to yield a protein concentration of nearly 15 - 20 mg/ml. The 27,000 × g pellet was resuspended in 10 ml of buffer A and Percoll to achieve a 60% suspension. The suspension was mixed and centrifuged at 27,000 × g for 60 min at 4°C. The resulting flocculent, white layer was collected and washed three times with buffer A at and centrifuged 27,000 × g for 30 min to yield a cell wall-enriched fraction (P60). This fraction was resuspended in 1ml of buffer A to yield a protein concentration of 5–6 mg/ml. Protein concentrations were determined using a BCA protein estimation kit from Pierce biotech.

2.3.3 Preparation of phospho[^{14}C]ribosylpyrophosphate (p[^{14}C]Rpp)

Radioactive p[C^{14}]Rpp was generated from uniformly labeled D-[^{14}C]glucose (American Radiochemicals Inc.) following the established procedures (Scherman et al., 1996). Briefly, 100 µCi (310 mCi/mmol) of D-[^{14}C]glucose was dried vacuum concentrator and suspended in 100 µl of 50 mM HEPES buffer (pH 7.6) containing 2 mM $MgCl_2$ and 0.5 mM $MnCl_2$.The enzymatic reaction was initiated with addition of 10 units of Hexokinase, 1 µM ATP and 4 µM of β–NADP and incubated at room temperature for 2 min. phosphatase inhibitors are added before adding ATP and hexokinase. Then, sequentially 10 units of glucose-6-phosphate dehydrogenase, 2 units of 6-phosphogluconate dehydrogenase, 10 units of phosphoriboisomerase, and a unit of phosphoribosyl

pyrophosphate synthetase were added along with additional 0.4 µM ATP. The reaction mixture was incubated at 37°C for another 1 hr. The entire sample was injected into a Dionex Carbopak PA1 column (9 X 250cm) and eluted at a flow rate of 1 ml/min with a linear gradient of 0.05-1 M Sodium acetate in water using a 30 min program run. 20 µl of each fraction were taken for scintillation counting. The p[C^{14}]Rpp containing fractions were pooled and frozen in aliquots of 500000 dpm. Since sodium acetate does not affect the arabinosyltransferase activity from our earlier results p[C^{14}]Rpp is used without removing salts.

2.3.4 Radioactive arabinosyltransferase assay using disaccharide arabinose acceptor.

All the transferase assay reactions in this Chapter were performed using radioactive p[^{14}C]Rpp unless otherwise specified. A typical cell free arabinosyltransferase assay reaction mixture contained 50 mM MOPS (pH 8.0), 4 mM 2-mercaptoethanol, 8.5 mM $MgCl_2$, 1 mM ATP, 3.8 µM p[^{14}C]Rpp (500,000 dpm), 300 µM of the disaccharide acceptor, membranes, and P60 fractions in a total volume of 200 µl. The reaction mixture was incubated at 37°C for 2 hr and, then terminated by adding 200 µl of ethanol. The resulting mixture was centrifuged at 14,000 × g, for 5 min and the supernatant was loaded onto a pre-packed strong anion exchange (SAX) column (Burdick and Jackson) pre-equilibrated with 2 ml of water. The column was eluted sequentially with 2 ml each of 50% ethanol. The eluent was evaporated to dryness and partitioned between the two phases (1:1) of water-saturated 1-butanol and water. The 1-butanol fractions were collected and measured for radioactive incorporation by liquid scintillation spectrometry.

Values reported are averages of duplicate reactions from representative experiments. Figure 2.3 depicts the experimental procedure of a cell free arabinosyltransferase assay.

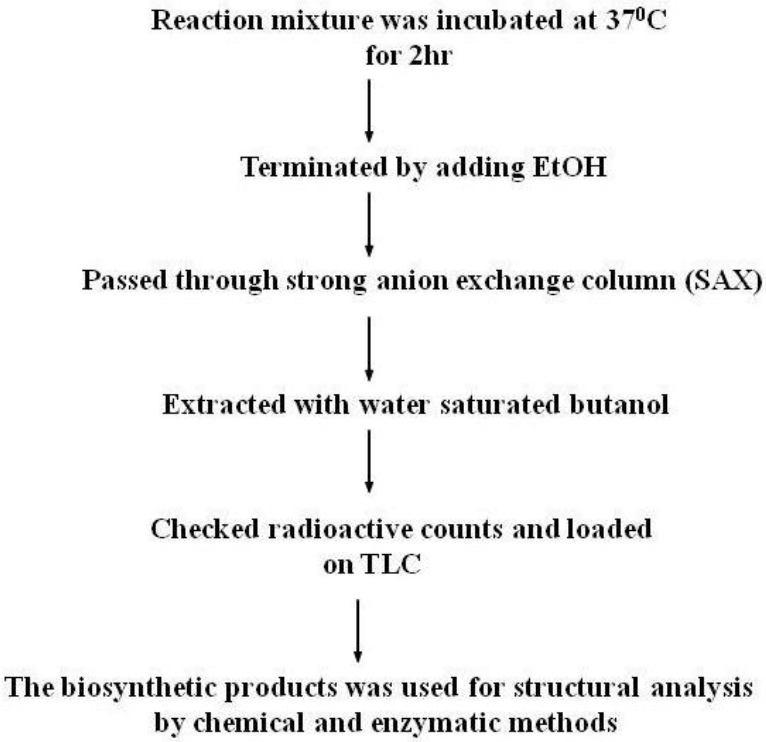

Figure 2.3 Illustration of an experimental procedure of cell free arabinosyltransferase assay.

2.3.5 Analytical procedures

2.3.5.1 TLC analysis of the enzymatic product

Equal volume of 1-butanol extract of the enzymatically synthesized radiolabeled product was used on silica gel TLC for further analysis. The plates were developed in the solvent system containing $CHCl_3$:MeOH:NH_4OH:H_2O (65:25:0.4:3.6) followed by autoradiography at −70°C using Biomax MR1 film (Kodak). A synthetic disaccharide

acceptor was visualized on TLC by spraying with α-napthol/sulphuric acid reagent (Jacin and Mishkin, 1965).

2.3.5.2 Monosaccharide composition analysis of the enzymatic product

Approximately 4000 dpm of the 1-butanol-soluble material were dried under nitrogen and hydrolyzed in 200 µl of 2M trifluoroacetic acid (TFA) at 120°C for 2 hr. The TFA was removed from a stream of air, and the hydrolysate was analyzed on a silica gel TLC plate developed in pyridine:ethyl acetate:acetic acid:water (5:5:1:3) followed by autoradiography. Radioactive spots corresponding to radioactivity were identified by co-chromatography with standard radiolabeled arabinogalactan, which were visualized by autoradiography.

2.3.5.3 Digestion with endoarabinanase and HPAEC analysis

The arabinosyltransferase assay radiolabeled enzymatic product was digestied with endoarabinanase isolated from *Cellulomonas gelida* (McNeil et al., 1994). In this case, approximately 10,000 dpm of the 1-butanol-soluble material were dried under nitrogen, reconstituted in 10 µl of water, sonicated, and treated with endoarabinanase for 16 hr at 37°C as previously described (McNeil et al., 1994). Aliquots from the digested mixture were subjected to Dionex high pH anion exchange chromatography (HPAEC) analysis.

2.3.5.4 Non-radioactive arabinosyltransferase assay for MALDI-TOF analysis

A set of 10 identical transferase assay reactions were set up to generate enough enzymatic products for MALDI-TOF anlaysis. In this case, we used non-radiolabeled pRpp (Sigma)

which was further purified by Dionex HPAEC. The typical non-radiolabeled assay contains 62.5 µM ATP reaction mixture contained 300 µM acceptor, 0.5 mM non-radiolabeled pRpp, membranes (0.6 mg), P-60 (0.3 mg) in buffer A (pH 7.9) in a total volume of 200 µl. The workup procedures were similarly done as described in section 2.3.4. The 1-butanol eluted product migrated on preparative TLC, co-chromatography with radioactive product to aid in further extraction of the non-radiolabeled product. The TLC extracted product was further subjected *to per-O*-methylation using the sodium hydroxide slurry method (Dell et al., 1994) and to MALDI-TOF analysis. Methylated sample was combined with 1 µl of 2, 5-dihydroxy benzoic acid (DHB, 10 mg/ml in 50 % acetonitrile, 0.1 % trifluoroacetic acid). The mixture was spotted on the MALDI target and allowed to air dry. The sample was analyzed by an Ultraflex-TOF/TOF mass spectrometer (Bruker Daltonics, Billerica, MA) in positive ion reflector mode using a 25 kV accelerating voltage. External calibrations were done using a peptide calibration mixture (4 to 6 peptides) on a spot adjacent to the sample. The data was processed using the FlexAnalysis software (version 2.4, Bruker Daltonics).

2.3.5.5 Glycosyl linkage analysis of the enzymatic product by alditol-acetates

In order to prove the position where additional arabinose was added onto the disaccharide acceptor, linkage analysis GC/MS was performed on the enzymatic product. In this case, the *per-O*-methylated samples were further hydrolyzed using 2 M trifluoroacetic acid, reduced with sodiumborohydride, *per-O*-acetylated, and analyzed by GC/MS as described (Daffe et al., 1990).

2.3.6 Arabinosyltransferase assay with Δ*embA*, *ΔembB* and Δ*embC* knockout mutants of *M. smegmatis*.

Crude membrane fractions are also a source of Emb arabinosyltransferases. To rule out the involvement of Emb proteins in the AftB product formation, individual knockout strains of *M. smegmatis* Δ*embA*, *ΔembB* and Δ*embC* were grown and harvested as described in section 2.3.1. Membrane and cell wall P-60 fractions were prepared as described in section 2.3.2 and the protein concentration was estimated using BCA protein estimation kit. A cell free arabinosyltransferase assay was performed with membrane (0.5 mg) and P-60 (0.3mg) fractions prepared from *M. smegmatis* Δ*embA*, *ΔembB* and Δ*embC* individual knockout mutants and *M. smegmatis* WT strain in buffer A containing 1 mM ATP, 3.8 μM p[^{14}C]Rpp (500,000 dpm), 300 μM of the disaccharide acceptor in a total volume of 200 μl. The reactions were incubated at 37°C for 2 hr and, then the reaction was terminated by adding 200 μl of ethanol. Extraction of the radiolabeled product was performed as described in section 2.3.4 and a TLC subjected to autoradiography was conducted as well.

2.3.7 Effect of ethambutol on arabinosyltransferase assay.

In order to see the effect of EMB on the transferase activity in a cell free arabinosyltransferase assay using disaccharide as an acceptor, *M. smegmatis* membrane and P-60 fractions were prepared and suspended in buffer A as described in section 2.3.2. A typical cell free arabinosyltransferase assay was carried out as described in section 2.3.4 with slight modifications. The membrane and P-60 fractions were pre-incubated for

30 min at 37°C with varying concentrations of ethambutol (6.25–50 µg/ml). After a 30 min of incubation, the reaction mixture was supplemented with buffer A containing 1 mM ATP, 3.8 µM p[^{14}C]Rpp (500,000 dpm), 300 µM of the disaccharide acceptor in a total volume of 200 µl. Extraction of the enzymatic product followed by TLC analysis was done as described in section 2.3.4.

2.3.8 Optimizing reaction parameters

2.3.8.1 Protein-dependent experiment

The experiment was performed to understand the optimal protein concentration required in the assay system. This experiment used the same basic assay as described in 2.3.4, but consisted of six different substrate concentrations (0.1-1 mg), while maintaining a constant ratio between the membranes (0.5 mg/ml) and the cell wall P-60 (0.3 mg/ml) that was used in the earlier assay systems in a final volume of 200 µl reaction. All other reaction conditions were identical. Extraction and analysis of the enzymatic products was carried as described in section 2.3.4.

2. 3.8.2 Time dependent experiment

To determine the optimal incubation time for better enzymatic activity, the enzymatic reactions were terminated at different time points 15, 30, 60, 120, 240 and 720 mins. Extraction and analysis of the enzymatic products were conducted similarly to the procedure described in earlier section 2.3.4.

2. 3.8.3 Substrate dependent

Cell free arabinosyltransferase assays were performed with varying concentrations of acceptor substrate (0.1-1 mM) while maintaining all other reaction conditions. Extraction and analysis of the enzymatic products were carried as described in earlier section 2.3.4.

2. 3.8.4 Buffers and pH

To determine the optimum pH for the arabinosyltransferase assay, 3 different buffers with pH ranging from 5.5 to 11.5 were applied and the appropriate counter ions were used to each buffer for pH increments of 1unit. 50 mM 2-(*N*-morpholino)ethanesulfonic acid (MES) was used for a pH of 5.5 to 6.5. Buffer A, containing 50 mM morpholinepropanesulfonic acid (MOPS), is used for a pH of 6-10. The third buffer, 50 mM *N*-cyclohexyl-3-aminopropanesulfonic acid (CAPS), was applied for a pH ranging from 10.5 to 11.5. The reaction mixture contained 5 mM β-mercaptoethanol, 10 mM $MgCl_2$, 1 mM ATP, 3.8 μM p[^{14}C]Rpp (500,000 dpm), 300 μM of the disaccharide acceptor in a total volume of 200 μl. Extraction and analysis of the enzymatic products were conducted in a similar fashion as described in earlier section 2.3.4.

2. 3.8.5 Divalent cations

Divalent cations are important for the catalytic activity of glycosyltransferases (Lairson et al., 2008). Endogenous divalent cations were removed from the crude membrane and P-60 fractions using DOWEX 50WX2-200 strong cation exchange resin. Then, varying concentrations of $MgCl_2$ (0.6-10 mM) were used in the *in vitro* assay conditions.

Extraction and analysis of the enzymatic products were carried as described in earlier section 2.3.4.

2.3.8.6 Effect of DTT, *N*-ethylmaleimide and iodoacetamide on AftB arabinosyltransferase activity

N-Ethylmaleimide and iodoacetamide alkylating SH reagents were used in the cell free arabinosyltransferase assay enzymatic reaction mixtures. These reagents covalently modify nucleophilic thiol residues of the active-sites and destroy the catalytic activity of the enzymes. Dithiothreitol (DTT), on the other hand, maintains SH groups in the reduced state for the activity of most enzymes in *in vitro* reactions. Based on these assumptions we tested the effect of these reagents on the arabinosyltransferase activity. A cell free arabinosyltransferase assay was carried out with varying concentration of DTT (0.625-10 mM) and the typical reaction contains buffer A, 1 mM ATP, 3.8 μM p[^{14}C]Rpp (500,000 dpm), 300 μM of the disaccharide acceptor in a total volume of 200 μl. *N*-ethylmaleimide and iodoacetamide were tested at 10 mM concentration while keeping all other reaction conditions same. Extraction and analysis of the enzymatic products were carried as described in sections 2.3.4.

2. 3.8.7 Screening detergents for the arabinosyltransferase activity

Solubilizing the membrane proteins is critical for their activity. We screened a number of non-ionic and ionic detergents to improve the transferase activity in crude membranes. The non-ionic detergents used were Tween-20, Tween-80, Brij-35, Brij-58, and Octyl-β-D-thioglucopyranoside while the ionic detergents include cholic and deoxycholic acids.

All the detergents were tested at one specific concentration of 0.1% in the assay buffer A, containing 1mM ATP, 3.8 μM p[^{14}C]Rpp (500,000 dpm), 300 μM of the disaccharide acceptor in a total volume of 200 μl. Extraction and analysis of the enzymatic products were carried as in section 2.3.4.

2.4 Results and Discussion

2.4.1 Development of a cell free arabinosyltransferase assay and characterization of the enzymatic product.

We developed a suitable and specific cell-free arabinosyltransferase assay using a linkage specific synthetic disaccharide acceptor. The reaction mixture contains a disaccharide acceptor along with the membrane and cell wall fraction isolated from *M. smegmatis* as an enzyme source in the presence of phospho[^{14}C]ribose pyrophosphate (pRpp); a precursor of the ultimate arabinose donor. Analysis of the enzymatic product after removal of the reactants using anion exchange chromatography indicated the formation of a radioactive product that is absent in the control reactions (without acceptor) shown in Figure 2.4. The migration of the enzymatically synthesized product was slower than the disaccharide indicating that radiolabeled arabinose was transferred from the donor (DP[^{14}C]Ara) to the disaccharide acceptor. Monosaccharide analysis of the radiolabeled product after trifluoroacetic acid hydrolysis indicated the presence of radioactive arabinose as shown in Figure 2.5.

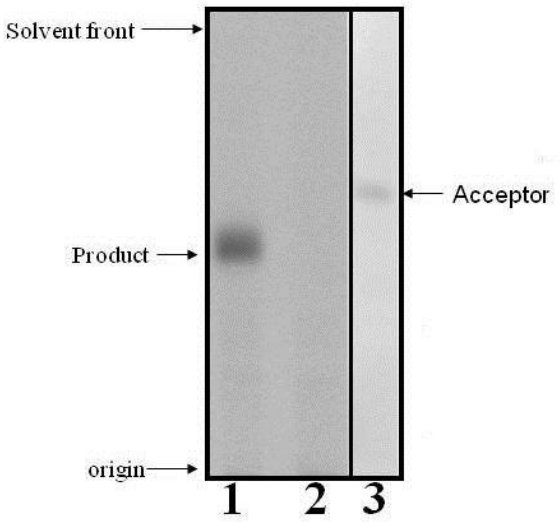

Figure 2.4 TLC analysis of the enzymatic product. Lane 1. Radioactive arabinosyltransferase assay reaction in presence of the arabinose disaccharide acceptor; lane 2. Radioactive arabinosyltransferase assay in absence of the arabinose disaccharide acceptor; lane 3. Arabinose disaccharide acceptor developed on TLC by sparying with α-napthol/sulphuric acid. Solvent system: $CHCl_3$:MeOH:NH_4OH:H_20 (65:25:0.4:6:3.6).

Monosaccharide analysis of the radiolabeled product after TFA hydrolysis

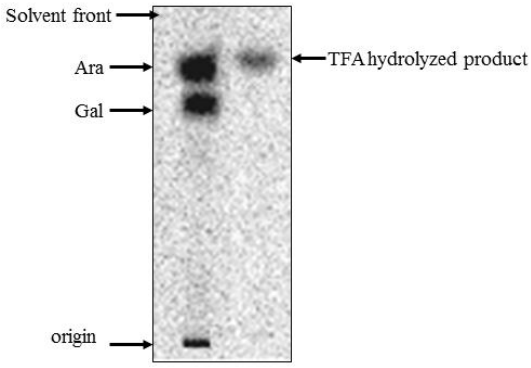

Figure 2.5 TFA hydrolysis breaks the glycosidic bonds in radioactive product. The results demonstrate the presence of only radiolabeled arabinose. Solvent system: pyridine: ethylacetate:acetic acid: water (5:5:1:3).

2.4.2 HPAEC, MALDI-TOF and GC/MS analysis of the arabinosyltransferase enzymatic product

HPAEC analysis of the enzymatic product after digestion with an endoarabinanase prepared from *Cellulomonas species* shows the intact peak at 17.5 min is shown in Figure 2.6. This peak is consistent with the retention time of the synthesized Ara_3.

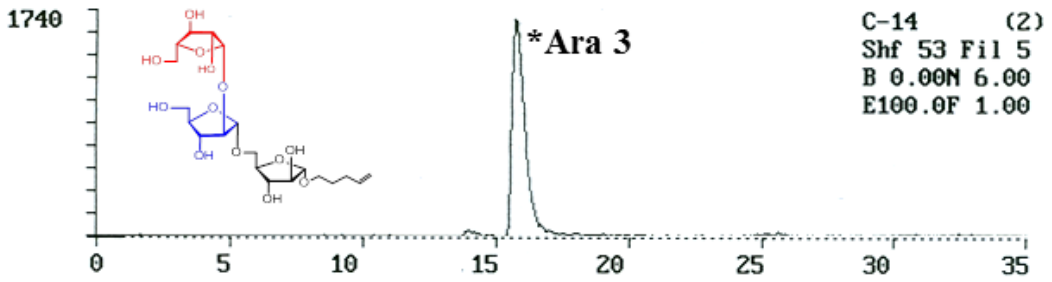

Figure 2.6 HPAEC profile of the endoarabinanase digested radioactive enzymatic. The presence of single prominent radioactive peak at 17.5 min, clearly demonstrates that enzymatic product formed is not intact and is not digested by endoarabinanase.

The mass spectrometry analysis of the *per*-*O*-methylated enzymatic product showed an additional arabinose transferred onto the synthetic disaccharide acceptor (Figure 2.7). The actual molecular mass for trisaccharide (Ara_3) enzymatic product with pentenyl aglycon corresponds to *m/z* 603 [$M+Na^+$], but the experimental mass for enzymatic product that is comigrating with radioactive product had *m/z* 605 [$M+Na^+$]. It is speculated that the reason for the increase in the two mass units in the enzymatic product may be due to the saturation of the pentenyl double bond present on the aglycon of the disaccharide acceptor during enzymatic conversion.

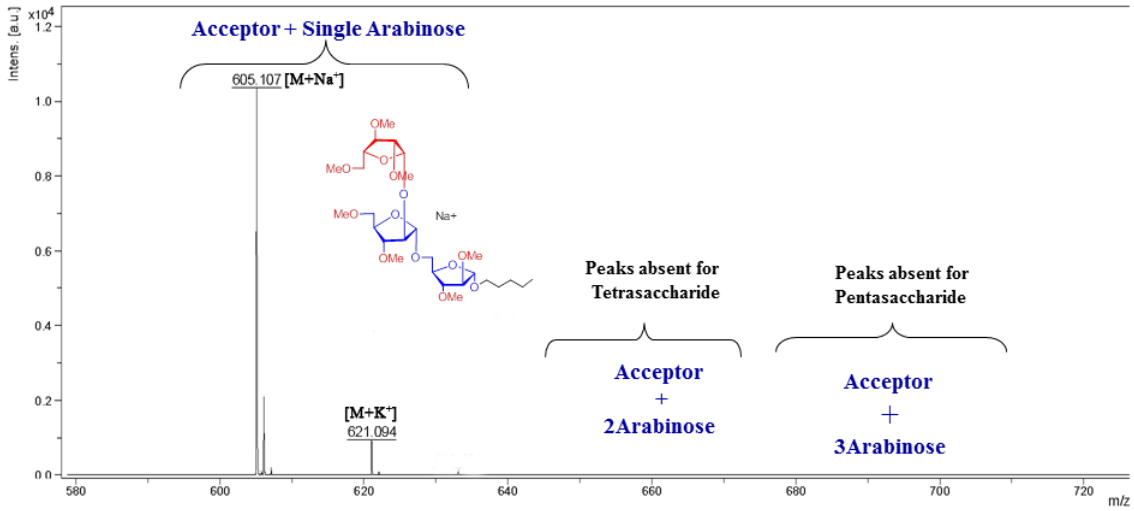

Figure 2.7 MALDI-TOF analysis of the non-radiolabeled enzymatic product. The presence of molecular ion corresponding to enzymatic product (*m/z* 605, 621) as sodium and potassium adducts indicates transfer of single arabinose moiety on to the acceptor molecule. No additional *m/z* was observed for acceptor with two or three arabinoses incorporated.

Linkage analysis was performed on the alditol acetate derivative of the enzymatic product after *per*-*O*-methylation, TFA hydrolysis, $NaBD_4$ reduction and *per*-acetylation. The formation of the molecular ion *m/z* 129 and *m/z* 130, with the loss of molecular ions of *m/z* 32(methanol), and 60 (aceticacid) revealed that the additional arabinose added to the acceptor was 1→2 linked as shown in Figure 2.8.

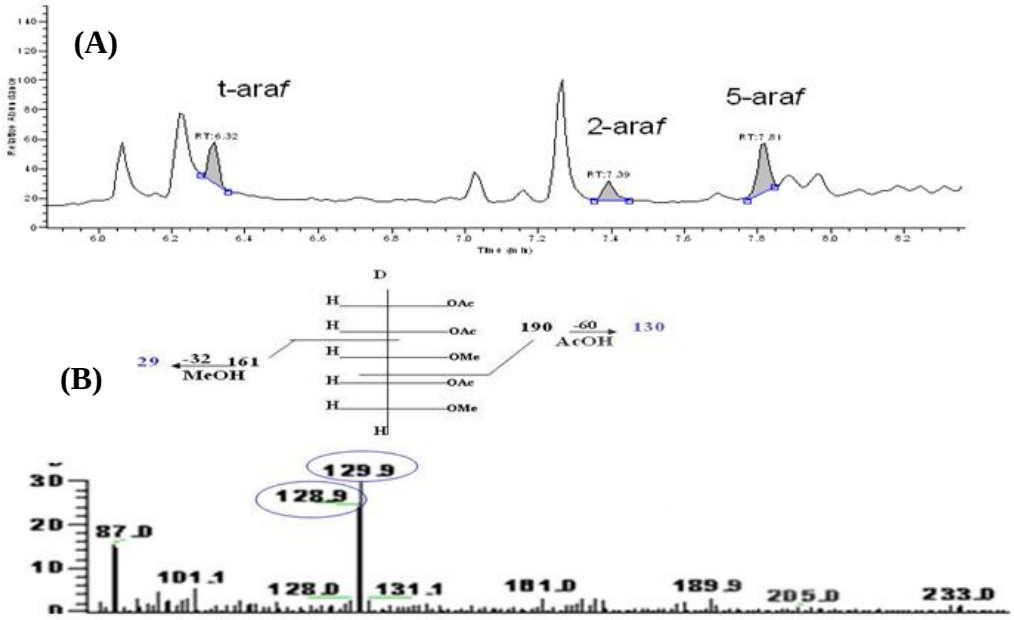

Figure 2.8 Linkage analysis of alditol acetate derivatives of the enzymatic product after per-O-methylation. **A)** Total ion chromatographs displaying the presence of terminal arabinose (t-Ara), 2-linked Ara and 5-linked Ara residues. **B)** Mass spectra showing fragmentation pattern for 2-linked arabinose residue. The diagnostic molecular ions with *m/z* values 129 and 130, with loss of MeOH, and HOAc indicates that the arabinose added on to the acceptor is 2-linked.

2.4.3 Involvement of Emb proteins and ethambutol in the product formation

Ethambutol (EMB), a front-line anti-TB drug is known to inhibit arabinosyltransferase activity in AG biosynthesis (Belanger et al., 1996). We assessed the capacity of the WT membrane to catalyze arabinosyltransferase activity in the presence of varying concentrations of ethambutol (6.25-50 µg/ml). TLC analysis of the 1-butanol fraction showed the formation of radioactive product with all the concentrations (Figure 2.9). TLC analysis of the butanol extractions from the arabinosyltransferase assay with the *M. smegmatis* Δ*embA, ΔembB* and Δ*embC* individual knockout mutants showed the formation of the radioactive product with all the strains as shown in Figure 2.10.

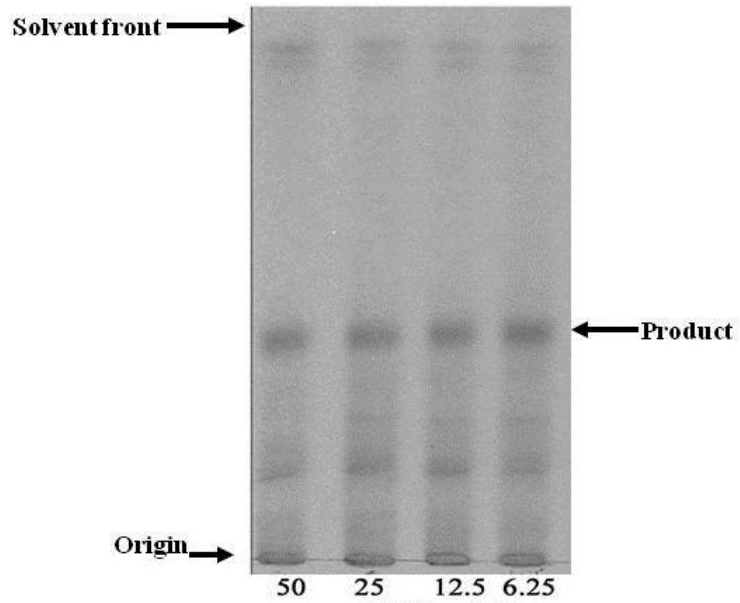

Figure 2.9 Effect of ethambutol on arabinosyltransferase activity. Transfer of radiolabeled arabinose from donor on to the synthetic disaccharide acceptor is not inhibited in the presence of varying concentrations of ethambutol (6.25-50 µg/ml).

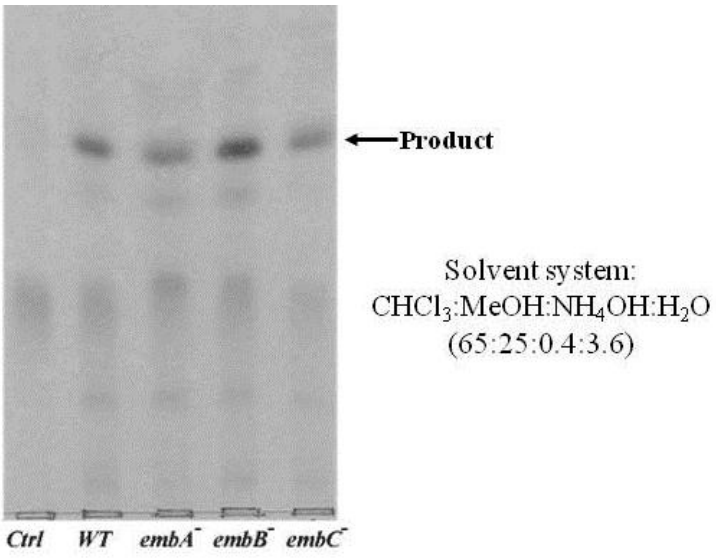

Figure 2.10 Cell free enzymatic assays with *M. smegmatis ΔembA, ΔembB* and *ΔembC* knockout strains. The formation of the radioactive product with individual knock out mutants indicated that this acceptor is not specific to the transferase activity of *emb* genes.

2.5 Optimization of reaction conditions

2.5.1 Protein and time dependency

The TLC profile of the enzymatic products (lanes 1-6) as shown in Figure 2.11(a) with increasing amounts of protein (membrane and P-60) showed linear increment in the incorporation of radioactive arabinose onto the disaccharide acceptor. Lane 7 served as the negative control without an acceptor in which there was no enzymatic product formed. The areas corresponding to the intensities of the radioactive product from the phosphoimager scanner was used to calculate the amount of enzymatic product in pmoles as shown in Figure 2.11(b).

Similar results were obtained from the time dependent experiment. There was a linear increase with the amount of enzymatic product with time (Figure 2.12 (a) & (b)).

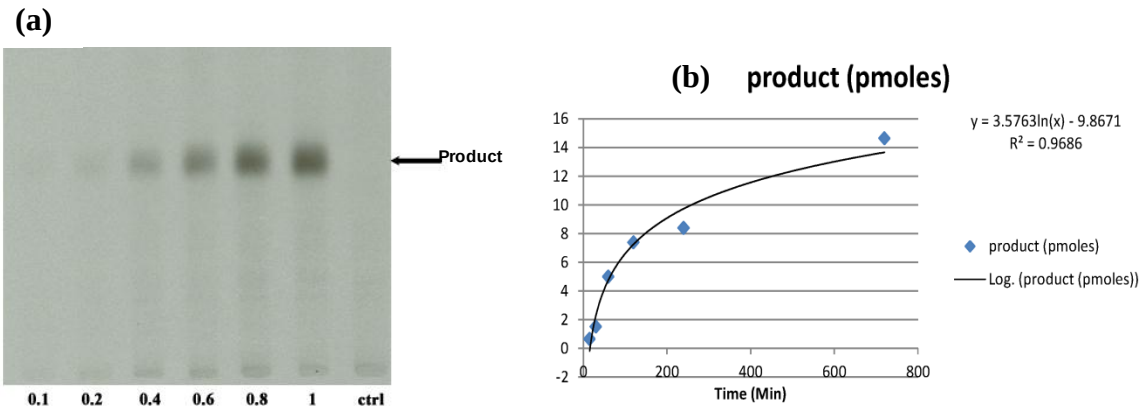

Figure 2.11 Protein Dependency
(a) TLC profile showed that formation of enzymatic product increases with increasing the concentration of protein (0.1-1 mg/ml). Control (Ctrl) lane showed no enzymatic product formation in the absence of the acceptor. (b) Graph showed radioactive enzymatic product in pmoles.

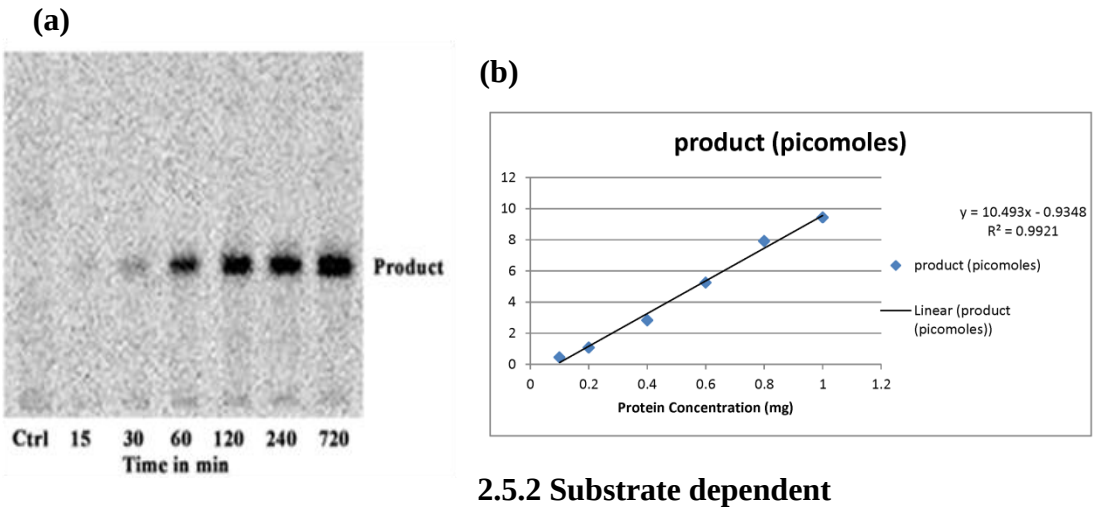

2.5.2 Substrate dependent

Figure 2.12 Time dependency
(a) TLC profile showed that formation of enzymatic product increases with increasing incubation period (15-720 min) of the cell free arabinosyltransferase assay. Control (Ctrl) lane showed no enzymatic product formation in the absence of the acceptor. (b) Graph showed the formation of enzymatic product in pmoles.

2.5.2 Substrate dependency

A linear increase in the amount of enzymatic product formed with an increasing concentration of disaccharide substrate was observed from the TLC analysis (Figure 2.13 (a)). Scintillation counting of the 1-butanol extracts also showed an increase in the total number of counts corresponding to the enzymatic product was increasing. The reaction, therefore, was not saturating with an increase in the substrate concentration (Figure 2.13 (b)).

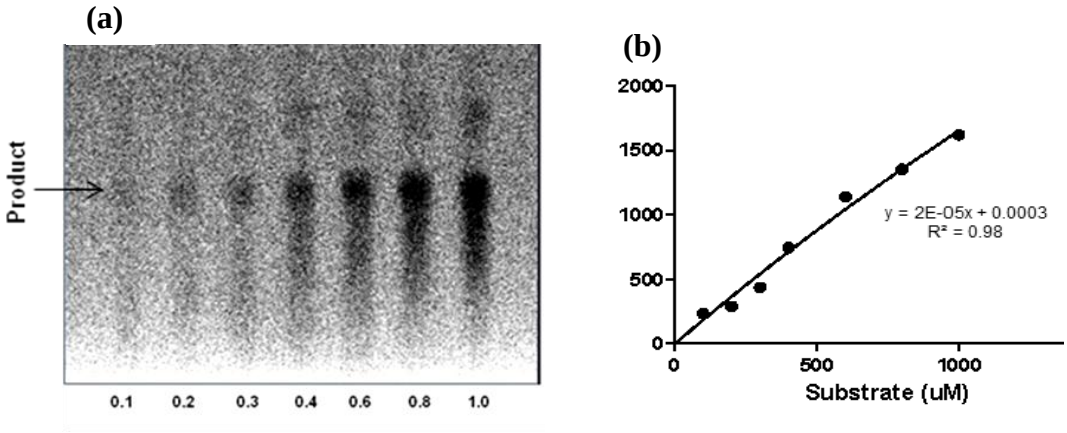

Figure 2.13 Substrate dependency
(a) TLC profile showed that formation of enzymatic product increases with increasing concentration of acceptor substrate (0.1-1 mM). (b) Total number of counts present in the enzymatic product showed linear relative proportion with substrate.

2.5.3 Buffers and pH

To determine the optimum pH for arabinosyltransferase activity, 3 different buffers with a range of pH between 6.5 - 11.5 were employed in the arabinosyltransferase assay reactions. From the TLC analysis, (Figure 2.14 (a)) Lane 1 corresponds to the negative control reaction in the absence of an acceptor substrate, and product was not formed as

expected. Lane 2 was a positive control reaction with MOPS buffer pH-7.9. It showed a strong band of the radioactive product. Lanes (3-5) correspond to the MOPS buffer ranging from a pH 6-10. It was observed that the amount of enzymatic product formed increased with the rise of one unit in MOPS until a pH of 9. At pH of 10, which is out of the buffering range of MOPS buffer, little product was formed. The total number of radioactive counts corresponding to the enzymatic product formed under different buffering conditions is shown in the Figure 2.14. The TLC profile of the CAPS buffer showed that it killed the arabinosyltransferase assay reaction with a pH of 9.5-11.5 (lanes 10-12). These results, it indicated that the MOPS buffer at a pH of 8 shows optimal transferase activity.

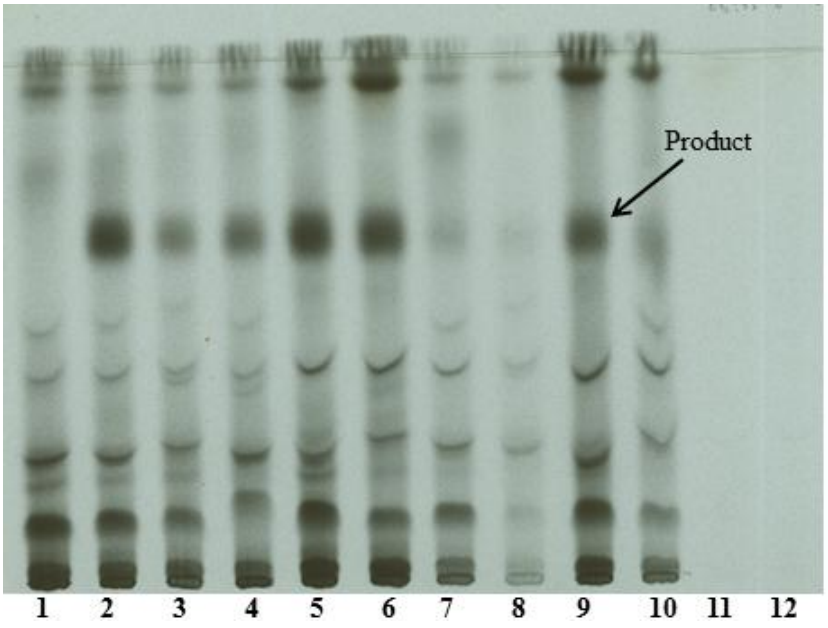

Figure 2.14 Effect of buffers on AftB arabinosyltransferase activity. Lane 1. Control without acceptor; lane 2. Positive control reaction; lane 3-7 MOPS buffer (pH 6-10); lane 8 and 9. MES buffer (pH 6.5 and 7.5); lanes 10-12 CAPS buffer (pH 9.5-11.5).

2.5.4 Effect of divalent Mg^{2+} ion concentration on arabinosyltransferase activity

The transferase assay reactions are absolutely dependent on the addition of Mg^{2+} ions as seen from the TLC profile where the addition of 10 mM EDTA put an end to the formation of the enzymatic product (Figure 2.15). In an another set of experiments, endogenous Mg^{2+} ions were removed from the crude membrane and cell wall P-60 preparations by using cation exchange resin DOWEX 50WX2-200 and replenished with titrating concentrations of $MgCl_2$ (0.6-10 mM). The TLC profile shows that the enzymatic product formed remains the same even with lowering concentration of $MgCl_2$.

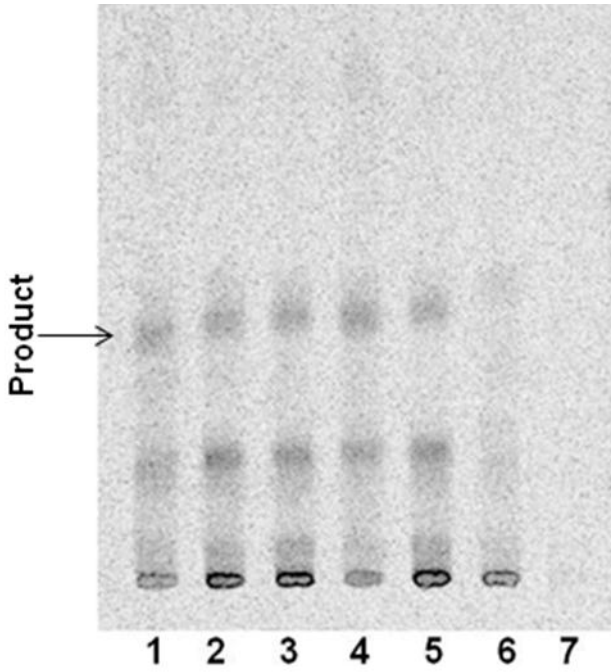

Figure 2.15 Effect of divalent cation and EDTA on arabinosyltransferase activity. Lane 1. 10 mM $MgCl_2$; Lane 2. 5 mM $MgCl_2$; Lane 3. 2.5 mM $MgCl_2$; Lane 4. 1.25 mM $MgCl_2$; Lane 5. 0.625 mM $MgCl_2$; Lane 6. Control without acceptor; Lane 7. 10 mM EDTA. The results demonstrated the formation of the enzymatic product with varying concentrations of $MgCl_2$ and its inhibition in the presence of 10 mM EDTA.

2.5.5 Reducing and alkyating agents:

Treatment of the arabinosyltransferase assay reaction mixtures with varying concentrations of dithiothreitol (DTT) (0.6-10 mM) showed the formation of a radioactive product, but in very low quantity (lanes 2-6 in Figure 2.16). Intensity of the radioactive band corresponding to the enzymatic product was consistent without any improvement. The TLC profile also demonstrated that the presence of reducing agents in the arabinosyltransferase assay aids in the formation of several non-specific bands that migrate much higher than the actual enzymatic product. Alkylating agents *N*-ethylmaleimide and iodoacetamide (lane 7 and 8) seem to inhibit the transferase activity at 10 mM concentration.

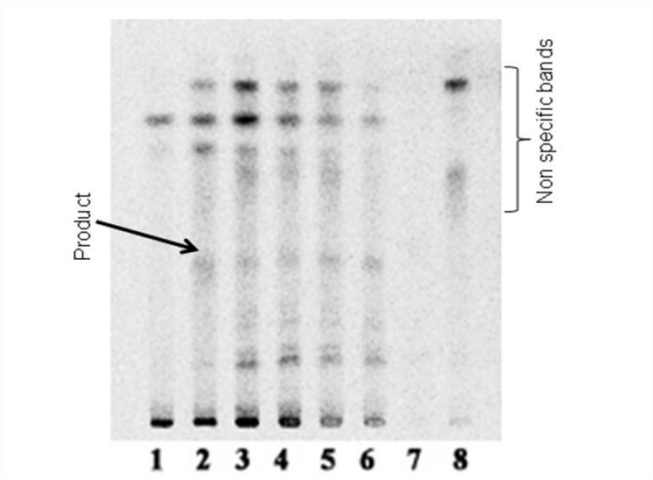

Figure 2.16 Effect of Reducing and Alkylating agents on arabinosyltransferase activity. Lane 1. Control without acceptor; Lane 2. 10 mM DTT; Lane 3. 5 mM DTT; Lane 4. 2.5 mM DTT; Lane 5. 1.25 mM DTT; Lane 6. 0.625 mM DTT; Lane 7. 10 mM *N*-ethylmaleimide (NEM); Lane 8. 10 mM iodoacetamide (IAA). TLC profile showed the formation of the enzymatic product in the presence of reducing agents.

2.5.6 Detergents:

The TLC profile of the arabinosyltransferase assays in the presence of 0.1% non-ionic detergents such as Tween-20 and Tween-80, showed the formation of the enzymatic product similar to that of WT positive control reaction (without detergent) revealing that these non-ionic detergents did not affect the arabinosyltransferase activity as shown in lane 1 Figure 2.17. Brij-35 and Brij-58 (lanes 4 & 5) completely abolished the formation of the enzymatic product. The non-ionic detergent Octyl-β-D-glucothiopyranoside (lane 8) did not influence the transferase activity but aided in the formation of non-specific products. Cholic acid (lane 6) did not affect the transferase activity, whereas, deoxycholic acid killed the formation of the enzymatic product.

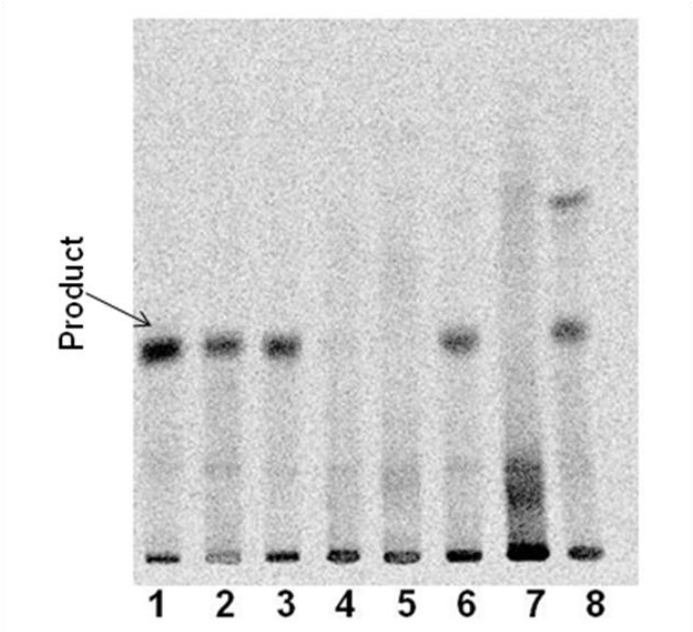

Figure 2.17 Effect of detergents on arabinosyltransferase activity. Lane 1. Positive control reaction with acceptor; Lane 2. Tween-20; Lane 3. Tween-80; Lane 4. Brij-35; Lane 5. Brij-58; Lane 6. Cholic acid; Lane 7. Deoxycholoic acid; Lane 8. Octyl-β-D-glucothiopyranoside.

2.6 Conclusions

In conclusion, a specific cell free radioactive arabinosyltransferase assay was developed using a synthetic arabinose disaccharide acceptor. MALDI-TOF, HPAEC and GC/MS analysis revealed that the enzymatic product formed is a trisaccharide with a (1→2) linkage. Furthermore, the results showed the formation of enzymatic products was independent of the action of ethambutol and EmbA, EmbB and EmbC arabinosyltransferases. We optimized the enzymatic reaction conditions and showed that the assay was dependent on both time and protein concentrations. In addition, the buffer and pH experiment indicated that optimal enzyme activity occurs with the MOPS buffer at pH-8.

2.7 References:

Ayers, J.D., T.L. Lowary, C.B. Morehouse, and G.S. Besra. 1998. Synthetic arabinofuranosyl oligosaccharides as mycobacterial arabinosyltransferase substrates. *Bioorg. Med. Chem. Lett.* 8:437-442.

Belanger, A.E., G.S. Besra, M.E. Ford, K. Mikusova, J.T. Belisle, P.J. Brennan, and J.M. Inamine. 1996. The *embAB* genes of *Mycobacterium avium* encode an arabinosyl transferase involved in cell wall arabinan biosynthesis that is the target for the antimycobacterial drug ethambutol. *Proc. Natl. Acad. Sci. U. S. A.* 93:11919-11924.

Besra, G.S., D. Chatterjee, and B. Bloom. 1994. Lipids and carbohydrates of *Mycobacterium tuberculosis*. *In* Tuberculosis: Pathogenesis, protection, and control. B.R. Bloom, editor. ASM Press: Washington, DC. 285-306.

Daffe, M., P.J. Brennan, and M. McNeil. 1990. Predominant structural features of the cell wall arabinogalactan of *Mycobacterium tuberculosis* as revealed through characterization of oligoglycosyl alditol fragments by gas chromatography/mass spectrometry and by 1H and 13C NMR analyses. *J. Biol. Chem*. 265:6734-6743.

Dell, A., A.J. Reason, K.H. Khoo, M. Panico, R.A. McDowell, and H.R. Morris. 1994. Mass spectrometry of carbohydrate-containing biopolymers. *Methods. Enzymol.* 230:108-132.

Escuyer, V.E., M.A. Lety, J.B. Torrelles, K.H. Khoo, J.B. Tang, C.D. Rithner, C. Frehel, M.R. McNeil, P.J. Brennan, and D. Chatterjee. 2001. The role of the *embA* and *embB* gene products in the biosynthesis of the terminal hexaarabinofuranosyl motif of *Mycobacterium smegmatis* arabinogalactan. *J. Biol. Chem*. 276:48854-48862.

Jacin, H., and A.R. Mishkin. 1965. Separation of carbohydrates on borate-impregnated silica gel G plates. *J. Chromatogr*. 18:170-173.

Lairson, L.L., B. Henrissat, G.J. Davies, and S.G. Withers. 2008. Glycosyltransferases: structures, functions, and mechanisms. *Annu. Rev. Biochem.* 77:521-555.

Lee, R.E., P.J. Brennan, and G.S. Besra. 1997. Mycobacterial arabinan biosynthesis: the use of synthetic arabinoside acceptors in the development of an arabinosyl transfer assay. *Glycobiology*. 7:1121-1128.

McNeil, M.R., K.G. Robuck, M. Harter, and P.J. Brennan. 1994. Enzymatic evidence for the presence of a critical terminal hexa-arabinoside in the cell walls of *Mycobacterium tuberculosis*. *Glycobiology*. 4:165-173.

Pathak, A.K., Y.A. El-Kattan, N. Bansal, J.A. Maddry, and R.C. Reynolds. 1998. Tin (IV) chloride mediated glycosylation in arabinofuranose, galactofuranose and rhamnopyranose. *Tetrahedron. Letters*. 39:1497-1500.

Scherman, M., A. Weston, K. Duncan, A. Whittington, R. Upton, L. Deng, R. Comber, J.D. Friedrich, and M. McNeil. 1995. Biosynthetic origin of mycobacterial cell wall arabinosyl residues. *J. Bacteriol.* 177:7125-7130.

Scherman, M.S., L. Kalbe-Bournonville, D. Bush, Y. Xin, L. Deng, and M. McNeil. 1996. Polyprenylphosphate-pentoses in mycobacteria are synthesized from 5-phosphoribose pyrophosphate. *J. Biol. Chem*. 271:29652-29658.

Snapper, S.B., R.E. Melton, S. Mustafa, T. Kieser, and W.R. Jacobs, Jr. 1990. Isolation and characterization of efficient plasmid transformation mutants of *Mycobacterium smegmatis*. *Mol. Microbiol.* 4:1911-1919.

Wolucka, B.A., M.R. McNeil, E. de Hoffmann, T. Chojnacki, and P.J. Brennan. 1994. Recognition of the lipid intermediate for arabinogalactan/arabinomannan biosynthesis and its relation to the mode of action of ethambutol on mycobacteria. *J. Biol. Chem*. 269:23328-23335.

Zhang, J., K.H. Khoo, S.W. Wu, and D. Chatterjee. 2007. Characterization of a distinct arabinofuranosyltransferase in *Mycobacterium smegmatis*. *J. Am. Chem. Soc.* 129:9650-9662.

CHAPTER 3

DEVELOPMENT OF PLATE BASED AFTB SPECIFIC ARABINOSYLTRANSFERASE ASSAY

3.1 Précis

AftB arabinosyltransferase terminates the arabinan biosynthesis in AG by adding a terminal β-(1→2) linked arabinose (Seidel et al., 2007; Zhang et al., 2010). In this Chapter, we have developed and evaluated an ELISA based arabinosyltransferase assay for AftB using CS35-mAb that recognizes lipoarabinomannan (LAM) (Kaur et al., 2002). Although this assay worked, we concluded that, for all practical purposes, the ELISA based method was time consuming with several intermediate washing steps. Hence, it is not an ideal platform for screening purposes. We therefore, decided to choose a more sensitive fluorescein labeling procedure. The fluorescein (6-FAM)-labeled disaccharide α-D-Ara*f*-(1-5)-α-D-Ara*f* was synthesized and assessed for its acceptor ability in cell free AftB arabinosyltransferase assays. However, efforts towards the identification of AftB specific fluorescein labeled enzymatic product using the fluorescence polarization assays were not successful.

3.2 Introduction

From our earlier studies described in Chapter 2, the use of the disaccharide acceptor (Ara_2) in a cell free arabinosyltransferase assay resulted in the formation of a specific trisaccharide (Ara_3) enzymatic product. Further analysis of this enzymatic product revealed that the additional arabinose added onto the synthetic acceptor is (1→2) linked. From the structural features of cell wall arabinan of AG and LAM, the *in vitro* observed (1→2) linkage is the characteristic feature of a terminal β-(1→2) capping of AG and LAM. Studies have shown that CS35-mAb recognizes the terminal β-(1→2) capping in the synthetic acceptors and is also essential for antibody binding (Hunter et al., 1986; Kaur et al., 2002; Rademacher et al., 2007). Based on this rationale, we hypothesized that the AftB enzymatic product may have an epitope that recognizes the binding region of CS35-mAb.

The aim of my study in this chapter focused on efforts towards developing a plate based assay for AftB. To date, several arabinosyltransferase assays specific for the AftB activity have been published (Seidel et al., 2007), but very few can be adapted to a high-throughput format. In this direction, the work described in this chapter focused on developing a plate based arabinosyltransferase assay using CS35-mAb in identifying AftB specific activity. In this chapter, we extended our approach from a calorimetric assay to a more sensitive fluorescence polarization method. The first part of this chapter focused on development of the plate based arabinosyltransferase assay using CS35-mAb (Figure 3.1) while the later section focused on converting this into a fluorescence based assay.

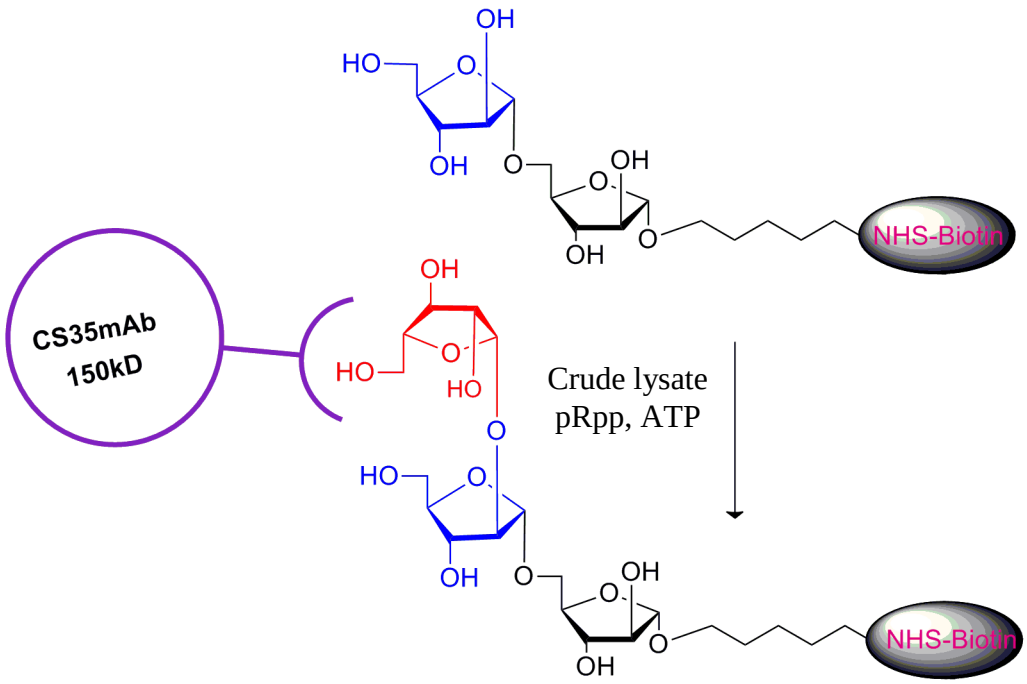

Figure 3.1 Schematic illustration of AftB arabinosyltransferase assay using CS35-mAb. In this transferase assay, AftB, present in the crude membranes, transfers arabinose from the donor DPA onto the biotinylated disaccharide acceptor that is bound to a streptavidin coated plate. This results in the formation of a β-(1→2) trisaccharide enzymatic product recognized by the CS35-mAb.

3.2.1 Principle of fluorescence polarization

Fluorescence polarization is described (Perrin, 1926), in principle, when a fluorescent molecule is excited with polarized light, small molecules rotate quickly during the excited state with low polarization values. Larger molecules created by binding of a

second molecule, such as antibodies, rotate little during the excited state and, therefore, have high polarization values. A schematic representation of AftB specific fluorescence polarization assay is shown in Figure 3.2.

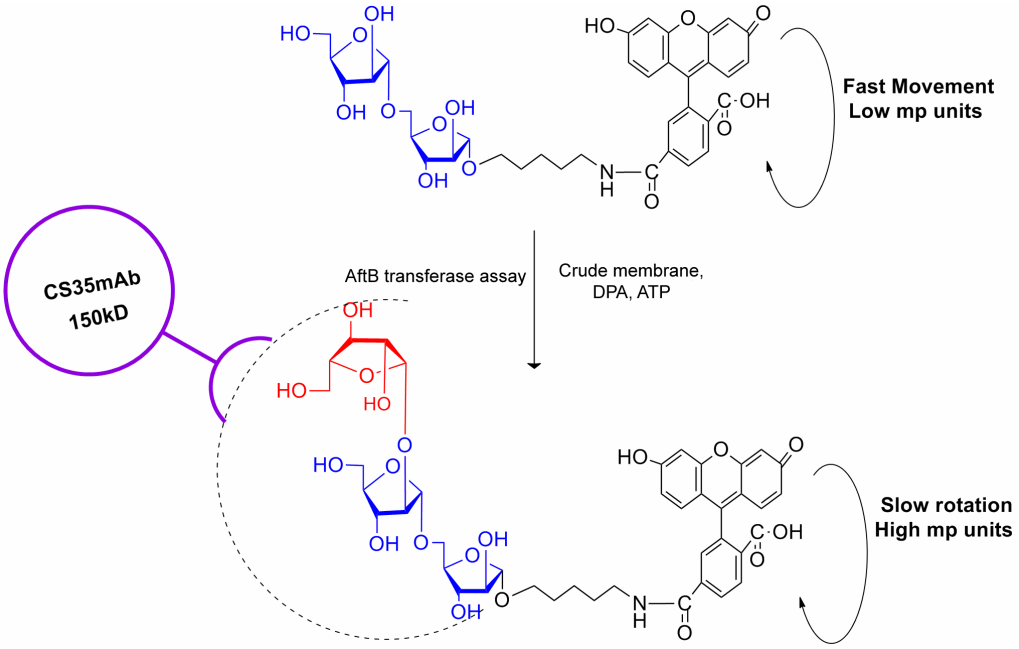

Figure 3.2 Schematic illustration of fluorescence polarization arabinosyltransferase assay. In this assay, AftB catalyzes the transfer of D-Ara*f* to the fluorescein labeled acceptor to generate a fluorescein labeled trisaccharide product with β-(1→2) D-Ara*f*. CS35-mAb is known to recognize β-D-Ara*f*-(1→2)-α-D-Ara*f* linkage formed on the fluorescein labeled disaccharide acceptor and causes an increase in millipolarization units compared to the free unbound fluorescein labeled acceptor.

3.3 Materials and methods

ImmunoPure Streptavidin was commercially obtained from Pierce Biotech (Rockford, IL U.S.A). The pRpp was purchased from Sigma. Secondary anti-Mouse IgG antibody coupled to a goat alkaline phosphatase was also purchased from Sigma (Cat # A5153).

The *p*-nitrophenylphosphate substrate was obtained from Kirkegaard and Perry Laboratories (Maryland U.S.A).

3.3.1 Bacterial strains and reagents

M. smegmatis mc^{2}155 was obtained from American Type Culture Collection ATCC (Snapper et al., 1990). The liquid cultures were grown to mid log phase O.D 600 nm of 0.7–0.8 at 37°C in Luria Bertani (LB) broth medium (Difco). The cells were harvested, washed with phosphate buffered saline (PBS) and stored at −80°C until further use. *M. smegmatis* membrane and P-60 cell wall fractions are prepared as described in Chapter 2, section 2.3.2. CS35-mAb was obtained from Dr. John Spencer, mycobacterial research laboratories (MRL). Lipid linked arabinose donor, DPA is prepared from an ethambutol sensitive strain *M. smegmatis 607* (Trudeau Mycobacterial collection), according to the established procedure and stored in chloroform: methanol (2:1) with 10% ammonia hydroxide at -20^{o}C (Wolucka et al., 1994).

3.3.2 Synthesis of biotinylated disaccharide acceptor

The structures of NHS-biotin, amine-linked disaccharide acceptor and biotinylated acceptors are shown in Figure 3.3. Amine-linked disaccharide acceptor (1 mg, 0.00234 mmol) was dissolved in water (0.1ml), and NHS-biotin (3.45 mg, 0.010 mmol) was dissolved in 15 µl of DMSO. Both these components were then dissolved in 400 µl of 100 mM $NaHCO_3$ buffer pH-8.3 and incubated overnight at room temperature with continuous stirring. Unlabeled biotin was removed by HPLC.

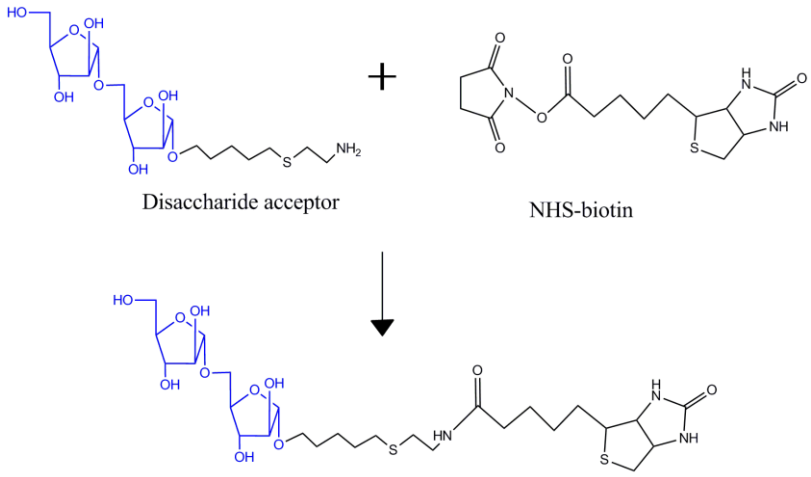

Figure 3.3 Structures of biotinylated arabinose disaccharide acceptor, Free NHS-biotin and biotinylated disaccharide acceptor.

3.3.3 Synthesis and HPLC separation of fluorescein labeled arabinose acceptor

The free amino group on the aglycon of arabinose disaccharide acceptor was coupled with fluorescein (6-FAM) the structures are given in Figure 3.4. The protocol was optimized for labeling 200 µg of amine containing arabinose disaccharide acceptor. The reaction mixture containing arabinose disaccharide acceptor and 6-FAM at a molar ratio of 1:4 in a 200 µl of 100 mM $NaHCO_3$ buffer pH-8.3 was incubated overnight at room temperature with continuous stirring. 6-FAM labeled arabinose disaccharide was separated from excess unlabeled fluorescein by reverse phase HPLC using a standard analytical (4.6 X 250mm) C18 column and eluted with linear gradient of 5-65 % acetonitrile over 30 min. The fraction containing colored fluorescein labeled sugar confirmed by ESI-MS were pooled and quantified by measuring the OD at 494 nm.

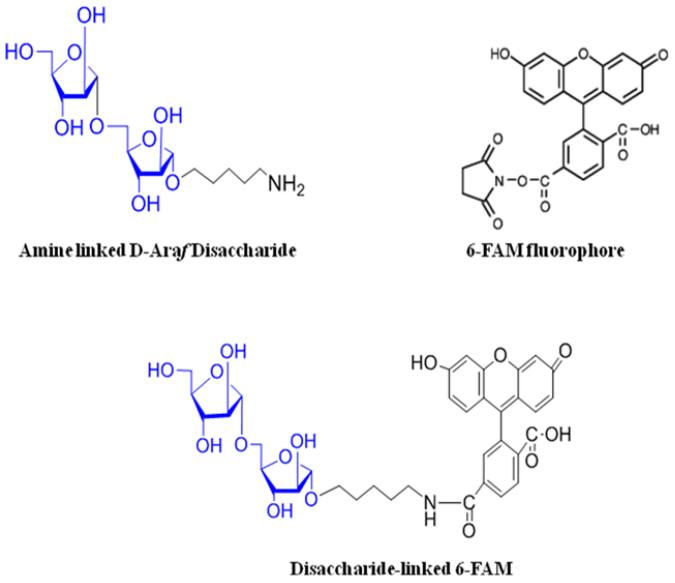

Figure 3.4 Structures of Synthetic amine-linked disaccharide, free fluorescein (6-FAM) and Disaccharide linked 6-FAM

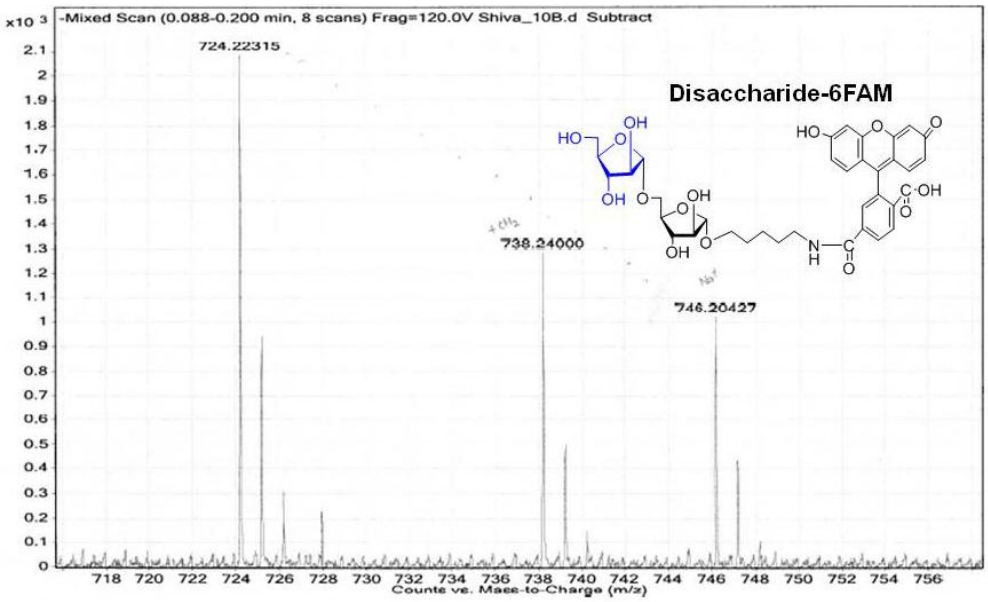

Figure 3.5 ESI-mass spectrum of HPLC separated 6-FAM fluorescein labeled disaccharide acceptor showing two isomers varying in lipid chain length. The *m/z* value of 724.2 [M-H] corresponds to the C5 lipid chain while *m/z* value 738.24 [M-H] corresponds to the C6 lipid chain.

3.3.4 ELISA based arabinosyltransferase assay procedure

The ELISA plate Dynex Immulon 4 was coated with streptavidin at a concentration of 50 µg/100 µl of Na_2HPO_4 buffer pH-9.0. The plate wells were then covered with clear adhesive sealing film to prevent evaporation, and place overnight at 4^oC. 200 µl of the blocking buffer (1% BSA, 0.05 % Tween 80 detergent in PBS, pH 7.4) were added to all the wells and incubated at room temperature for 1hr. The blocking solution was removed and a biotinylated disaccharide acceptor was added at a concentration of 50 µg/100 µl in PBS (pH 7.4), and the plate was further incubated at room temperature for 2 hr. the standard reaction contained 1 mM ATP, 0.1 mM pRpp, membrane proteins (0.6 mg), P-60 fraction (0.3 mg) were added into Buffer A (50 mM MOPS (pH 8.0), 5 mM β-mercaptoethanol, 10 mM $MgCl_2$) to a total volume of 200 µl and incubated overnight at 37^oC. All wells were washed five times with wash buffer. Primary antibody (CS35-mAb) was diluted in the blocking buffer at 1:500 dilution. The plate was washed six times with 200 µl OF wash buffer (PBS with 0.05% Tween). 100 µl of secondary antibody was added at 1:2500 dilution in wash buffer and incubated for 2 hr at room temperature. After, the plate was washed six times with 200 µl of PBS, 100 µl of p-nitrophenylphosphate was added to all the wells. The plate was maintained at room temperature for 1 hr and the O.D. was read at 405 nm in spectrophotometer.

3.3.5 Development of FP arabinosyltransferase assay

A typical reaction mixture contained a fluorescein-labeled disaccharide acceptor of 100 nM spiked with 100 µM of a non-labeled disaccharide acceptor in buffer A (50 mM MOPS pH-7.8, 10 mM $MgCl_2$). The reaction mixture also contained 100 µM DPA, ATP (6.25 µM), 0.1% Igepal and 0.2 mg of crude membranes from WT *M. smegmatis*

prepared as in section 2.3.2 in a total volume of 200 µl. All the components were added in a 96-well plate and incubated at 37^{o}C for 2 hr. The reaction with 6FAM-labeled disaccharide served as a control. After incubation, CS35-mAb (1:100) was added and the absorption was measured for millipolarization units (mp) in a Victor V3 microplate reader in the Department of Biochemistry.

3.3.6 Time dependent AftB specific FP arabinosyltransferase assay

Similar reaction conditions were employed as described in the Section 3.2.3.2, but the individual reactions were terminated at different time points (1, 5, 10, 20, 40, 60, 90 and 120 mins).

3.4 Results and discussion

The ELISA based AftB specific transferase assay is illustrated schematically in Figure 3.1. Transferase activity was assessed in a streptavidin coated 96 well plate in which a biotinylated arabinose disaccharide acceptor was bound to streptavidin through an avidin-biotin complex. AftB arabinosyltransferase activity present in the crude membranes catalyzes the β-(1→2) linkage by transferring an arabinose from the lipid linked arabinose donor (DPA) to the biotinylated acceptor bound to streptavidin. The trisaccharide enzymatic product formed was further confirmed by the recognition of CS35-mAb and color development. In Figure 3.6, lane 2 is a negative control reaction without a biotinylated acceptor whereas lane 4 serves as a positive control reaction containing standard tetrasaccharide arabinose obtained from Dr. John Spencer at CSU. Lane 1 is the arabinosyltransferase reaction in presence of a biotinylated acceptor

showing a positive color development indicating AftB transferase activity and recognition of an AftB specific enzymatic product by CS35-mAb.

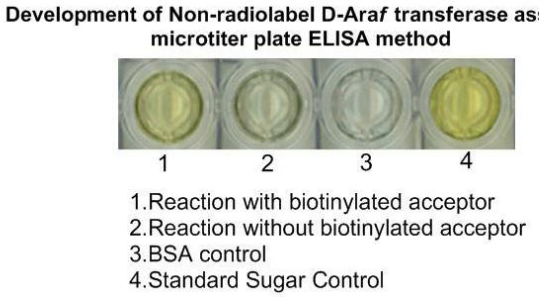

Figure 3.6 Development of non-radiolabeled AftB specific arabinosyltransferase assay in a micro-titer plate based ELISA method. A positive color development in the assay reaction (lane 2) indicates recognition of enzymatic product with CS35-mAb.

3.4.1 Fluorescence polarization assay for AftB

In order to develop a sensitive method, we chose to synthesize the fluorescein labeled acceptor for AftB arabinosyltransferase activity. Labeling with fluorescein was performed by allowing a free amino group on the acceptor to react with commercially available *N*-hydroxysuccinimide (NHS)-ester of fluorescein (6-FAM) to form a stable amide bond (Hermanson, 1996). The fluorescein labeled arabinose disaccharide was then separated by the reverse phase HPLC system. The purified compound obtained was further confirmed by ESI-mass spectrometry as shown in Figure 3.5. The final yield of the fluorescein labeled disaccharide acceptor was 60 µg (33% of starting material) as determined by the O.D. at 494 nm. The arabinosyltransferase assay reaction in the presence of the fluorescein labeled acceptor resulted in increased mp units. In Figure 3.7, the 20 unit increase in mp values in the assay reaction compared to the fluorescein labeled disaccharide acceptor and free fluorescein controls potentially indicated the

presence of transferase activity. The increase in mp value might be a result of increase in molecular mass of the fluorescein labeled disaccharide with additional arabinose.

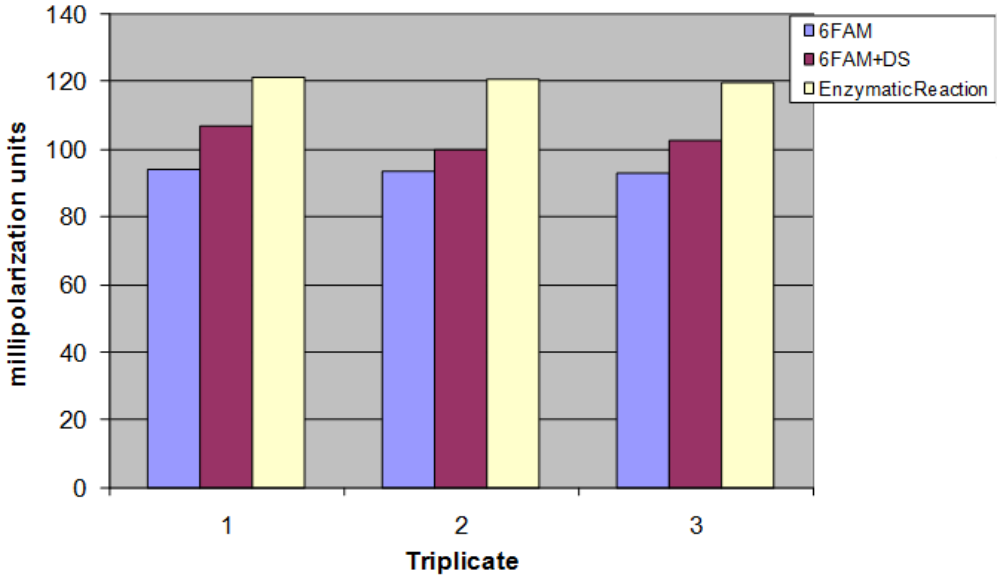

Figure 3.7 Fluorescence polarization AftB specific arabinosyltransferase assay (performed in triplicates). There is a consistent increase in mp values in the enzymatic reaction compared to free fluorescein.

In order to determine the optimal conditions for the assay, the time dependent appearance of the fluorescence polarization signal was studied by terminating the reaction at various time points. Linear increase in the fluorescence signal was observed with time as shown in Figure 3.8. Unfortunately, this linearity altered with the addition of CS35-mAb. Failure to increase in the mp values after addition of CS35-mAb, may be due to interference of 6-FAM with the epitope recognition of the enzymatic product. Because of the very little amount of the fluorescein labeled substrate used in the reaction mixtures, we preferred to analyze the formation of the AftB enzymatic product by mass spectrometry. ESI-mass spectrometry analysis of the reaction mixture confirmed the absence of molecular ions corresponding to 6-FAM labeled disaccharide and its enzymatic product.

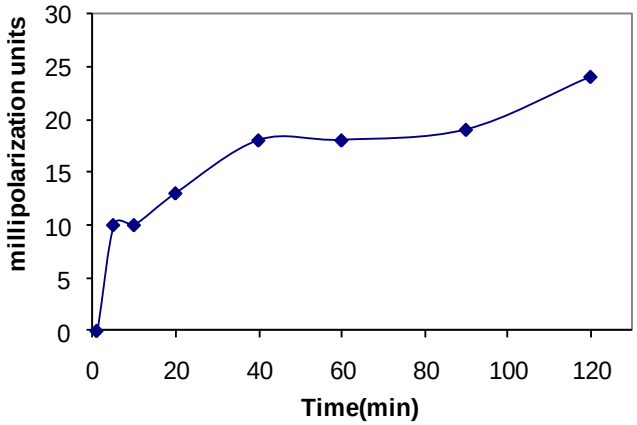

Figure 3.8 Time dependency of FP arabinosyltransferase. Linear increase in the fluorescence signal (mp units) with time confirms true enzymatic activity.

3.5 Conclusions

We successfully synthesized biotinylated and fluorescein labeled disaccharide acceptors for AftB arabinosyltransferase assays. We were also successful in developing a plate based ELISA method for AftB specific arabinosyltransferase activity using a biotinylated disaccharide acceptor. The additional arabinose transferred onto the biotinylated acceptor was bound to the streptavidin coated plate and later recognized using CS35-mAb.

The development of fluorescence polarization AftB arabinosyltransferase assay was not successful. Unfortunately, we were not able to identify either a fluorescein labeled acceptor or its enzymatic product by mass spectrometry. This may be due to the modifications of a fluorescein compound by endogenous enzymes present in the crude membranes. Moreover, due to the limited availability of the amine-linked arabinose disaccharide acceptor, further characterization of the fluorescein labeled acceptor and its enzymatic product was not possible to be used in development of an assay system specific for AftB transferase activity.

3.6 References

Hermanson, G.T. 1996. Chemistry of reactive groups. *In* Bioconjugate techniques. Academic Press, Amsterdam, Chapter 2. 169-213.

Hunter, S.W., H. Gaylord, and P.J. Brennan. 1986. Structure and antigenicity of the phosphorylated lipopolysaccharide antigens from the leprosy and tubercle bacilli. *J. Biol. Chem*. 261:12345-12351.

Kaur, D., T.L. Lowary, V.D. Vissa, D.C. Crick, and P.J. Brennan. 2002. Characterization of the epitope of anti-lipoarabinomannan antibodies as the terminal hexaarabinofuranosyl motif of mycobacterial arabinans. *Microbiology*. 148:3049-3057.

Perrin, F. 1926. Polarization of light of fluorescence, average life of molecules in the excited state (Polarisation de la lumière de fluorescence. Vie moyenne des molécules dans l'etat excité). *J. Phys. Radium*. 7:390-401.

Rademacher, C., G.K. Shoemaker, H.S. Kim, R.B. Zheng, H. Taha, C. Liu, R.C. Nacario, D.C. Schriemer, J.S. Klassen, T. Peters, and T.L. Lowary. 2007. Ligand specificity of CS-35, a monoclonal antibody that recognizes mycobacterial lipoarabinomannan: a model system for oligofuranoside-protein recognition. *J. Am. Chem. Soc.* 129:10489-10502.

Seidel, M., L.J. Alderwick, H.L. Birch, H. Sahm, L. Eggeling, and G.S. Besra. 2007. Identification of a novel arabinofuranosyltransferase AftB involved in a terminal step of cell wall arabinan biosynthesis in Corynebacterianeae, such as *Corynebacterium glutamicum* and *Mycobacterium tuberculosis*. *J. Biol. Chem*. 282:14729-14740.

Snapper, S.B., R.E. Melton, S. Mustafa, T. Kieser, and W.R. Jacobs, Jr. 1990. Isolation and characterization of efficient plasmid transformation mutants of *Mycobacterium smegmatis*. *Mol. Microbiol.* 4:1911-1919.

Wolucka, B.A., M.R. McNeil, E. de Hoffmann, T. Chojnacki, and P.J. Brennan. 1994. Recognition of the lipid intermediate for arabinogalactan/arabinomannan biosynthesis

and its relation to the mode of action of ethambutol on mycobacteria. *J. Biol. Chem*. 269:23328-23335.

Zhang, J., A.G. Amin, A. Holemann, P.H. Seeberger, and D. Chatterjee. 2010. Development of a plate-based scintillation proximity assay for the mycobacterial AftB enzyme involved in cell wall arabinan biosynthesis. *Bioorg. Med. Chem.* 18:7121-7131.

CHAPTER 4

RECONSTITUTION OF FUNCTIONAL MYCOBACTERIAL ARABINOSYLTRANSFERASE AftC PROTEOLIPOSOME AND ASSESSMENT OF DECAPRENYLPHOSPHORYL-ARABINOSE ANALOGUES AS ARABINOFURANOSYL DONORS

These studies were initiated by our former laboratory member Jian Zhang. I contributed in AftC expression, purification and reconstitution into proteoliposomes and assessment of acceptor analogs for its transferase activity. Quantification of enzymatic product by MALDTI-TOF analysis and mass spectrometry analysis of lipid specificity.

Jian Zhang, Shiva K. Angala, Pradeep K. Pramanik, Kai Li, Mary Jackson, Dean C. Crick, Abraham Liav, Adam Jozwiak, Ewa Swiezewska, Mike R. McNeil and
Delphi Chatterjee, Reconstitution of functional mycobacterial arabinosyltransferase AftC proteoliposome and assessment of decaprenylphosphoryl-arabinose analogues as arabinofuranosyl donors. ACS Chem Biol, 2011.

4.1 Précis

Arabinosyltransferases are a family of membrane bound glycosyltransferases involved in the biosynthesis of arabinan segment of two key glycoconjugates arabinogalactan and lipoarabinomannan in the mycobacterial cell wall. All arabinosyltransferases identified have been found to be essential for the growth of Mtb and are potential targets for developing new anti-tuberculosis drugs. Technical bottlenecks in designing enzyme assays for screening for inhibitors are: 1) the enzymes are membrane proteins and refractory to isolation; and 2) there are no commercial substrate and the sole arabinose donor, decaprenylphosphoryl-D-arabinofuranose is sparsely produced and difficult to

isolate. In this study, we have synthesized several substitutes for decaprenylphosphoryl-D-arabinofuranose by varying the chain length and investigated their arabinofuranose (Ara*f*) donating property. In parallel, an essential arabinosyltransferase (AftC), enzyme that introduces α-(1→3) branch points in the internal arabinan domain in arabinogalactan and lipoarabinomannan synthesis has been expressed and purified for the first time. Furthermore, it has been shown that the AftC is active only when reconstituted in a proteoliposome using mycobacterial phospholipids, and has a preference for diacylated phosphatidylinositoldimannoside (Ac_2PIM_2). The α-(1→3) branched arabinans were generated when AftC-liposome complex was used in an assay with the *Z,Z*-farnesylphosphoryl D-arabinose (*Z*-FPA) and linear α-D-Ara*f*-$(1\rightarrow5)_{3\text{-}5}$ linked linear oligosaccharide acceptors but not when a α-(1→3) branchpoint is preintroduced.

4.2 Introduction

According to the 13th (2010) annual tuberculosis report by the World Health Organization (WHO) there were an estimated 9.27 million new cases of tuberculosis (TB) worldwide in 2007. It is now prioritized to find new affordable and effective anti-tuberculosis drugs to reduce the physical and economical burden of TB patients. The mycobacterial cell wall has been regarded as a validated target for developing new anti-TB drugs supported by the fact that several first-line anti-TB drugs such as ethambutol and isoniazid, inhibit synthesis of the arabinan and the mycolic acid, key constituents of cell wall of Mtb. Common to all pathogenic Mycobacterium *sp*., including the etiological agents of TB and leprosy, a fully elaborated cell wall is essential for growth and survival in the infected host.

The majority of the glycosyltransferases (GTs) involved in the synthesis of the common and rare sugars of the cell envelope of *Mycobacterium sp*. are essential for viability and, conceivably, are suitable targets for new drug development against multidrug and extensively-drug resistant tuberculosis as reviewed earlier. It has been shown that all Ara*f* residues in mycobacterial D-arabinan originate from the pentose phosphate pathway/hexose monophosphate shunt and the immediate precursor is decaprenylphospho-D-arabinofuranose (DPA). The biosynthetic pathway for the DPA formation has been recently elucidated (Mikusova et al., 2005). Recently, an enzyme, decaprenylphosphoryl-β-D-ribose-2'-epimerase (DprE) involved in the synthesis of decaprenylphosphoryl-D-arabinofuranose (DPA), the arabinose donor for arabinan synthesis has been identified as the target for benzothiazinone and dinitrobenzamide derivatives, new classes of anti-tuberculosis candidates (Makarov et al., 2009). These compounds are now in a Phase 2 clinical trials (Koul et al., 2011).

Although the structural scaffold and the biosynthetic steps in the arabinan formation in AG have been almost completely elucidated (Alderwick et al., 2007; Belanger et al., 1996; Berg et al., 2005) compound screening against arabinosyltransferase activity has not been pursued due to difficulties in obtaining soluble, active proteins for biochemical assays. This is largely due to the fact that all arabinosyltransferases are membrane proteins with multiple membrane spanning domains. As shown in Figure 4.1, arabinosyltransferases dedicated for arabinogalactan (AG) pathway include AftA (Rv3792), apparently responsible for the transfer of the first Ara*f* residue to the galactan domain of AG (Alderwick et al., 2006), the terminal β-(1→2)-capping arabinosyltransferase, AftB (Rv3805c) (Seidel et al., 2007), AftC (Rv2673) involved in

the internal α-(1→3)-branching of the arabinan domain of AG (Birch et al., 2008) and the EmbA and EmbB proteins involved in the formation of the [β-D-Ara*f*-(1→2)-α-D-Ara*f*]2-3,5-α-D-Araf-(1→5)-α-D-Ara*f*- (Ara_6) termini of arabinan (Escuyer et al., 2001). On the contrary, interestingly, only three enzymes -EmbC, AftC and AftD (Rv0236c) − have been implicated in lipoarabinomannan (LAM) arabinan synthesis (Skovierova et al., 2009; Zhang et al., 2003).

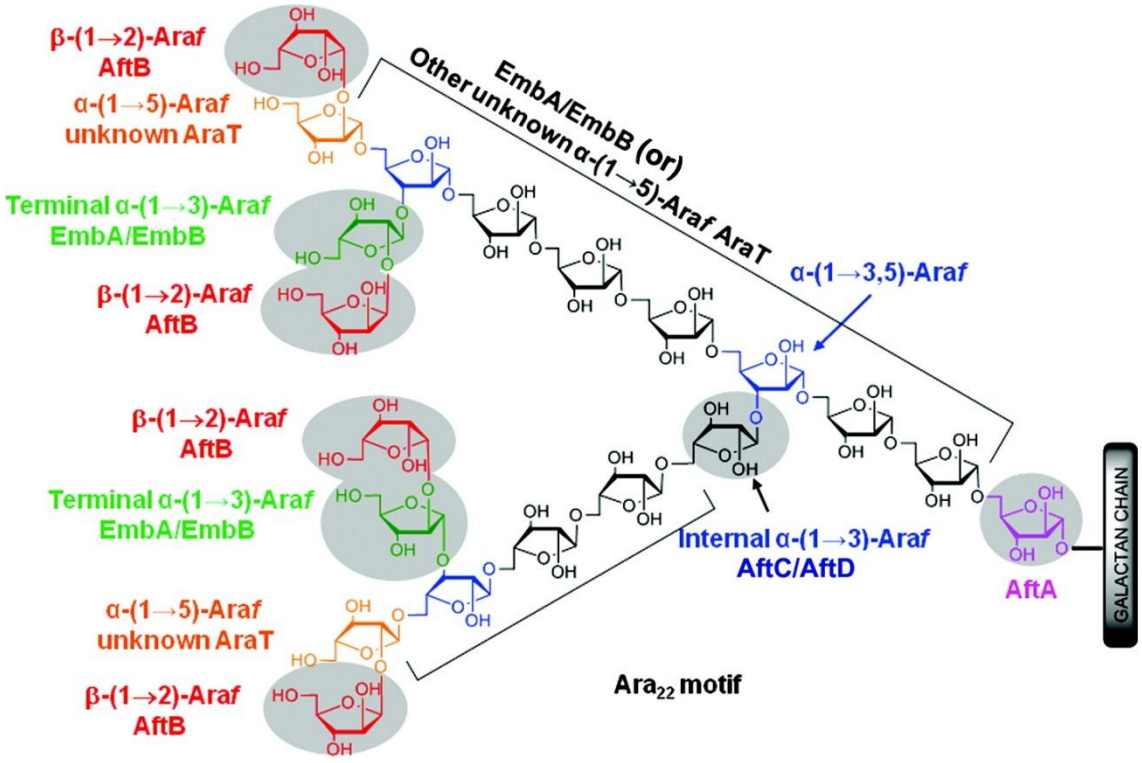

Figure 4.1 Putative biosynthesis of arabinan in AG in mycobacterium.

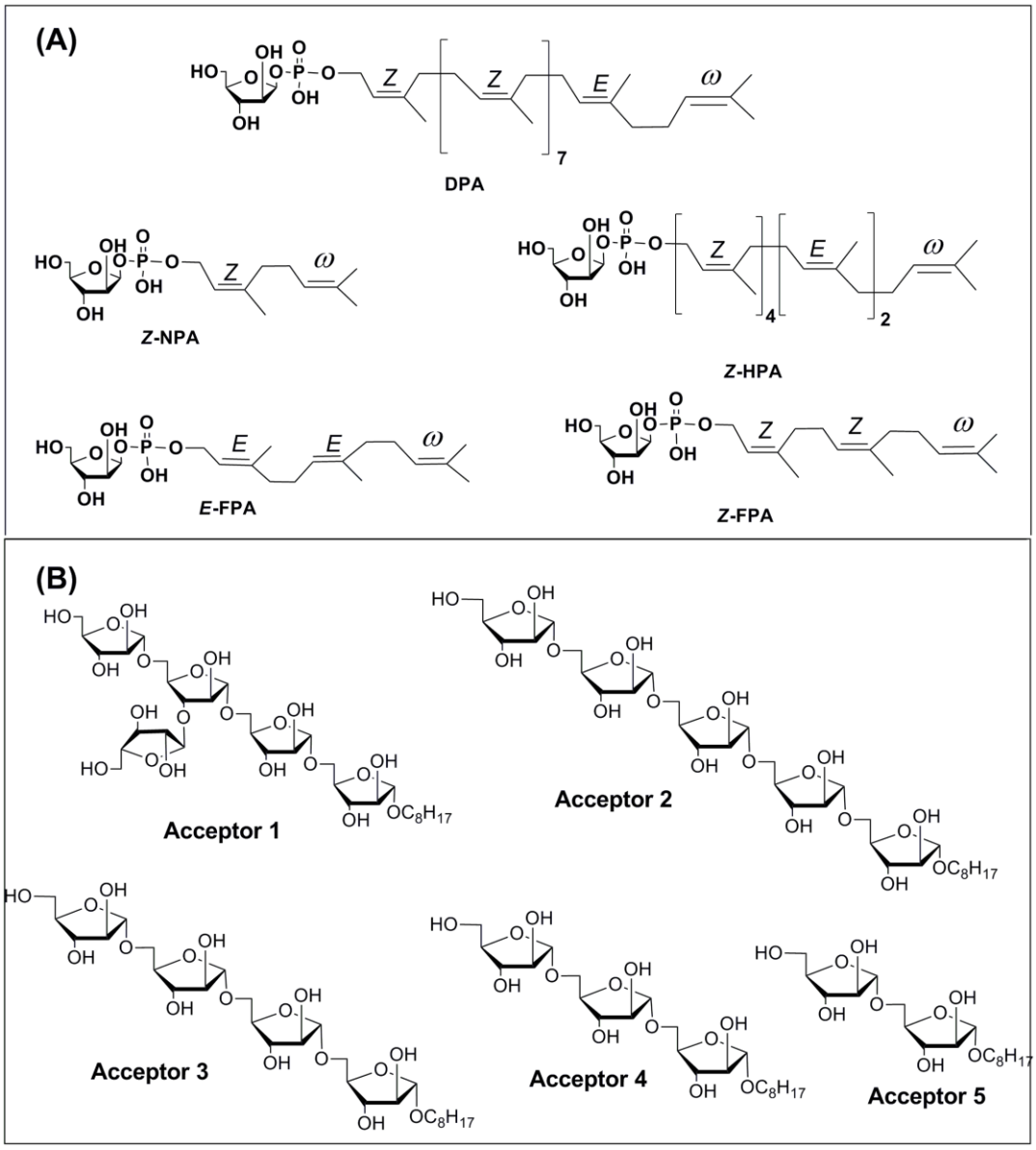

Figure 4.2 (A) Structure of DPA and DPA analogues used in this study. "*Z*", "*E*", and "ω" represent the configuration of the double bonds in the lipids in DPA and DPA analogues. Abbreviation: *Z*-nerylphosphoryl D-arabinose (*Z*-NPA), *Z,Z*-farnesylphosphoryl D--arabinose (*Z*-FPA), *E,E*-farnesylphosphoryl D-arabinose (*E*-FPA), *Z,Z,Z*-heptaprenylphosphoryl D-arabinose (*Z*-HPA); **4.2 (B)** The structure of the acceptors **1**-**5** used in the assays. Acceptor **1** is a branched pentasaccharide that was used for probing a α-(1→5) arabinosyltransferase activity and acceptors **2-5** are linear oligosaccharides from dimer to pentamer that was used for probing the α-(1→3) arabinosyltransferase (AftC) or β-(1→2) arabinosyltransferase (AftB)

The donor substrate (DPA) used in the arabinosyltransferase enzymatic assays is sparsely produced by *Mycobacterium sp.* and is not commercially available. Preparation of DPA from mycobacteria is laborious and time-consuming and is often obtained in poor yield (Wolucka et al., 1994), and therefore not suitable for development of high throughput plate-based assays. Moreover, due to the long-chain length in the lipid, DPA has poor solubility in an aqueous reaction buffer, which greatly impedes its efficiency in enzymatic reactions. As an alternate, phosphoribose pyrophosphate (pRpp) has been utilized in many assays (Khasnobis et al., 2006; Skovierova et al., 2009). This highly soluble precursor of DPA can transform to DPA *in situ* in an enzymatic reaction (Mikusova et al., 2005). However, due to the five steps involved in the conversion of pRpp to DPA, overall product formation is often in low efficiency (approximately 4% overall yield).

In this study, we were able to express and purify recombinant AftC in *M. smegmatis*, and reconstituted in a proteoliposome to retain its arabinosyltransferase activity in enzymatic assays. In addition, we synthesized several DPA analogues carrying shorter lipid chains (C10, C15 and C35). These compounds (Figure 4.2A), *Z*-nerylphosphoryl D-arabinose (*Z*-NPA), *Z,Z*-farnesylphosphoryl D-arabinose (*Z*-FPA), *E,E*-farnesylphosphoryl D-arabinose (*E*-FPA), and *Z,Z,Z,Z,E,E*-heptaprenylphosphoryl D-arabinose (*Z*-HPA) were assessed as artificial donors for Arabinosyltransferase assays with specific synthetic linear arabinofuranosyl acceptors.

4.3 Materials and methods

4.3.1 Syntheses of the DPA analogues

The syntheses of DPA analogues were performed according to the established methods (Liav and Brennan, 2005; Liav et al., 2009). The detailed synthetic procedure are presented in the section 4.7 as supplemental section.

4.3.2 Cell free assays and structural analyses of the enzymatic products

Typical assay reaction mixtures contained buffer A that has 50 mM MOPS (pH 7.9), 5 mM 2-mercaptoethanol and 10 mM $MgCl_2$, ATP (62.5 μM), DPA analogues (1 mM), acceptor **1** (200 μM), and membranes (1.0 mg) in a total volume of 100 μl. The cell membranes were prepared from *M. smegmatis* according to the established procedure (Zhang et al., 2007). The reaction mixtures were incubated at 37°C for 2 h and terminated by adding 666 μl of 1:1 $CHCl_3$/MeOH to make a final solution of $CHCl_3$/MeOH/H_2O, 10:10:3. The reaction mixture was centrifuged at 14,000 rpm for 10 min. The supernatant was then evaporated to dryness. The dried reaction mixtures without further processing were per-*O*-methylated (Zhang et al., 2007) and resulting residues were dissolved in 50 μl of $CHCl_3$. 1 μl of sample was mixed with 1 μl of 2,5-dihydroxy benzoic acid (DHB, 10 mg/ml in 50 % acetonitrile, 0.1 % trifluoroacetic acid). The mixture was spotted on the MALDI target and allowed to air dry. The sample was analyzed by an Ultraflex-TOF/TOF mass spectrometer (Bruker Daltonics, Billerica, MA) in positive ion, reflector mode using a 25 kV accelerating voltage. External calibration is done using a peptide calibration mixture (4 to 6 peptides) on a spot adjacent to the sample. The data was processed in the FlexAnalysis software (version 2.4, Bruker Daltonics).

4.3.3 Competitive assay

The competition assays were performed according to the typical radioactive assay (Zhang et al., 2007) using DPA analogues as competitors. In brief, reaction mixtures contained buffer A, 62.5 μM ATP, 0.8 μM p[^{14}C]Rpp (100,000 dpm), acceptor **1** (300 μM), 80 μM unlabeled competitors (*Z*-NPA, *Z*-FPA, *E*-FPA or *E*-HPA), membranes (0.5 mg) and cell wall extracts (P60, 0.3 mg) (Khasnobis et al., 2006) in a total volume of 160 μl. The reaction mixtures were incubated at 37°C for 1 h and then terminated by adding 160 μl of ethanol. The resulting mixture was centrifuged at 14,000 x g and the supernatants were passed through pre-packed strong anion exchange (SAX) columns. The columns were eluted with 2 ml water. The eluent was evaporated to dryness and partitioned between the two phases (1:1) of water saturated 1-butanol and water. Using liquid scintillation counting, the 1-butanol fractions were measured for radioactivity incorporation. For TLC analysis of the enzymatic products formed in the competition assay, an aliquot of the 1-butanol fraction was dried under air and the residue was reconstituted in milli-Q water (10 μL) for analysis by silica gel TLC. The TLC plate was chromatographed in $CHCl_3$/MeOH/1 M NH_4OAc/NH_4OH/H_2O (180:140:9:9:23) followed by autoradiography at -70^{o}C using Biomax MR film (Kodak).

4.3.4 Overexpression of AftC (Rv2673) in *M. smegmatis*

The entire coding sequence of *Rv2673* was PCR amplified from Mtb H_{37}Rv genomic DNA using the primers Rv2673pJAMS (5'-cggagatctgtgtacggtgcgctggtgacgg-3') and Rv2673pJAMS (5'-ccctctagaccgctggccctcccgctcgg-3'), excised with BglII and XbaI, and cloned into the compatible BamHI and XbaI restriction sites of the expression vector

pJAM2. The resulting plasmid, pJAM*Rv2673*, allows the inducible expression of *aftC* under control of the acetamidase promoter. The recombinant protein produced with this system had a hexa-histidine at its carboxyl terminus allowing its purification using metal affinity columns and detection by immunoblotting with the monoclonal Penta-His antibody from QIAGEN. Synthesis of AftC in mc^2155/pJAM*Rv2673* cells grown at 37°C in MM63 broth was induced during log phase with 0.2% acetamide for 12 hr. The *M. smegmatis* control strain carried the empty plasmid, pJAM2. Cells were harvested by centrifugation (3,000 rpm) and frozen at -80^{o}C until further use.

4.3.5 Generation of His_6-AftC

Frozen cells were thawed on ice and suspended in 50 mM Tris-HCl buffer containing 150 mM NaCl (pH 8.0) and protease inhibitor (EDTA-free, Roche), DNAase, and Igepal CA-630 [1.0 % (vol/vol)] were added to the cell suspension. Cells were disrupted by probe sonication on ice (10 cycles at 60 s on and 90 s off). Cell debris was removed by centrifugation (10,000 × g, 15 min, 4^{o}C). Soluble cell lysate was applied to affinity column containing Ni-NAT agarose (0.4 ml, QIAGEN). The column was washed with 20 ml of Tris-HCl buffer with 0.1% Igepal CA-630. Then, a gradient elution buffer (Tris-HCl) containing 5 mM to 300 mM of imidazole (pH 8.0) and 0.1% Igepal CA-630 was applied to elute the column over 15 column volumes. Fractions containing His_6-AftC (150-200 mM of imidazole) were identified by SDS-PAGE and Western-blot. Protein identity was confirmed using trypsin digestion and Mascot search engine (Proteomics and Metabolomics Facility located at Colorado State University). The His_6-AftC was desalted on PD-10 column (GE Healthcare) and stored in 10 % (vol/vol) of glycerol at -80 ^{o}C until further use.

4.3.6 AftC liposome reconstitution

$CHCl_3/CH_3OH$ extracted lipids (5 mg) from Mtb $H_{37}Rv$ obtained from the Tuberculosis Research Material Contract (NIH) at Colorado State University was suspended in $CHCl_3$ (20 mg / mL in a glass tube) and then dried under a gentle stream of nitrogen to give a thin, homogeneous lipid film. 1mL of the suspension buffer (1% Igepal CA-630 in 50 mM buffer A) was added to the film, and gently resuspended to clarity by pipetting. The solution was left at room temperature without disturbing for 2 h and was then sonicated to obtain a yellow solution. Purified recombinant AftC (200 µg, 1.0 ml) was added to the lipid-detergent mixture. The mixture was allowed to stand for 30 minutes on ice. Activated and washed BioBeads (300 mg) were added, and the mixture was stirred overnight at 4^oC to allow gentle removal of the detergent and incorporation of the AftC into the lipid bilayer. The BioBeads were removed and 250 µL of the fresh batch was added and the suspension was stirred for one hour at 4^oC. The mixture was centrifuged for 15 min (10,000 × g, 4^oC) and separated into a pellet and a milky supernatant containing AftC proteoliposome. The protein concentration of proteoliposome was determined by BCA method.

4.3.7 Arabinosyltransferase assays using AftC proteoliposome and DPA analogues and analysis by MALDI-TOF-MS

A typical reaction mixture of 100 µl total volume contained 10 µg protein concentration (2 µM) of AftC proteoliposome, 1 mM acceptor **1-5,** 2 mM Ara*f* donor (*Z*-FPA or *Z*-HPA) in buffer A. Reactions were incubated at room temperature for 2 h at 37^oC and then terminated by adding 666 µl of 1:1 $CHCl_3$/MeOH to make a final $CHCl_3$/MeOH/H_2O of

10:10:3. The reaction mixture was centrifuged at 14,000 rpm for 10 min. The supernatant was evaporated to dryness in a SpeedVac. The dried samples were directly per-*O*-methylated and the subjected to MALDI-TOF-MS according to the methods described previously (Zhang et al., 2007). Since the penta-arabinosyl donor and the hexa-arabinosyl acceptor are expect to have very similar properties during MALD-TOF-MS and are present together in the sample and their ions collected in the same laser acquisition, we hypothesized that the area of the $[M+Na^+]$ ions peaks would be proportional to the abundance of the actual oligosaccharides. This hypothesis was tested using known ratios of synthetic octyl hexa-arabinoside and synthetic octyl penta-arabinoside (ratios of 1, 0.5, 0.25, and 0.125 were tested). Indeed a linear relationship between the molar ratio of the two oligosaccharides and the ratio of their respective $[M+Na^+]$ ion peaks was found. A standard curve was generated as presented in Figure 4.8. This standard curve was then used to calculate the ratio of product to substrate from the ratio of the $[M+Na^+]$ ion peaks in actual samples.

4.4 Results and discussion

4.4.1 Chemical syntheses of DPA analogues (Section 4.7 as supplement).

The chemical syntheses of all DPA analogues used a common intermediate, 2,3,5-(Tri *tert*-butyldimethylsilyl)-D-arabinosyl phosphate, that was obtained by coupling of a dibenzyl phosphate with a 2,3,5-(Tri *tert*-butyldimethylsilyl)-D-arabinosyl bromide (Liav et al., 2006). The β-anomer of the arabinoside was produced in 75% yield in the α/β mixture (as estimated by ^{1}H NMR). In the reaction step of coupling arabinosyl bromide with dibenzyl phosphate, a rigorous drying of bromide and dibenzyl phosphate intermediates in advance was necessary to improve the proportion of β-anomer in the

products of arabinosyl phosphate. Although the β-anomer could not be completely separated from the α-anomer by column chromatography, the early eluting fractions were enriched in the β-anomer (~ 88%). Alcohols containing the short lipid chains (C10, C15, C35) were activated by forming trichloroacetimidate intermediates. Although the trichloroacetimidates were sensitive to moisture and temperature, they could be stored at -20°C in a desiccator for several days. Finally, the arabinosyl phosphate was coupled with trichloroacetimidates in toluene. Deprotection of the coupled products with ammonium fluoride in a 15% methanolic ammonium hydroxide followed by chromatography on silica gel gave pure DPA analogues.

Chemical synthesis of DPA was described initially that used phosphoramidite-phosphite triester methodology which yielded a β/α ratio of 0.25 (Lee et al., 1995). However, only the β-anomer of DPA has proven to be a suitable donor for Ara*f*. In our present work for the synthesis of DPA analogues, an optimized approach was applied to increase the proportion of the β-anomer in an anomeric mixture (β/α ratio of 3) and with this anomeric mixture also increased the yield of the product by three folds compared to using the ones synthesized earlier.

4.4.2 Cell free Assay

We first wanted to determine whether the DPA analogues would be effective in a cell free assay using membrane preparation (100,000×g pellet) from *M. smegmatis* as the enzyme source. One specific pentasaccharide, a linear Ara_5 (acceptor **2**, Figure 4.2B), octyl α-D-Ara*f*-(1→5)-α-D-Ara*f*-(1→5)-α-D-Ara*f*-(1→5)-α-D-Ara*f*-(1→5)-α-D-Ara*f* (Zhang et al., 2007) was used as an acceptor. In order to examine the contribution of the

length (C10, C15 or C35) and configuration (*Z* or *E*) of the lipid chains to the donor efficiency in the assay, we assessed the ability of *Z*-NPA, *Z*-FPA, *E*-FPA, and *Z*-HPA in serving as donor substrates. The enzymatic reaction mixture without further processing was per-*O*-methylated and directly analyzed by MALDI-TOF-MS. As shown in Figure 4.3 A-D, molecular ions corresponding to unreacted acceptor (*m/z* 967) and an enzymatic product (*m/z* 1127) as sodium adducts were observed.

Additionally, several phosphatidylinositol mannoside (PIMs) and other endogenous components present in the membranes could also be detected (methylated PIM_2 at *m/z* 877, methylated PIM_3 at *m/z* 1081, methylated PIM_4 at *m/z* 1285, methylated PIM_5 at *m/z* 1489, methylated PIM_6 at *m/z* 1693). By quantification of the relative intensity of the acceptor (*m/z* 967) and the product (*m/z* 1127) reflected in the mass spectrum using a standard curve (see materials and methods section 4.3.7), the conversion rate (activity) of DPA analogues could be estimated. The *Z*-FPA exhibited the best Ara*f*-donating activity (Figure 4.3B). However, the *E*-FPA that possessed the same length of lipid as *Z*-FPA had no Ara*f*-donating activity (Figure 4.3C). The *Z*-NPA and *Z*-HPA exhibited moderate conversions (Figure 4.3A and 4.3D).

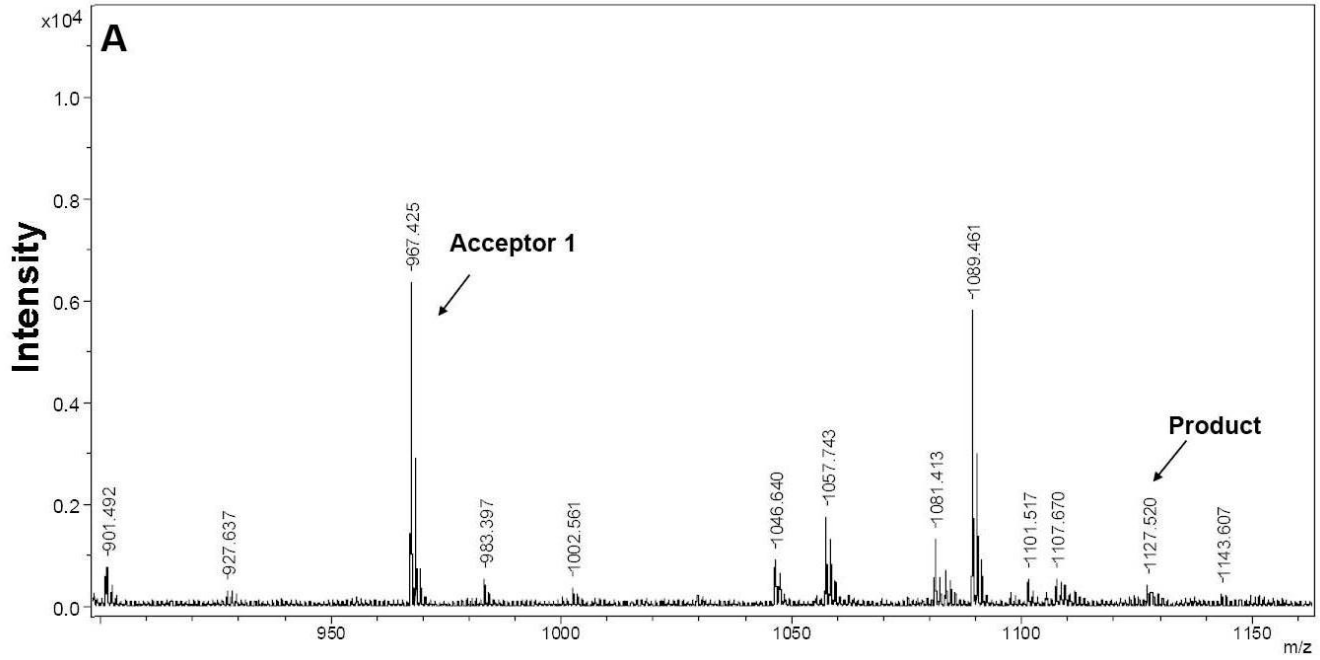

Figure 4.3.A. MALDI-TOF-MS spectra of enzymatic product by using *Z*-NPA in a cell free arabinosyltransferase assay in presence of crude membranes as enzyme source for the transferase activity. Arrows showing molecular ions corresponding to unreacted acceptor (*m/z* 967) and its enzymatic product (*m/z* 1127) as sodium adducts

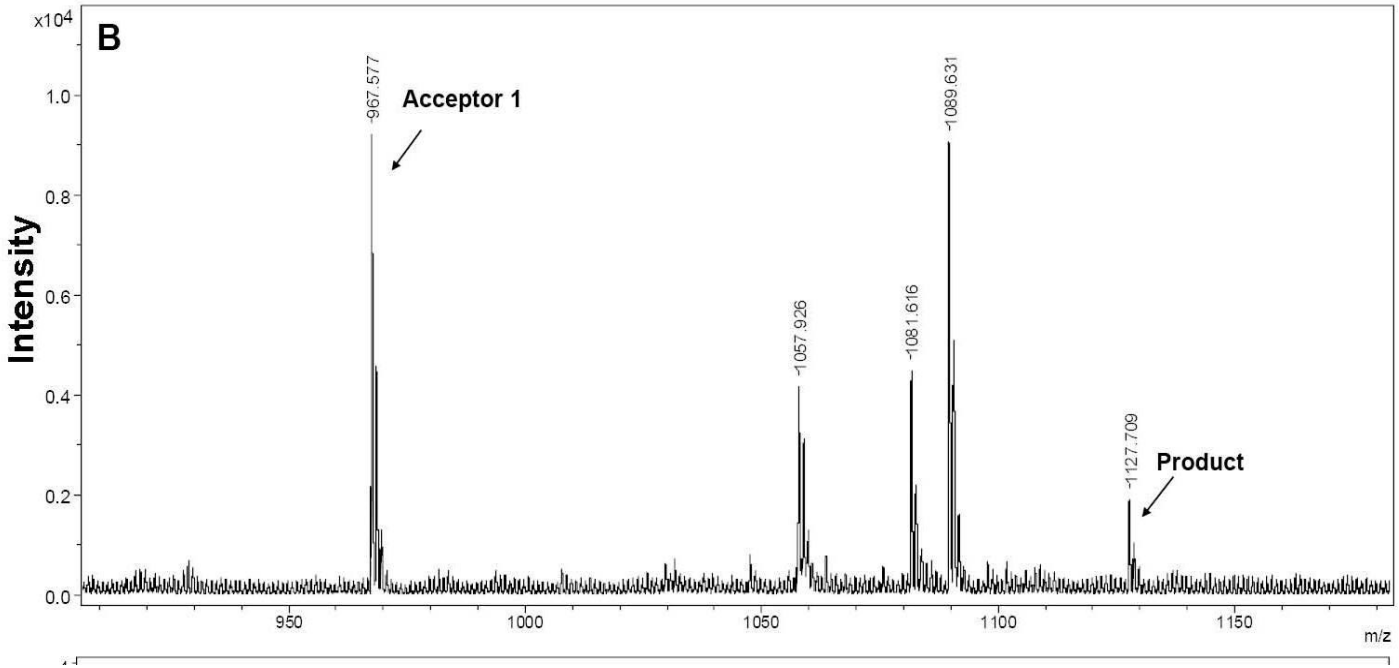

Figure 4.3.B. MALDI-TOF-MS spectra of enzymatic product formed using *Z*-FPA as donor analog in cell free arabinosyltransferase assay. Arrows showing molecular ions corresponding to unreacted acceptor (*m/z* 967) and its enzymatic product (*m/z* 1127) as sodium adducts

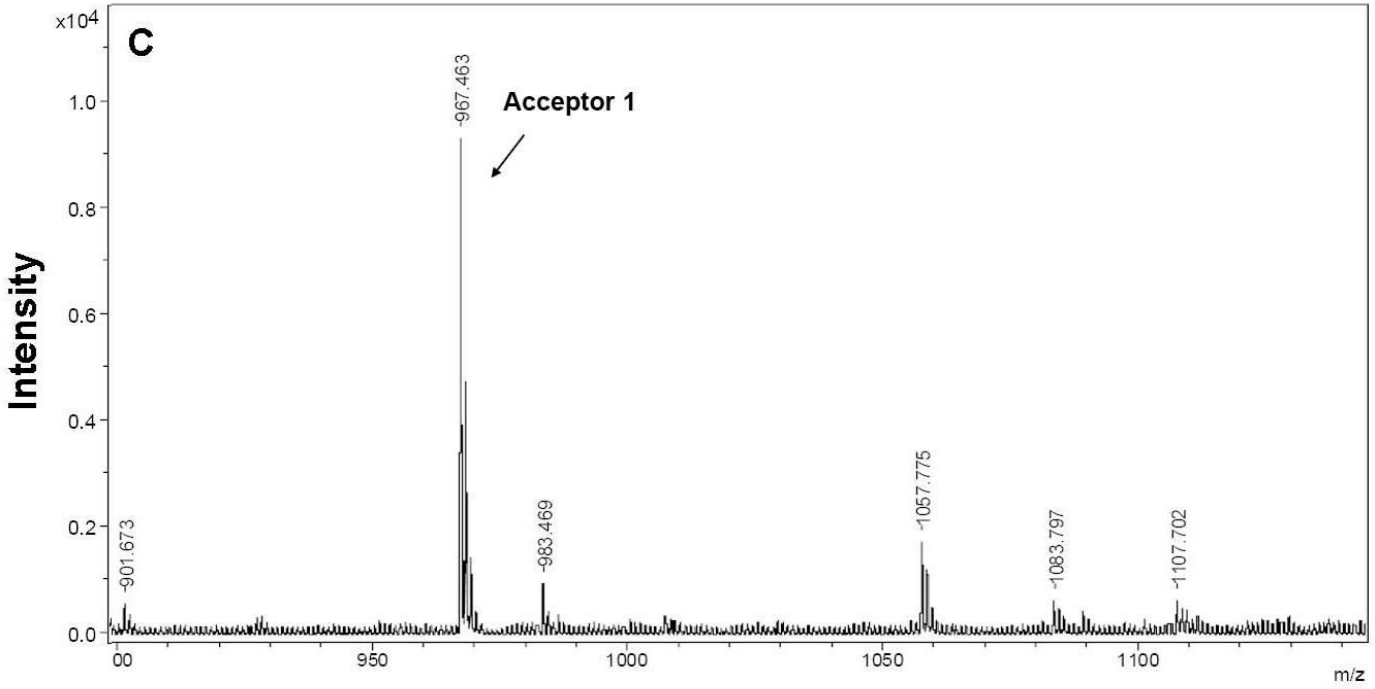

Figure 4.3.C. MALDI-TOF-MS spectra of *per-O-methylated* enzymatic product by using *E*-FPA. Arrows showing molecular ions corresponding to unreacted acceptor (*m/z* 967) as sodium adducts and absence of molecular ion (*m/z* 1127) corresponding to its enzymatic product indicates lack of transferase activity in presence of *E*-FPA as an alternate donor analog.

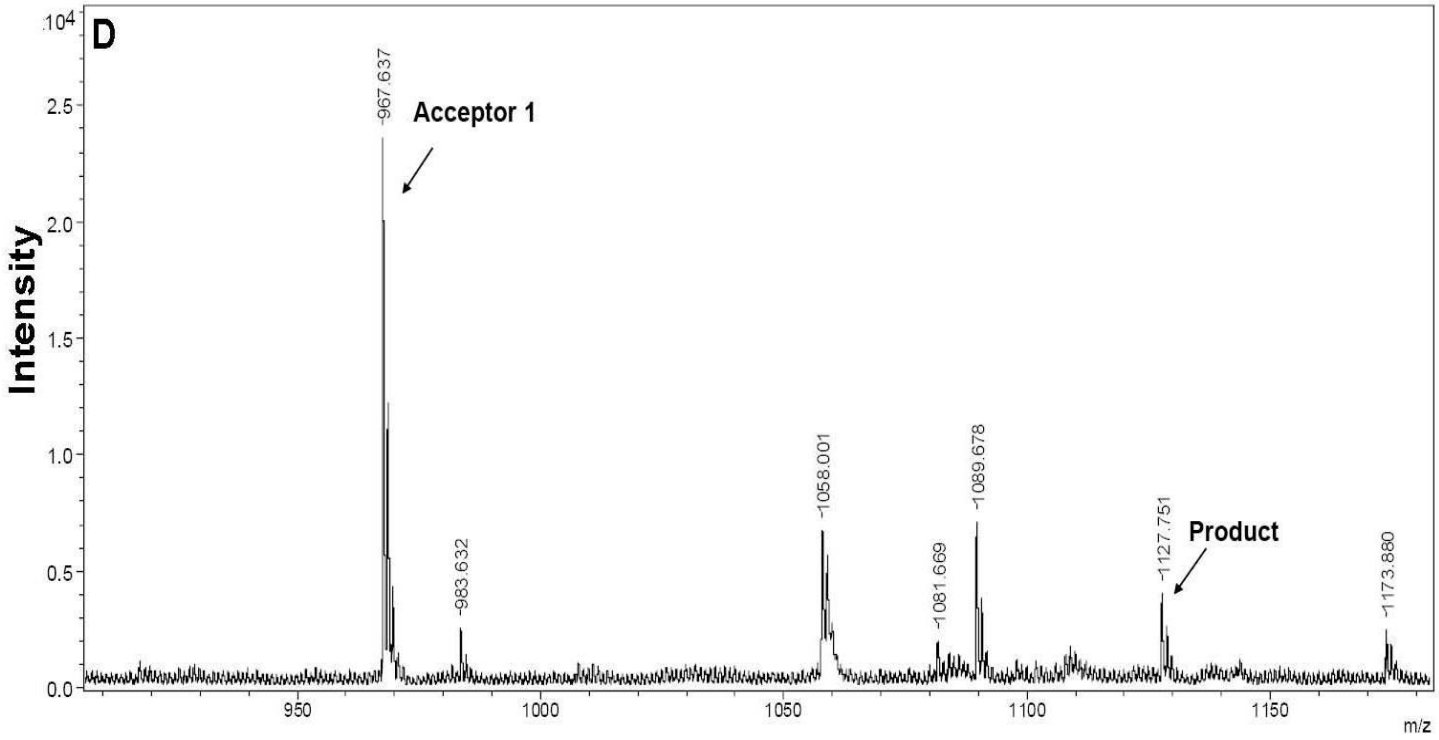

Figure 4.3.D. MALDI-TOF-MS spectra of enzymatic product by using *Z*-HPA. Arrows pointing molecular ions for unreacted acceptor (*m/z* 967) as sodium adducts, while molecular ion (*m/z* 1127) for its enzymatic product indicating transferase activity in presence of *Z*-HPA.

4.4.3 Competition arabinosyltransferase assay

To confirm the arabinosyltransferase activities of DPA analogues, we evaluated the ability of unlabeled polyprenyl-P-Ara*f* (*Z*-NPA, *Z*-FPA, *E*-FPA, and *E*-HPA) to inhibit the incorporation of labeled Ara*f* from (DP[^{14}C]A) generated *in situ* from the p[^{14}C]Rpp into the product.

The results showed that the addition of *Z*-FPA led to 54% inhibition of the DP[^{14}C]A (Figure 4.4.B). In contrast, *E*-FPA only marginally affected the DP[^{14}C]A incorporation (11% inhibition) indicating a limited competition of the lipids in the *E*-configuration. In addition, *Z*-NPA and *Z*-HPA showed 10% and 35% inhibitory ability, respectively. As is evident from the TLC (Figure 4.4.A), formation of DPA and DPR (decaprenylphospho-D-ribofuranose) also decreased dramatically using *Z*-FPA as competitor. It indicates that one of the biosynthetic steps in the transformation of p[^{14}C]Rpp to DP[^{14}C]A could also be inhibited by *Z*-FPA.

Thus, we have been successful in finding the differential inhibitory properties of the DPA analogues in arabinosyltransferase assay using DP[^{14}C]A as donor. The enzyme has a preference for *Z*-FPA compared to all other DPA analogues synthesized in this work (Figure 4.4.B).

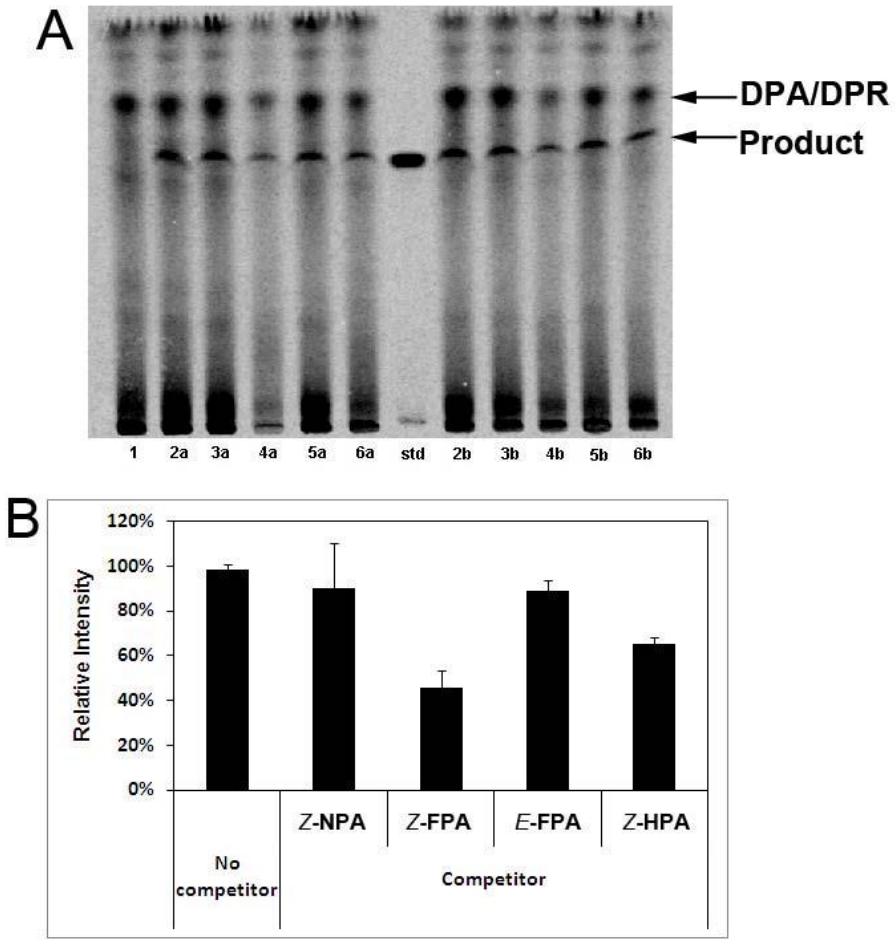

Figure 4.4 Competitive assay. **(A)** The TLC profile of the reactions (using [^{14}C]-DPA) competed against the DPA analogues including *Z*-NPA (lanes 3a and 3b), *Z*-FPA (lane 4a and 4b), *E*-FPA (lane 5a and 5b), and *Z*-HPA (lane 6a and 6b). Lane 2a and 2b represent the reaction without using any competitor (negative control). Lane 1 exhibits the reaction without using acceptor **1** (positive control). The 'std' lane represents the enzymatic product purified by column chromatography. 'a' and 'b' represent the duplicate of one competitive assay. The bands that migrated above the enzymatic product contained the [^{14}C]-DPA and [^{14}C]-DPR that were produced from p[^{14}C]Rpp**. (B)** The comparison of the scintillation intensity of the competitive assays using the DPA analogues as the competitors. The relative intensity was evaluated according to the assay without using the competitors that was normalized to 100%.

4.4.4 Expression of aftC and development of arabinosyltransferase assays using AftC-proteoliposome and DPA analogues.

A recombinant His_6-tagged AftC was efficiently produced in *M. smegmatis* mc^2155/pJAM/*Rv2673* upon induction of the expression of the *aftC* gene with acetamide (Triccas et al., 1998). The His_6-tagged recombinant protein could be detected by Western-blot (migrating at ~38kDa) in the transformants. Cells from AftC overexpressor were disrupted by sonication and solubilized in 1% Igepal CA-630, a detergent proven to retain arabinosyltransferase activity (Seidel et al., 2007). The resulting supernatant after centrifugation was nickel-affinity column purified by eluting with imidazole. Fractions (50 mM-200 mM of imidazole) containing His_6-tagged AftC were monitored by SDS-PAGE (Figure 4.5) and western-blot and ~200 μg of purified protein was obtained from 1 L of cell culture. The identity of the AftC protein was confirmed using in-gel trypsin digestion and analyzing the peptides by mass spectrometry, and matching the masses with MASCOT searching (score 122, Figure 4.6).

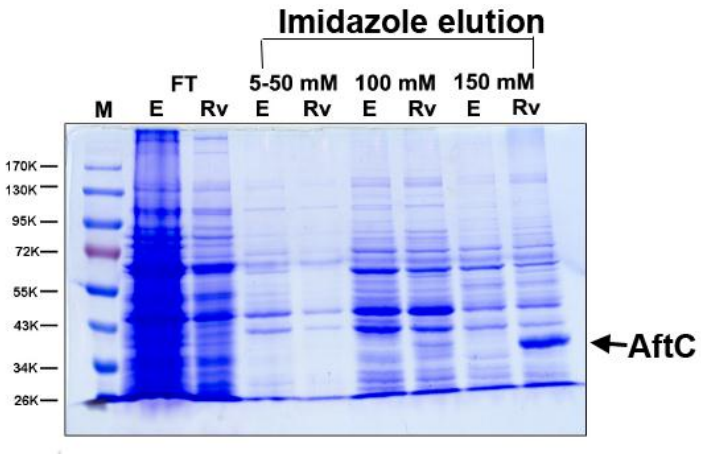

Figure 4.5. SDS-PAGE analysis of AftC (Rv2673). The cell lysate was applied to affinity chromatography and the column was washed with 20 ml of Tris-HCl buffer with 0.1% Igepal CA-630 (pH 8.0) and eluted with Tris-HCl buffer containing 5 mM to 300 mM of imidazole. The AftC was eluted in the buffer containing 150 mM of imidazole. "E" represents the *M. smegmatis* control strain carried the empty plasmid, pJAM2 and "Rv" represents the pJAMRv2673 strain with expression of AftC.

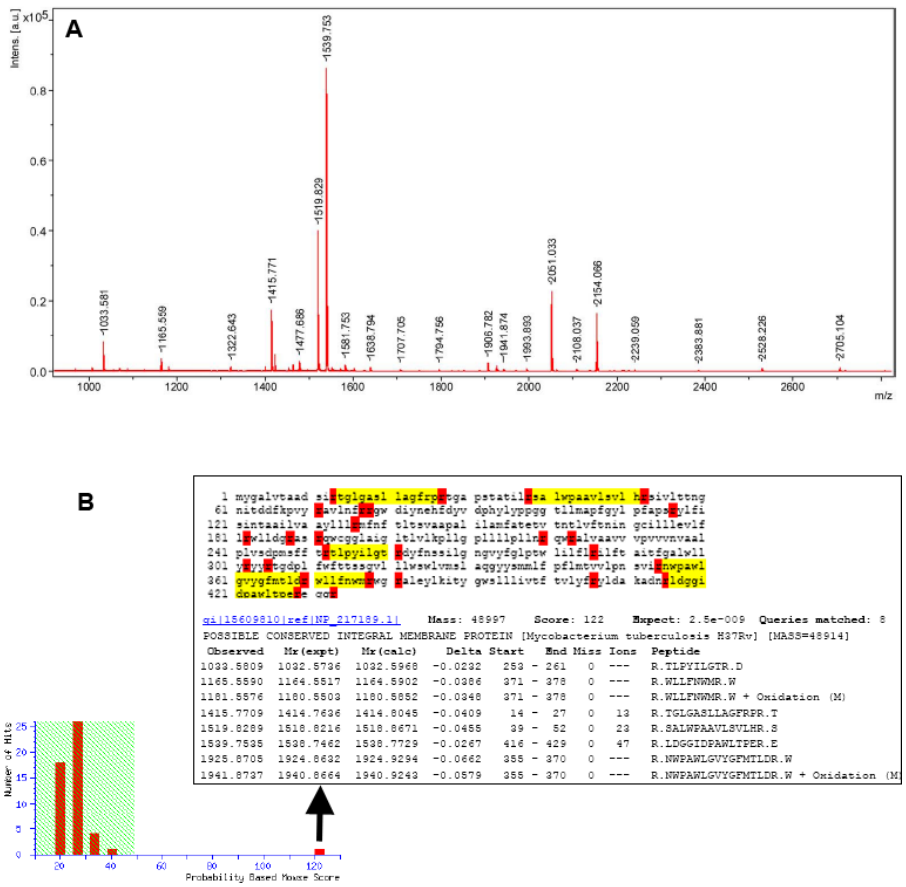

Figure 4.6. MALDI analysis of purified AftC (Rv2673). To prepare MALDI sample, AftC was subjected to SDS-PAGE (15%), stained with Coomassie Brilliant Blue, and AftC band was cut from the gel and subjected to in-gel tryptic digestion. (A) MALDI spectrum of peptides (assigned in the frame in panel B) after tryptic digestion. (B) Results on the MASCOT searching engineer. The score of 122 in MASCOT (left) represented AftC whose peptide fragments and coverage map are shown in the frame.

Enzymatic assays were next designed to compare the ability of *M. smegmatis* mc^{2}155/pJAM and mc^{2}155/pJAM/*aftC* cell free extracts to transfer Ara*f* from the DPA analogues onto acceptor **2**. No significant increase in product formation was observed (1.3 fold, increase over the control). However, when only the affinity purified recombinant AftC protein was used in the assay, we were unable to detect any product. On the other hand, when recombinant AftC was combined with *M. smegmatis*

membranes from the over expressing strain, product formation increased 2.3 fold (results not shown).

We reasoned that the failure of the recombinant protein to catalyze product formation was perhaps due to its lack of normal environment and as it has been reported that GT-C membrane proteins require lipids for folding to retain structure and glycosyltransferase activity (Newby et al., 2009). Based on this hypothesis, we developed a reconstitution system forming a liposome using lipid extracts. At first we used commercially available dipalmitoyl phosphatidylcholine (DPPC) to reconstitute but the resulting liposome failed to generate active enzyme. Then the purified AftC was reconstituted with native lipids ($CHCl_3$:CH_3OH:H_2O (10:10:3)) extracts of from Mtb H_{37}Rv cells to form AftC proteoliposome. Since both *Z*-FPA (C15) and *Z*-HPA (C35) worked well in the arabinosyltransferase assay, we use these compounds as sugar donors in separate reactions from which AftC would transfer Ara*f*(s) to the acceptors.

Five different arabinofuranosyl acceptors were tested in the enzymatic reactions using the AftC proteoliposome and DPA analogues. One of the acceptors was a branched pentasaccharide octyl (α-D-Ara*f*)$_2$-(1→3,5)-α-D-Ara*f*-(1→5)-α-D-Ara*f*-(1→5)-α-D-Ara*f* (acceptor **1)**, and the others were linear oligosaccharides (acceptors **2-5**, structures shown in Figure 4.2B) including Ara_5-octyl α-D-Ara*f*-(1→5)-α-D-Ara*f*-(1→5)-α-D-Ara*f*-(1→5)-α-D-Ara*f*-(1→5)-α-D-Ara*f* (acceptor **2**); Ara_4-octyl α-D-Ara*f*-(1→5)-α-D-Ara*f*-(1→5)-α-D-Ara*f*-(1→5)-α-D-Ara*f* (acceptor **3**), Ara_3- octyl α-D-Ara*f*-(1→5)-α-D-Ara*f*-(1→5)-α-D-Ara*f* (acceptor **4**) and Ara_2 octyl α-D-Ara*f*-(1→5)-α-D-Ara*f* (acceptor **5**).

Direct mass spectral analyses of the reaction mixtures revealed that the products formed in reactions with acceptors **2-4** only, and showed evidence of transfer of a single Ara*f* onto each of the acceptors tested. No products were detected for either acceptor **1** or **5**. We concluded that AftC can only transfer Ara*f* when a minimum of three Ara*f* residues are present as in acceptors **2-4** in order to introduce an α-D-Ara*f*-(1→3) branch point (Birch et al., 2008) (Figure 4.7). In fact, in AG or LAM branching is evident only after three linear α-(1→5)-Ara*f* have been assembled (Lee et al., 2006; Torrelles et al., 2004). Consequentially, the $Ara_{2,}$ acceptor **5** could not form a trisaccharide with AftC as it is recognized as a substrate for AftB to form a β-(1→2)-Ara*f* linkage (Seidel et al., 2007; Zhang et al., 2010) (data not shown). Furthermore, linear Ara_5 acceptor **2** could generate a enzymatic product with a mass at 1127 $[M+Na]^+$ and 1143 $[M+K]^+$ as shown in Figures 4.3A and 4.3B when using *Z*-FPA and *Z*-HPA as a donor, respectively, acceptor **1** with a α-(1→3)-Ara*f* branch already introduced could not yield any product with AftC proteoliposome (Figure 4.3.C). The acceptor **1** has been proven to be specific for a α-(1→5) arabinosyltransferase that has yet to be identified (Zhang et al., 2007).

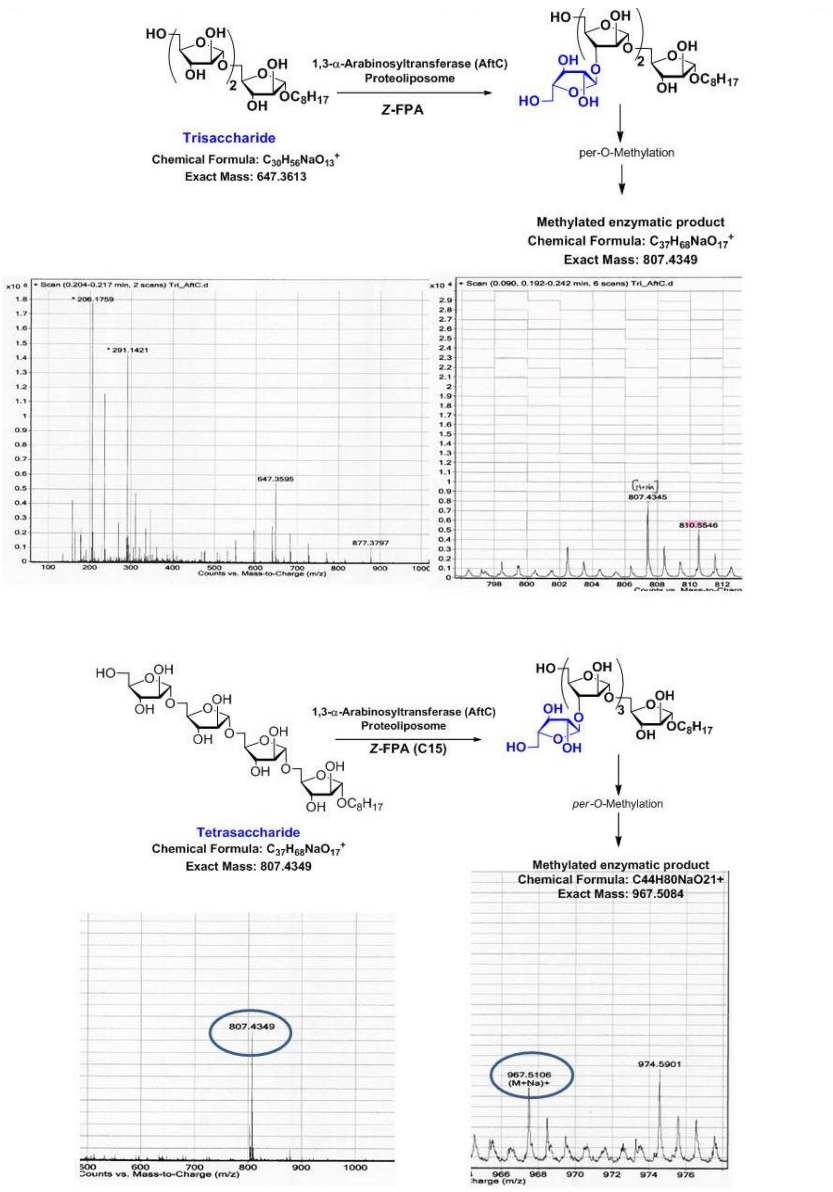

Figure 4.7 Arabinosyltransferase assays in AftC proteoliposome using a linear trisaccharide (A) and a linear tetrasaccharide (B) as acceptor. The enzymatic products were immediately subjected to methylation and ESI-MS analysis after completing the assay reactions. The linear disaccharide could not produce its enzymatic product when using AftC proteoliposome.

AftC, a bifunctional enzyme has recently been reported to display a α-(1→3) branching arabinosyltransferase activity on a synthetic linear α-(1→5) linked Ara_5 acceptor *in vitro* (Birch et al., 2008). One characteristic feature of AftC is that unlike other arabinosyltransferases described, the gene is nonessential in *M. smegmatis* and knock-out mutants could be generated an attribute reminiscent of the Emb proteins (Escuyer et al., 2001; Zhang et al., 2003). Phenotypic analysis of the mutants in *C. glutamicum* and *M. smegmatis* showed that this enzyme is responsible for α-(1→3) branching of the inner core of arabinan domain of AG (Figure 4.1) and LAM. Although AftC encodes a membrane-associated protein carrying the proposed GT-C motif of polyprenyl-dependent GTs (Berg et al., 2005), we have been successful in overexpressing and purifying AftC and shown that it retains activity in an *in vitro* assay after successful reconstitution in proteoliposome using native mycobacterial lipids.

We have also shown that use of DPA can be substituted with using some of the short chain synthetic DPA analogues, preferably, the analogue containing a moderate-length lipid (C15). In mass spectrometric analysis, the *Z*-FPA exhibited the best Ara*f*-donating activity, 19.4% conversion (Figure 4.8). However, the *E*-FPA that possessed the same length of lipid as *Z*-FPA had no ions at *m/z* 1127 and hence was considered as zero percent conversion (Figure 4.8). The *Z*-NPA (8% conversion) and *Z*-HPA (17% conversion) exhibited moderate conversions. Moreover, the DPA analogues containing lipids with *Z*-configuration are competitive substrates for DPA in the arabinosyltransferase assays. We believe that lipids in the *Z*-configuration are favored because structurally, *Z*-FPA is very similar to DPA which also contains *Z*-isoprene units and should be able to adopt all configurations of the double bond as in DPA.

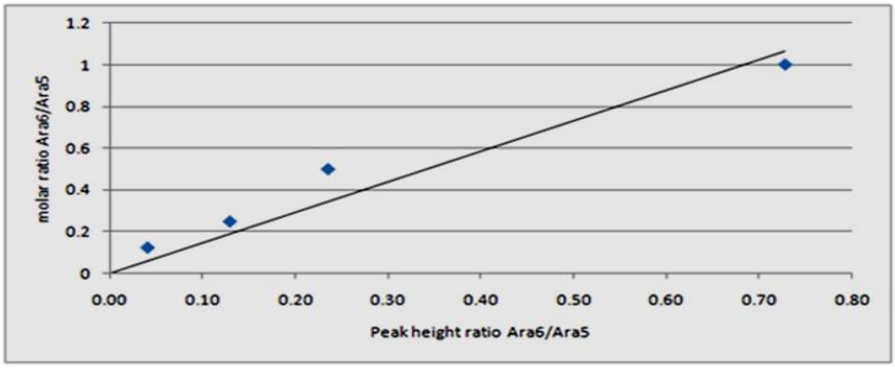

Quantitation of Enzymatic Product

	Peak heights					
	Ara6	Ara5	Ratio (height)	Experimental Ratio	Actual Ratio	Enzymatic product % conversion
Z-NPA	790	13386	0.059016883	0.059016883	0.086283	7.9
Z-FPA	1577	9577	0.164665344	0.164665344	0.240741	19.4
E-FPA	0	36595	0	0	0	0.0
Z-HPA	3299	22946	0.143772335	0.143772335	0.210195	17.4

Figure 4.8 Quantification of enzymatic product based on peak heights.

The excellent solubility of *Z*-FPA (C15) could be another favorable factor for its optimal Ara*f*-donating activity. One reason that *Z*-NPA was shown to be inactive in the past (Lee et al., 1998) is perhaps due to the presence of predominantly α anomer in the preparation. All arabinosyltransferases described so far are membrane proteins of GT-C family. One characteristic feature of these proteins is that these are all membrane bound, which beat all odds of isolation and purification. Even if these are isolated with difficulty, after expression and purification, GT-C membrane proteins are mostly insoluble and aggregate easily (Newby et al., 2009). Therefore, developing an efficient assay to pursue functional studies on AftC or to screen for inhibitors has been problematic. We have been able to express and purify AftC and shown that it has α-(1→3) arabinosyltransferase activity (Birch et al., 2008). Repeated attempts to express AftC and obtain in large amounts in *E. coli* pLySS, BL21, C41 or C43 strains (Dumon-Seignovert et al., 2004) have failed suggesting toxicity of the protein in a non-mycobacterial host.

In vitro assay using the purified recombinant AftC and DPA failed to give any product. However, with the successful reconstitution of AftC-proteoliposome and replacing DPA with analogues *Z*-FPA or *Z*-HPA, we were able to improve the *in vitro* assay with product formation in reasonable amounts. For restoring arabinosyltransferase activity for AftC, reconstructing a lipid environment seemed to be a crucial factor. The inactivity of the proteoliposome using DPPC might be due to 1) commercial DPPC is not identical to the DPPC of mycobacterium; 2) a combination of multiple lipids from Mtb are necessary for creating a "real" mycobacterial membrane environment mimicking the cell membrane that will foster proper folding of arabinosyltransferase.

In an initial attempt to test the individual lipids isolated from Mtb total lipid extracts using preparative TLC, a lipid (Band IV) (Figure 4.9) has shown better activity than other lipids for fabricating AftC proteoliposome. Mass spectral analysis revealed Band IV contained predominantly diacylPIM$_2$ (Ac$_2$PIM$_2$) with considerable heterogeneity in the fatty acyl composition of Ac$_2$PIM$_2$'s indicating that mycobacterial phospholipids are important aspects in retaining arabinosyltransferase activity. We speculate that there is a specific binding pocket in AftC that fits the Ac$_2$PIM$_2$ in order to fold properly.

.

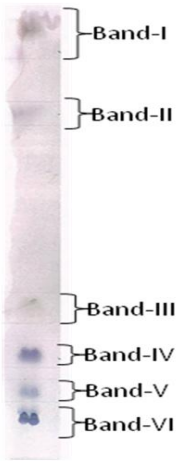

Figure 4.9 Thin Layer Chromatography plate of lipid extract from Mtb H_{37}Rv cells. The total lipid extracts where subjected to preparative TLC, bands were excised as labeled on the TLC plate and extracted from the silica gel with $CHCl_3$:CH_3OH (2:1, V:V). Organic solvents were removed and aliquot of lipid preparations were analyzed by Mass spectrometry.

4.5 Conclusions

D-Ara*f* is unique to mycobacteria and is the constituent of two most important macromolecules, AG and LAM that play significant physiological and biological roles. The enzymes involved in the polymerization of AG and LAM have been suggested to present future opportunities for developing new therapeutics (Wolucka, 2008). The fact that Ethambutol, a first line anti tuberculosis drug inhibits arabinan synthesis (Mikusova et al., 1995) and new compounds have identified that are capable of inhibiting the formation of DPA, which also inhibits Mtb grown intracellularly support this notion (Makarov et al., 2009). Our present study describes isolation of one important arabinosyltransferase whose functional studies can now be pursued due to its availability in a recombinant form. The assay developed bypasses use of radioactive pRpp, isolation of DPA and use of membrane preparations in which all arabinosyltransferases are present. Our ongoing effort encompasses refining several parameters in the assays, such as optimizing detergents for dissolving protein and lipids for forming proteoliposome to increase the conversion rate of the enzymatic reaction, and more importantly, replacing the aglycon on the acceptors (i.e., introduce an "octylamine" tag) for developing novel assays based on carbohydrate microarrays (Park and Shin, 2007) or for screening small molecule inhibitors.

4.5.1 Acknowledgments: This work was supported by Grants AI037139, AI064798, AI049151, and RR023763 from the National Institutes of Health to DC, MJ, DCC, and JZ respectively. Shiva Angala was supported by departmental Bridge Fund. The MALDI-TOF-MS analyses were performed at the Proteomics and Metabolomics Facility located at Colorado State University.

4.6 References

Alderwick, L.J., H.L. Birch, A.K. Mishra, L. Eggeling, and G.S. Besra. 2007. Structure, function and biosynthesis of the *Mycobacterium tuberculosis* cell wall: arabinogalactan and lipoarabinomannan assembly with a view to discovering new drug targets. *Biochem. Soc. Trans.* 35:1325-1328.

Alderwick, L.J., L.G. Dover, M. Seidel, R. Gande, H. Sahm, L. Eggeling, and G.S. Besra. 2006. Arabinan-deficient mutants of *Corynebacterium glutamicum* and the consequent flux in decaprenylmonophosphoryl-D-arabinose metabolism. *Glycobiology*. 16:1073-1081.

Belanger, A.E., G.S. Besra, M.E. Ford, K. Mikusova, J.T. Belisle, P.J. Brennan, and J.M. Inamine. 1996. The *embAB* genes of *Mycobacterium avium* encode an arabinosyl transferase involved in cell wall arabinan biosynthesis that is the target for the antimycobacterial drug ethambutol. *Proc. Natl. Acad. Sci. U. S. A.* 93:11919-11924.

Berg, S., J. Starbuck, J.B. Torrelles, V.D. Vissa, D.C. Crick, D. Chatterjee, and P.J. Brennan. 2005. Roles of conserved proline and glycosyltransferase motifs of EmbC in biosynthesis of lipoarabinomannan. *J Biol Chem.* 280:5651-5663.

Birch, H.L., L.J. Alderwick, A. Bhatt, D. Rittmann, K. Krumbach, A. Singh, Y. Bai, T.L. Lowary, L. Eggeling, and G.S. Besra. 2008. Biosynthesis of mycobacterial arabinogalactan: identification of a novel alpha(1-->3) arabinofuranosyltransferase. *Mol. Microbiol.* 69:1191-1206.

Dumon-Seignovert, L., G. Cariot, and L. Vuillard. 2004. The toxicity of recombinant proteins in *Escherichia coli*: a comparison of overexpression in BL21 (DE3), C41 (DE3), and C43 (DE3). *Protein Expr. Purif.* 37:203-206.

Escuyer, V.E., M.A. Lety, J.B. Torrelles, K.H. Khoo, J.B. Tang, C.D. Rithner, C. Frehel, M.R. McNeil, P.J. Brennan, and D. Chatterjee. 2001. The role of the *embA* and *embB* gene products in the biosynthesis of the terminal hexaarabinofuranosyl motif of *Mycobacterium smegmatis* arabinogalactan. *J Biol Chem.* 276:48854-48862.

Khasnobis, S., J. Zhang, S.K. Angala, A.G. Amin, M.R. McNeil, D.C. Crick, and D. Chatterjee. 2006. Characterization of a specific arabinosyltransferase activity involved in mycobacterial arabinan biosynthesis. *Chem. Biol.* 13:787-795.

Koul, A., E. Arnoult, N. Lounis, J. Guillemont, and K. Andries. 2011. The challenge of new drug discovery for tuberculosis. *Nature*. 469:483-490.

Lee, A., S.W. Wu, M.S. Scherman, J.B. Torrelles, D. Chatterjee, M.R. McNeil, and K.H. Khoo. 2006. Sequencing of oligoarabinosyl units released from mycobacterial arabinogalactan by endogenous arabinanase: identification of distinctive and novel structural motifs. *Biochemistry (Mosc).* 45:15817-15828.

Lee, R., K. Mikusova, P. Brennan, and G. Besra. 1995. Synthesis of the mycobacterial arabinose donor beta-D-arabinofuranosyl-1-monophosphoryldecaprenol, development of a basic arabinosyl-transferase assay, and identification of ethambutol as an arabinosyl transferase inhibitor. *J. Am. Chem. Soc.* 117:11829-11832.

Lee, R.E., P.J. Brennan, and G.S. Besra. 1998. Synthesis of beta-D-arabinofuranosyl-1-monophosphoryl polyprenols: examination of their function as mycobacterial arabinosyl transferase donors. *Bioorg. Med. Chem. Lett.* 8:951-954.

Liav, A., and P.J. Brennan. 2005. Stereoselective synthesis of farnesylphosphoryl [beta]-d-arabinofuranose. *Tetrahedron letters*. 46:2937-2939.

Liav, A., E. Ciepichal, E. Swiezewska, A. Bobovská, P. Dianisková, J. Blasko, K. Mikusová, and P.J. Brennan. 2009. Stereoselective syntheses of heptaprenylphosphoryl [beta]-d-arabino-and [beta]-d-ribo-furanoses. *Tetrahedron letters*. 50:2242-2244.

Liav, A., H. Huang, E. Ciepichal, P.J. Brennan, and M.R. McNeil. 2006. Stereoselective synthesis of decaprenylphosphoryl [beta]-d-arabinofuranose. *Tetrahedron letters*. 47:545-547.

Makarov, V., G. Manina, K. Mikusova, U. Mollmann, O. Ryabova, B. Saint-Joanis, N. Dhar, M.R. Pasca, S. Buroni, A.P. Lucarelli, A. Milano, E. De Rossi, M. Belanova, A. Bobovska, P. Dianiskova, J. Kordulakova, C. Sala, E. Fullam, P. Schneider, J.D. McKinney, P. Brodin, T. Christophe, S. Waddell, P. Butcher, J. Albrethsen, I. Rosenkrands, R. Brosch, V. Nandi, S. Bharath, S. Gaonkar, R.K. Shandil, V. Balasubramanian, T. Balganesh, S. Tyagi, J. Grosset, G. Riccardi, and S.T. Cole. 2009. Benzothiazinones kill *Mycobacterium tuberculosis* by blocking arabinan synthesis. *Science*. 324:801-804.

Mikusova, K., H. Huang, T. Yagi, M. Holsters, D. Vereecke, W. D'Haeze, M.S. Scherman, P.J. Brennan, M.R. McNeil, and D.C. Crick. 2005. Decaprenylphosphoryl arabinofuranose, the donor of the D-arabinofuranosyl residues of mycobacterial arabinan, is formed via a two-step epimerization of decaprenylphosphoryl ribose. *J Bacteriol*. 187:8020-8025.

Mikusova, K., R.A. Slayden, G.S. Besra, and P.J. Brennan. 1995. Biogenesis of the mycobacterial cell wall and the site of action of ethambutol. *Antimicrob. Agents Chemother.* 39:2484-2489.

Newby, Z.E., J.D. O'Connell, 3rd, F. Gruswitz, F.A. Hays, W.E. Harries, I.M. Harwood, J.D. Ho, J.K. Lee, D.F. Savage, L.J. Miercke, and R.M. Stroud. 2009. A general protocol for the crystallization of membrane proteins for X-ray structural investigation. *Nat Protoc*. 4:619-637.

Park, S., and I. Shin. 2007. Carbohydrate microarrays for assaying galactosyltransferase activity. *Organic Letters*. 9:1675-1678.

Seidel, M., L.J. Alderwick, H.L. Birch, H. Sahm, L. Eggeling, and G.S. Besra. 2007. Identification of a novel arabinofuranosyltransferase AftB involved in a terminal step of cell wall arabinan biosynthesis in Corynebacterianeae, such as *Corynebacterium glutamicum* and *Mycobacterium tuberculosis*. *J. Biol. Chem*. 282:14729-14740.

Skovierova, H., G. Larrouy-Maumus, J. Zhang, D. Kaur, N. Barilone, J. Kordulakova, M. Gilleron, S. Guadagnini, M. Belanova, M.C. Prevost, B. Gicquel, G. Puzo, D. Chatterjee, P.J. Brennan, J. Nigou, and M. Jackson. 2009. AftD, a novel essential arabinofuranosyltransferase from mycobacteria. *Glycobiology*. 19:1235-1247.

Torrelles, J.B., K.H. Khoo, P.A. Sieling, R.L. Modlin, N. Zhang, A.M. Marques, A. Treumann, C.D. Rithner, P.J. Brennan, and D. Chatterjee. 2004. Truncated structural variants of lipoarabinomannan in *Mycobacterium leprae* and an ethambutol-resistant strain of *Mycobacterium tuberculosis*. *J Biol Chem*. 279:41227-41239.

Triccas, J.A., T. Parish, W.J. Britton, and B. Gicquel. 1998. An inducible expression system permitting the efficient purification of a recombinant antigen from *Mycobacterium smegmatis*. *FEMS Microbiol. Lett.* 167:151-156.

Wolucka, B.A. 2008. Biosynthesis of D-arabinose in mycobacteria - a novel bacterial pathway with implications for antimycobacterial therapy. *FEBS J*. 275:2691-2711.

Wolucka, B.A., M.R. McNeil, E. de Hoffmann, T. Chojnacki, and P.J. Brennan. 1994. Recognition of the lipid intermediate for arabinogalactan/arabinomannan biosynthesis and its relation to the mode of action of ethambutol on mycobacteria. *J. Biol. Chem*. 269:23328-23335.

Zhang, J., A.G. Amin, A. Holemann, P.H. Seeberger, and D. Chatterjee. 2010. Development of a plate-based scintillation proximity assay for the mycobacterial AftB enzyme involved in cell wall arabinan biosynthesis. *Bioorg Med Chem*. 18:7121-7131.

Zhang, J., K.H. Khoo, S.W. Wu, and D. Chatterjee. 2007. Characterization of a distinct arabinofuranosyltransferase in *Mycobacterium smegmatis*. *J. Am. Chem. Soc*. 129:9650-9662.

Zhang, N., J.B. Torrelles, M.R. McNeil, V.E. Escuyer, K.H. Khoo, P.J. Brennan, and D. Chatterjee. 2003. The Emb proteins of mycobacteria direct arabinosylation of lipoarabinomannan and arabinogalactan via an N-terminal recognition region and a C-terminal synthetic region. *Mol. Microbiol*. 50:69-76.

4.7 - SUPPLEMENT

RECONSTITUTION OF FUNCTIONALLY ACTIVE MYCOBACTERIAL ARABINOSYLTRANSFERASE AFTC PROTEOLIPOSOME AND ASSESSMENT OF DECAPRENYLPHOSPHORYL-ARABINOSE ANALOGUES AS ARABINOFURANOSYL DONORS

1. Synthesis of *Z*-NPA, *E*-FPA and *Z*-HPA

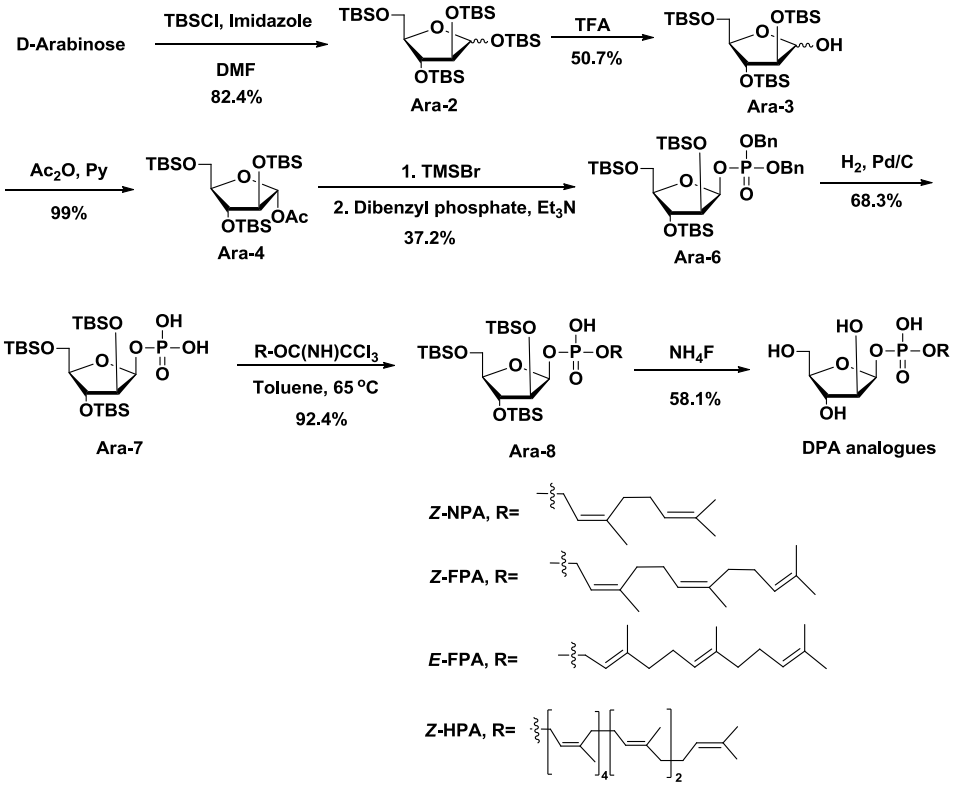

Scheme S1. Synthesis of DPA analogues

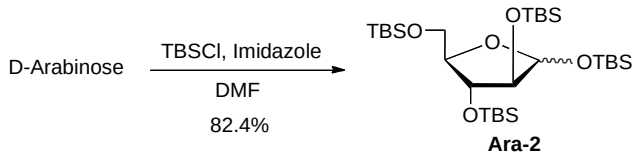

Ara-2

1,2,3,5-(Tetra *tert*-butyldimethylsilyl)-D-**arabinose (Ara-2).** D-Arabinose (2 g, 13.3 mmol) and imidazole (4.5 g, 66 mmol) were dissolved in DMF (100 mL) and to the stirred solution TBSCl (12 g, 80 mmol) was slowly added. The mixture was stirred at room temperature over night. Ice water was added to the reaction until no more precipitate was produced. The reaction was filtered and the pellet was washed with water, dissolved in acetone and concentrated by rotatory evaporator. The residue was purified by silica-gel column chromatography at EtOAc/Hexane, 1:40 to give **Ara-2** (6.631 g, 84.2%). ^{1}H NMR (400 MHz, $CDCl_3$): δ 5.13 (s, 1 H), 4.01 (dd, J = 9.6, 4.8 Hz), 3.93 (m, 2 H), 3.68 (m, 2 H), 0.90 (m, 36 H), 0.10 (m, 24 H).

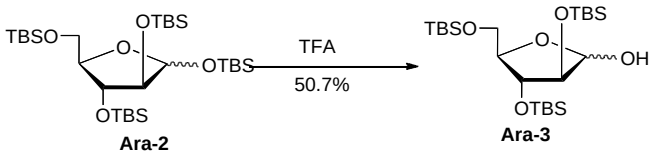

Ara-2 **Ara-3**

2,3,5-(Tri *tert*-butyldimethylsilyl)-D-**arabinose (Ara-3).** To a solution of Ara-2 (6.631 g) in dichloromethane (200 ml), trifluoroacetic acid (43 ml) was added. The mixture was stirred for two minutes before being poured into a stirred solution of NH_4OH (16 ml) in MeOH at -20^{o}C. The mixture was then allowed to warm to room temperature before partitioning between CH_2Cl_2 (50 mL) and water (50 mL). The organic phase was taken, washed with NaCl, dried over Na_2SO_4 and concentrated by rotatory evaporator followed by column chromatography (EtOAc/Hexane, 1:15) to give Ara-3 (2.8g, 50.7%). ^{1}H NMR (400 MHz, $CDCl_3$): δ 5.56 (dd, J = 6.3, 3.5 Hz, 1 H), 5.34 (dt, J = 6.6, 1.1 Hz, 1 H), 5.13-5.06 (m, 2 H), 4.21 (m, 2 H), 4.09 (m, 1 H), 4.00 (m, 1 H), 3.94-3.56 (m, 3 H), 0.90 (m,

27 H), 0.11-0.08 (m, 18 H). ^{13}C NMR (400 MHz, $CDCl_3$): δ 104.46, 96.77, 88.36, 85.19, 81.19, 78.10, 77.85, 63.85, 26.16, 25.92, 18.58, 18.06, -4.677, -5.195.

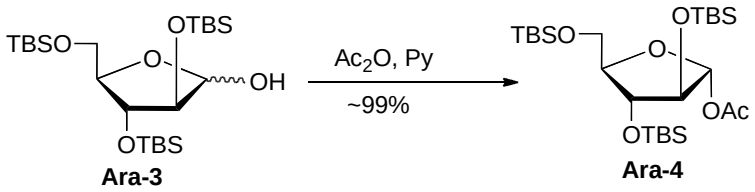

Ara-3 **Ara-4**

Acetyl 2,3,5-(Tri *tert*-butyldimethylsilyl)-D-arabinose (Ara-4). To a solution of Ara-3 (2.8 g, 1 mmol) in dry pyridine (5 mL) at 0 ^{o}C, Ac_2O (0.78 mL, 1.5 mmol) was added drop-wise with a syringe. The solution was stirred for 4 h at room temperature before being diluted with CH_2Cl_2 and washed with 5% HCl and water. The CH_2Cl_2 layer was dried over Na_2SO_4, and concentrated to give rough product. The crude product was then purified by chromatography on silica gel (hexane/EtOAc, 60:1 → 40:1) to give Ara-4 (2.7 g, 99%). TLC performed on hexane/EtOAc, 40:1. ^{1}H NMR (400 MHz, $CDCl_3$): δ 5.92 (s, 1 H), 4.16-4.05 (m, 8 H), 3.80-3.61 (m, 2 H), 2.05 (s, 3 H), 0.90 (m, 27 H), 0.11-0.08 (m, 18 H). ^{13}C NMR (400 MHz, $CDCl_3$): δ 170.45, 103.40, 89.21, 82.56, 78.30, 63.44, 21.37, 18.55, 18.02, 17.94, -3.97, -4.62, -4.82, -5.17, -5.20.

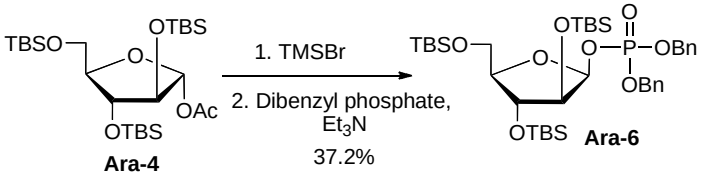

Ara-4 **Ara-6**

Dibenzyl 2,3,5-(Tri *tert*-butyldimethylsilyl)-D-arabinosyl phosphate (Ara-6). To a solution of Ara-4 (450 mg, 0.8 mmol) in CH_2Cl_2 (5 mL) was added TMSBr (0.51 ml, 4.0 mmol). The reaction mixture was stirred at room temperature for 2 h and dried in vacuo for 2 h. The resulting Ara-5 (345 mg, 1.1 mmol) and dibenzyl phosphate (460 mg, 1.65 mmol) were dried under vacuum for an additional hour and then dry toluene (5 mL) was added to the reaction mixture. Dry triethylamine (0.34 mL, 1.82 mmol) was added to the

mixture. A precipitate was observed within 1–2 minutes and the reaction mixture was allowed to stir for 16 hours at room temperature under an atmosphere of nitrogen. The solvent was removed *in vacuo.* The product was purified by chromatography on silica gel (hexane/EtOAc, 8:1 → 4:1) to yield Ara-6 (0.225 g, 37.2% 2 step yield). TLC was performed with hexane/EtOAc 8:1. ^{1}H NMR (400 MHz, $CDCl_3$): δ 5.72 (dd, 0.75 H, J = 3.2, 5.2 Hz, H-1β), 5.65 (d, 0.25 H, J = 5.2 Hz, H-1α), 5.08-5.01 (m, 4 H), 4.04 (m, 2 H), 3.84-3.56 (m, 3 H), 0.90-0.82 (m, 27 H), 0.111- -0.026 (m, 18 H). HRMS (ES$^-$) calculated $C_{37}H_{65}O_8PSi_3$ 775.3617 [M-H]. Found 775.3614.

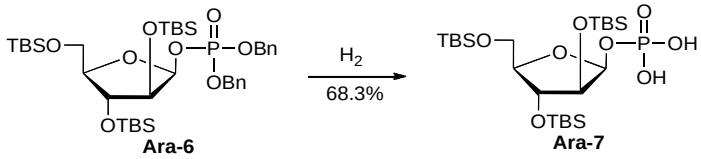

2,3,5-(Tri *tert*-butyldimethylsilyl)-D**-arabinosyl phosphate (Ara-7).** Ara-6 (149 mg, 0.06 mmol) was dissolved in a mixture of ethanol (5 mL) and triethylamine (0.1 mL, 3.0 mmol). Then 10% Pd/C (15 mg, 30% w/w) was added. The reaction vessel was evacuated and flushed three times with hydrogen gas before allowing the reaction mixture to stir for 48 hours at room temperature under a balloon of hydrogen. TLC tracked the reaction using $CHCl_3$/MeOH/NH_4OH, 50:10:0.6. The catalyst was filtered and washed with ethanol. The filtrate was concentrated and the residue was dried under vacuum to afford the triethlammonium salt **Ara-7** as an oil (0.102 g, 90%). HRMS (ES$^-$) calculated $C_{23}H_{52}O_8PSi_3$ 571.2713 [M-H]. Found 571.2716.

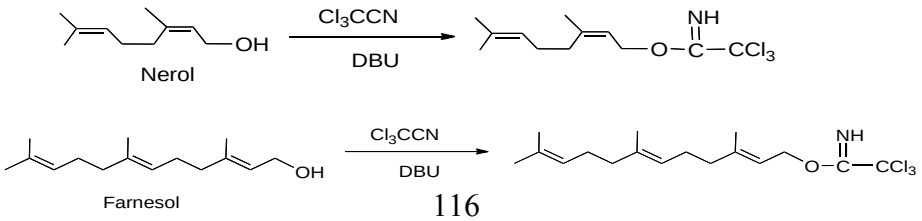

To an ice-cold solution of Nerol or Farneol (88 μl, 0.5 mmol) in DCM (5 ml) was added trichloroacetonitrile (0.1 ml, 1.0 mmol) and DBU (10 μl). The mixture was stirred at room temperature for 90 mins and dried. The mixture was purified by column chromatography (EtOAc/Hexane, 1:8) to give the trichloroacetimidate products.

***Z*-Nerosyl trichloroacetimidate**. ^{1}H NMR (400 MHz, $CDCl_3$): δ 5.45 (t, 1 H, J = 6.4 Hz), 5.08 (m, 1 H), 4.79 (d, 2 H, J = 9.6 Hz), 2.14 (m, 4 H), 1.80 (s, 3 H), 1.69 (s, 1 H), 1.61 (s, 3 H). ^{13}C NMR (400 MHz, $CDCl_3$): δ 163.09, 143.80, 132.43, 123.82, 118.71, 66.30, 32.54, 26.92, 25.92, 23.81, 17.92.

***E*-Farnesyl trichloroacetimidate.** ^{1}H NMR (400 MHz, $CDCl_3$): δ 5.45 (t, 1 H, J = 6.4 Hz), 5.08 (m, 2 H), 4.79 (d, 2 H, J = 7.2 Hz), 2.11-1.93 (m, 8 H), 1.71 (s, 3 H), 1.66 (s, 1 H), 1.59 (s, 3 H), 1.53 (s, 3 H).

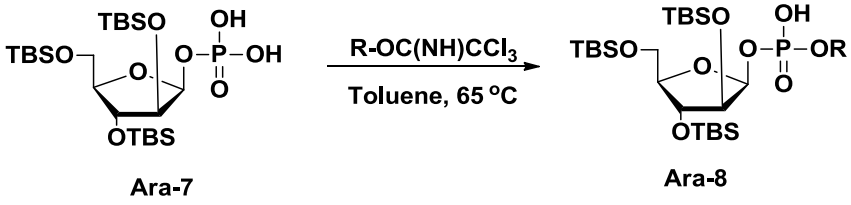

Ara-7 Ara-8

***Z*-Nerosyl-2,3,5-(Tri *tert*-butyldimethylsilyl)-D-arabinosyl phosphate (Ara-8a).** A solution of trichloroacetimidate (35 mg, 0.06 mmol) in toluene (2.5 ml) was added to triethyl amine salt of Ara-7 (30 mg, 0.19 mmol) and mixture was stirred at 65 ^{o}C for 3 h. It was then dried and the residue was purified by chromatography with silica gel ($CHCl_3$:MeOH, 5:1) to give Ara-8a (40 mg, 92.4%). ^{1}H NMR (400 MHz, $CDCl_3$): δ 5.85 (m, 0.75 H, H-1β), 5.45 (m, 0.25 H, H-1α), 5.38 (t, J = 6.0 Hz, 0.25 H, H-3α), 5.05 (m, 1 H), 4.40 (m, 1 H), 4.00 (m, 2 H), 3.62 (m, 2 H), 2.11-2.00 (m, 6 H), 1.67, 1.65, 1.56 (3 ×

Me), 0.91-0.85 (m, 18 H), 0.13-0.03 (m, 27 H). HRMS (ES^-) calculated $C_{33}H_{68}O_8PSi_3$ 707.3965 [M-H]. Found 707.3966.

***E*-Farnesyl-2,3,5-(Tri *tert*-butyldimethylsilyl)-D-arabinosyl phosphate (Ara-8b).** A solution of trichloroacetimidate (25 mg, 0.3 mmol) in toluene (2.5 ml) was added to triethyl amine salt of Ara-7 (30 mg, 0.19 mmol) and mixture was stirred at 65 ^oC for 3 h. It was then dried and the residue was purified by chromatography with silica gel ($CHCl_3$:MeOH, 5:1) to give Ara-8b (65 mg). ^1H NMR (400 MHz, $CDCl_3$): δ 5.73 (dd, J = 10.8, 20.0 Hz, 0.75 H, H-1β), 5.46 (d, J = 6.0 Hz, 0.25 H, H-1α), 5.39 (t, J = 6.0 Hz, 0.25 H, H-3α), 5.32 (t, J = 6.4 Hz, 0.75 H-3β), 5.16-5.06 (m, 5 H), 4.14-3.98 (m, 2 H), 3.91 (d, 1 H, J =6.8 Hz), 3.81-3.59 (m, 1 H), 3.30 (s, 1 H), 3.13 (s, 1 H), 2.30-2.00 (m, 10 H), 1.65 (s, 6 H), 1.57 (s 6 H), 0.90-0.86 (m, 18 H), 0.11-0.03 (m, 27 H).

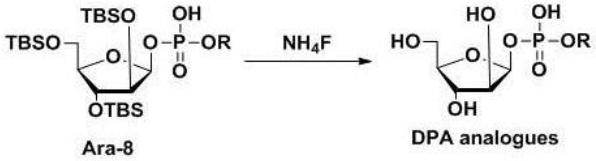

Ara-8 DPA analogues

***Z*-Nerylphosphoryl D-arabinose (*Z*-NPA).** Ara-8a (30 mg, 0.042 mmol) was deprotected by treatment with ammouium fluoride (100 mg) and 15% methanolic ammonium hydroxide (2 ml) in MeOH (5 ml) at 65 ^oC for 22 h. The mixture was cooled and diluted with DCM. The precipitate was filtered off and washed with DCM/MeOH, 5:1. The filtrate was dried and residue was chromatographed on silica gel. The product was eluted with mixture of 65:125:4, DCM/MeOH/NH_4OH to give ***Z*-NPA** (9 mg, yield: 58.1%). HRMS (ES^-) calculated $C_{15}H_{26}O_8P$ 365.1371 [M-H]. Found 365.1369.

***E,E*-Farnesylphosphoryl D-arabinose (*E*-FPA).** *E*-FPA was synthesized following the procedure of preparing *Z*-NPA. HRMS (ES^-) calculated $C_{20}H_{34}O_8P$ 433.1997 [M-H]. Found 433.2000.

***Z,Z*-Farnesylphosphoryl D-arabinose (*Z*-FPA).** Z-FPA was synthesized following the procedure of preparing *Z*-NPA. ^{1} H NMR (300 MHz, CD_3OD): d 5.49 (m, 1H, partially overlapped with the H-1 signal), 5.48 (d, *J* =4.5 Hz,1H, H-1), 5.44 (t, *J* =7.2 Hz), 4.44 (t, *J* =6.6 Hz, 2H), 4.08 (t, *J* =7.5 Hz, 1H), 3.98 (m, 1H), 3.75 (dd, *J* =3.0, 11.8 Hz), 3.63 (dd, *J* =5.7, 12.0 Hz, 1H), 2.20-1.92 (m, 8H), 1.75 (s, 3H), 1.67 (s, 3H), 1.61 (s, 3H), 1.60 (s, 3H). HRMS (ES^-) calculated $C_{20}H_{34}O_8P$ 433.1997 [M-H]. Found 433.2050.

***Z,Z,Z,Z,E,E*-heptaprenylphosphoryl D-arabinose (*Z*-HPA).** *Z*-HPA was synthesized according to an established procedure[1]. NMR data (500 MHz, CD3OD): d 5.48 (d, *J* =4.8 Hz, 1H, H-1), 5.42 (t, *J* =6.8 Hz, 1H), 5.16–5.09 (m, 4 H), 4.41 (t, *J* =6.6 Hz, 2H), 4.30 (dd, *J* =4.4, 7.3 Hz, 1H), 3.99 (d, *J* =4.4 Hz, 1H), 3.98–3.95 (m, 1H), 3.82 (dd, *J* =2.9, 12.2 Hz, 1H), 3.63 (dd, *J* =5.37, 12.2 Hz 1H), 2.14–1.97 (m, 20H), 1.76 (s, 3H), 1.70 (s, 9H), 1.69 (s, 3H), 1.63 (s, 3H), 1.61 (s, 6H), 1.37–1.31 (m, 6H). HRMS (ES^-) calculated $C_{40}H_{66}O_8P$ 705.4495 [M-H]. Found 705.4480.

CHAPTER 5

RAPID SCREENING OF INHIBITORS OF *M. TUBERCULOSIS* GROWTH USING TETRAZOLIUM SALTS

This chapter has been published (Methods Mol Biol, 2009. 465: p. 187-201).
Anita G. Amin, Shiva K. Angala, Delphi Chatterjee and Dean C. Crick

Contributions: I contributed in developing the Alamar Blue based MIC screening with Mtb, Anita Amin performed cytotoxic studies on Vero cell lines.

5.1 Introduction

Tuberculosis (TB) is the major cause of death due to an infectious agent worldwide and treatment of this ancient disease now faces new challenges due to the increase in multidrug resistant tuberculosis (MDR-TB) (Kritski et al., 1996). Most of the TB treatment drugs, as we know them today, were developed some decades ago. The current treatment for the disease spans a period of 6 to 8 months, with a combination of four drug regimen of isoniazid (INH), rifampin (RIF), ethambutol (EMB) and pyrazinamide (PZA), which when followed as recommended is highly effective. However, due to unpleasant side effects of the drug regimen, many patients find it difficult to continue treatment for such a prolonged period of time. This results in the treatment failure and development of drug resistance. The second line drugs used to treat patients, who do not respond to treatment with first line drugs, are less effective and very expensive (Espinal et al., 2000). In addition, treatment of the disease is complicated by the presence of latent, non-replicating bacilli harbored by a large portion of the population throughout the world.

These bacilli have the potential to reactivate and cause active disease(Stead, 1967; Stead et al., 1968), but current TB therapy is mainly effective against replicating and metabolically active bacteria. Therefore, to improve the existing treatment crisis for TB there is a need to discover novel drugs that would attack the disease causing bacillus in new ways, overcoming the increasing problems of MDR strains, duration of treatment and latent infections. According to the guidelines set by Global Alliance for TB drug development www.tballiance.org (Scientific Blueprint)] selection of a lead compound generally starts with an initial evaluation of a compound's preliminary characteristics such as *in vitro* determination of the minimum inhibitory concentration (MIC) of the compound against Mtb and assessment of toxicity on a eukaryotic cell line followed by evaluation of bioavailability and efficacy in animal models. While substantial progress has been made in understanding the molecular basis of drug resistance in Mtb in the last decade (Musser, 1995), understanding the mechanisms of action of antimicrobial agents is important in designing the novel antibiotics that are active against the resistant strains. Many factors are involved in understanding the mode of action of antimicrobial agents but the first and foremost is the susceptibility of microorganisms to these agents (Piatek et al., 2000).

5.1.1 Minimum inhibitory concentration

Minimum inhibitory concentrations (MICs) are considered the gold standard for determining the susceptibility of organisms to antimicrobials and are usually defined as the lowest concentrations of antimicrobial agents that inhibit more than 99% of the bacterial growth. MIC is often used to confirm susceptibility or resistance to a drug, but it is also used as a research tool to determine the *in vitro* activity of new antimicrobials. For

the purpose of this chapter, MIC is defined as the lowest concentration of the antimicrobial that inhibits the visible growth of a microorganism using a microplate based Alamar Blue assay (MABA) system.

Drug susceptibility testing or MIC determination using solid culture systems such as Lowenstein-Jensen (LJ) medium or Middlebrook agar take about 3 weeks to get results (Canetti et al., 1969; Canetti et al., 1963). Various other methods have been developed, with variable results and costs (Norden et al., 1995; Wanger and Mills, 1996; Wilson et al., 1997). However, two methods of choice for determination of MIC using Mtb have emerged: 1) the radiometric BACTEC 460 TB method using BACTEC 12B vials and 2) the colorimetric microtiter plate based method using Alamar Blue (Collins and Franzblau, 1997). Both methods have the advantage of evaluating new compounds that can be tested without the problem of standardization and the time required to complete a test is around 14 days. The BACTEC 460 system is a radiometric assay used to determine susceptibility to an antimicrobial very rapidly and has long been the system of choice, but it is less useful for high throughput screening due to high cost, high volume and generation of radioactive waste. The MABA assay is a simple, rapid, low-cost, high throughput system which does not require expensive instrumentation as the growth of bacteria can be measured by a visual color change (Collins and Franzblau, 1997).

5.1.2 Bacterial growth inhibition assay

The MABA method is used for measuring the cell proliferation and, as with the tetrazolium salts, Alamar Blue measures viability by monitoring the oxidation-reduction environment of cellular growth. Alamar Blue is soluble as well as stable in culture medium and non-toxic(Ansar Ahmed et al., 1994). The redox dye is a viable cell

indicator where the blue, nonfluorescent, oxidized form turns pink and fluorescent upon reduction. Growth can, therefore, be determined by a visual color change or, alternatively, can be measured using a fluorometer or spectrophotometer. Alamar Blue has been successfully used to assess the susceptibility of Mtb to various antimicrobials in several laboratories (Collins and Franzblau, 1997; Franzblau et al., 1998; Yajko et al., 1995).

5.1.3 Toxicology

The design of new therapeutic regimens relies on preclinical data to choose promising drugs and dosage schedules to be evaluated further in clinical trials. The identification of compounds with potential toxic activity is, therefore, an important aspect in the testing of new antimicrobials. The relatively high costs, low throughput and animal distress involved in testing compounds in whole animal models has led to development of *in vitro* assays making use of human and animal cell lines that can be used for the cytotoxicity determination assays.

5.1.4 Eukaryotic cytotoxicity assay

Cytotoxicity may be defined simply as the cell killing property of a chemical compound independent from the mechanism of death. Most cytotoxicity assays measure the amount of cell death that has occurred in a culture. When cell membranes are compromised they become porous and allow molecules to leak out, these molecules can then be quantitated and utilized to estimate viability. For example, a typical assay might measure the presence of intracellular enzymes, such as lactate dehydrogenase in the culture supernatant (Nachlas et al., 1960). The reduction of tetrazolium salts is now widely used as a reliable way to determine cytotoxicity. The yellow tetrazolium compound ([3-(4,5-

dimethylthiazol-2-yl)-5-(3-carboxymethoxyphenyl)-2-(4-sulfophenyl)-2H-tetrazolium, inner salt, MTS) is reduced by metabolically active cells into a purple formazan product, in part, by the action of dehydrogenase enzymes, which generate reducing equivalents such as NADH and NADPH (Barltrop et al., 1991; Cory et al., 1991). The resulting intracellular formazan can then be quantitated using a spectrophotometer(Mosmann, 1983).

In this chapter we describe a rapid *in vitro* method using the MABA to determine MIC values for novel growth inhibitors. In addition, we discuss the use of a color change based spectrophotometric method for determining the cytotoxic effects of the compounds. We will briefly mention how to maintain the eukaryotic cell line and determination of the concentration of the test compound causing 50% loss of cell viability (also referred to as IC_{50}).

5.2. Materials

5.2.1. Mycobacterial growth inhibition

1. Mtb $H_{37}Rv$ reference strain ATCC # 25618 (American Type Culture Collection).
2. Stock cultures containing 2 x 10^7cfu/ml of Mtb $H_{37}Rv$ strain stored frozen at -80^{o}C.
3. Middlebrook 7H9 broth (Difco), dissolved in deionised water at 4.7 g per 900 ml, autoclave sterilized.
4. Middlebrook 7H11 agar (Difco), dissolved in deionized water at 21.0 g per 900 ml, autoclave sterilized and poured in 100 mm x 15 mm Petri dishes.

5. Middlebrook OADC (Oleic acid, albumin, dextrose, catalase) enrichment (10% in 7H9 broth and/or 7H11 agar), filter sterilized (**Note 1**).

   Formula per litre purified water:

   i) 8.5 g Sodium chloride (Sigma)

   ii) 50.0 g Bovine Albumin (fraction V) (Sigma)

   iii) 0.04 g Catalase (Fisher Scientific)

   iv) 0.3 ml Oleic acid (Sigma)

   v) 20.0 g Dextrose (Sigma)

6. Tween-80 (Sigma) Prepare a 20% v/v stock (**Note 2**).
7. Tryptic soy agar (Difco) (**Note 3**)
8. Dimethyl sulfoxide (DMSO) (Sigma)
9. Isoniazid (INH) (Sigma)
10. Alamar Blue dye 10X solution (Biosource International)

5.2.2 Growth of eukaryotic cells and toxicity test

1. African green monkey kidney cell line [VERO] ATCC # CCL-81 (American Type Culture Collection).
2. Human hepatocellular liver carcinoma cell line [HepG2] ATCC # HB-8065 (American Type Culture Collection).
3. RPMI 1640 with L-glutamine tissue culture growth media (Invitrogen) (**Note 4**).

   Complete culture media includes the following supplements per litre of RPMI 1640 with L-glutamate

1.5 g Sodium bicarbonate (Sigma)

10 ml Sodium pyruvate (100 mM) [Mediatech]

140 ml Non-essential amino acids (100X) [Mediatech]

100 ml Penicillin/streptomycin solution (100X, 10000 I.U/10000 µg/ml) [Mediatech]

10% Bovine calf serum (BCS) [Hyclone] (**Note 5**)

4. Trypsin EDTA (0.05%) [Mediatech]
5. Phosphate buffered saline (PBS) (1X, pH 7.2, without calcium chloride and magnesium chloride)
6. Dimethyl sulfoxide
7. Incubator at 37^{o}C with 5% CO_2 and 75% humidity
8. Promega Cell Titer 96 Aqueous One Solution Cell Proliferation Kit
9. Microplate reader with 490 nM wavelength filter.

5.3. Methods

5.3.1 Inhibition of Mycobacterial growth

5.3.1.1 Preparation of *Mtb* working stocks

1. Starting from the ATCC stock of Mtb H37Rv, streak a loopful on a plate containing 7H11 agar supplemented with OADC and incubate at 37^{o}C to obtain isolated colonies. Pick a colony from the plate and add to 10 ml of 7H9 broth supplemented with 10% OADC and 0.05% Tween-80 in a glass culture tube with a stir bar (**Note 6**). Incubate at 37^{o}C with stirring. In addition, spread 0.5 ml from the newly made tube culture onto an LJ slant and/or 7H11 agar plate supplemented with OADC as a low passage back-up.

2. Take periodic readings of the culture at OD_{600}. Transfer 1 ml of the mid log phase culture (O.D. 600 = 0.6 – 0.9) into a new tube containing 10 ml of medium and a stir bar, and incubate with stirring at 37^{o}C, for future use (**Note 7**). Simultaneously, spread a loopful of the 10 ml culture onto a Tryptic soy agar plate. (**Note 3**).
3. Divide the rest of the inoculum from step 1 between two Erlenmeyer flasks containing 50 ml of medium each. This is passage 1 (**Note 8**). Incubate the flask cultures on a rotary shaker at 125 rpm and tube cultures on a stir plate at 37^{o}C till they reach an OD_{600} of 0.6 – 0.9. For a second scale up, divide the 50 ml culture between two 1 liter flasks each containing 500 ml media. This is passage 2. Spread a loopful of this culture on a Tryptic soy agar plate to check for contamination.
4. The 500 ml culture is the working stock and is ready to be frozen in aliquots when it reaches an OD_{600} of 0.6 – 0.9. Add 1.5 ml aliquots of the 500 ml culture to 2.0 ml cryovials, swirling the culture flask frequently to keep the bacteria in suspension. Place the vials in appropriately labeled freezer boxes in the order in which they were filled. Store the culture stocks frozen at -80^{o}C. Take one cryovial from each freezer box and thaw on ice. Make 8 x 1:10 serial dilutions of each stock culture vial taken from the freezer box and plate 0.1 ml on 7H11 agar plates containing OADC. Spread the inoculum and incubate at 37^{o}C. The plates should be ready to count in 2-3 weeks. Identify a plate with about 100 – 200 colonies, count the colonies and correct for the appropriate dilution factor. The cfu/ml should be approximately 2 x 10^{7} cfu/ml (**Note 9**).

5.3.1.2 Compound stock solutions and Solubility

1. Test compounds are prepared as 20 mg/ml stocks in appropriate solvents such as deionized water, dimethyl sulfoxide or ethanol, depending on the solubility of the compound and then further diluted to 5 mg/ml working stocks (**Note 10**).
2. Isoniazid (INH) is used as a positive control in all MABA plates and is prepared in deionized sterile water at 10 mg/ml stock concentration which is further diluted to 25 µg/ml working stock.

5.3.1.3 Alamar blue susceptibility assay

1. Take a sterile 96 well round bottom microplate and add 200 µl of sterile deionized water to all of the wells on the outer perimeter (Figure.5.1). This helps to minimize the evaporation of the medium in the test wells during incubation.
2. Add 98 µl of 7H9 broth supplemented with 10% OADC and 0.05% Tween-80 in the wells in column 2, rows B to G. Add 50 µl media to the rest of the wells from B3 to G11 (Figure.5.1).
3. Add 2 µl of the test compound from the 20 µg/ml stock concentration to the wells in column 2, rows B to F, and 2 µl of INH from the 25 µg/ml stock concentration to well G2 (Figure.5.1).
4. Take 50 µl from column wells B2 to G2 and transfer to column wells B3 to G3. Identical serial dilutions (1:2) are made up to B10 to G10, and the excess 50 µl medium is discarded from the wells B10 to G10.
5. Thaw the frozen stock vial of Mtb $H_{37}Rv$ on ice and add 100 µl to 10 ml fresh medium. Add 50 µl of this mixture to wells B2 to G11 so the final concentration is 1 x 10^5 cfu/ml in each. The wells B11 to G11 serve as a compound free

control. The final concentration for the test compounds now ranges from 50 µg/ml to 0.19 µg/ml (**Note 11**) and 0.25 µg/ml to 0.0009 µg/ml for INH. Negative control wells (B11 to G11) have only the solvent and bacterial culture added.

6. The plate is sealed with parafilm and incubated at 37°C for 5 days (**Note 12**).
7. At the end of a 5 day incubation, 10 µl of Alamar Blue reagent is added to well B11. The plate is reincubated at 37°C for 24 h. If well B11 turns pink, the reagent mixture should be added to all the remaining wells in the microplate (**Note 13**).
8. The plate is resealed and incubated for an additional 24h at 37°C, and the color change in all of the wells recorded at the end of incubation. Blue indicates no growth whereas pink indicates growth (**Note 14**).

Figure 5.1 Representative 96 well microplate format for screening compounds to determine their MICs on Mtb $H_{37}Rv$ using MABA.

5.3.1.4 Compounds tested against Mtb growth inhibition by micro-titer Alamar blue assay method.

In this study we screened nearly 2000 compounds against Mtb growth inhibition. The library consisted of a diverse range of compounds which were further modified based on their preliminary inhibitory effect of the parent compound on the validated drug targets of Mtb (Figure 5.2). The librarycompounds belongs to various classes, 1) sulphonamides, 2) 5-amino thymidine analogs, 3) 5-amino-deoxy uridine analogs, 4) allylaminomethanone-A, 5) *N*- *N'*-bis[*p*-(isoamyloxyl) phenyl] thiourea derivatives (THC).

The RmlC and GlfT enzymes of Mtb are validated drug targets with an already established assay (Ma et al., 2001; Scherman et al., 2003) for screening novel compounds for their activity. Libraries of sulphonamides, 5-amino-deoxythymidine and 5-amino-deoxyuridine were generated to target these enzymes. These libraries were screened initially at two different concentrations 400 µM (200 µg/ml with MW of 500) and 20 µM (10 µg/ml with MW of 500). The compounds identified active to be inhibitory at a concentration of 20 µM against the Mtb growth were further screened for their MIC but none of them have showed any significant effect at lower concentrations.

Derivatives of allylaminomethanone-A, targets MenA biosynthesis in mycobacteria (Kurosu et al., 2007). Compounds of this class were tested against the mycobacterial growth inhibition and a series of compounds with higher inhibitory activities ranging from 0.58-2.4 µM (Dhiman et al., 2009) were identified.

Thiocarlide (THC; *N*-*N'*-bis[*p*-(isoamyloxyl) phenyl] thiourea) also known as isoxyl, has been used in the past to treat TB but later discontinued because of its poor bioavailability. Several THC derivatives were synthesized at Colorado state university, in an effort to

improve its therapeutic value and it was found that the arabino analog derivative was the most promising candidate with an MIC of 1.5-3.1 µg/ml against Mtb. These compounds were further tested for bioavailability assays in mice (Liav et al., 2008).

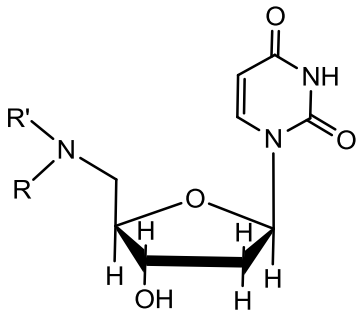

5-amino-deoxy-uridine

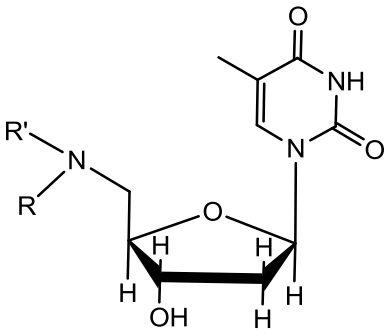

5-amino-deoxy-thymidine

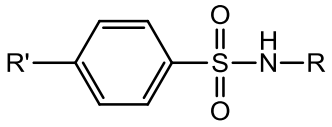

Sulphonamides

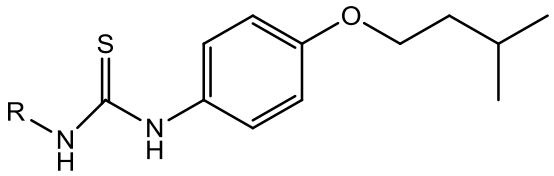

N-*N'*-bis[*p*-(isoamyloxyl) phenyl] thiourea (THC)

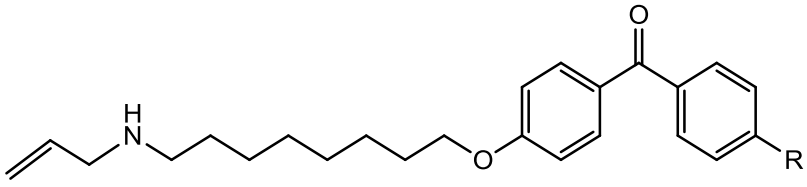

Allylaminomethanone-A

Figure 5.2 Parental scaffold structures of library compounds tested against Mtb growth inhibition by micro-titer Alamar blue assay.

5.3.2 Cytotoxicity

5.3.2.1 Maintenance of eukaryotic cell lines

The African green monkey kidney cells (Vero), a cell line that does not generally modify compounds that are added to it (Yasumura and Kawakita, 1963) and the human hepatoma cell line (HepG2), a cell line capable of modifying compounds (Bassi et al., 1991; Ferro et al., 1988), are grown as monolayers. In order to keep the cell cultures healthy and actively growing, it is necessary to subculture them at regular intervals. The most common method of sub cultivation is the use of proteolytic enzymes such as trypsin or collagenase to break the cell to substrate and intercellular connections. After the proteolytic disassociation of cells into a single cell suspension, the cells are diluted with fresh media and transferred into new culture flasks. The cells attach to the surface of the flask and begin to grow and divide and reach near confluency when they are again ready to be sub-cultured or used for testing purposes.

1. Cells are grown in 75 cm^2 tissue culture flasks in RPMI 1640 complete media.
2. To harvest a cell monolayer, remove and discard the culture medium. Rinse the cell layer with 5 ml of the phosphate buffered saline (PBS) before adding trypsin (**Note 15**). Add 2-3 ml of trypsin solution to the cell layer and check the progress of the enzyme treatment every 5 minutes for a maximum of 15 minutes. Monolayers that are particularly difficult to detach can be placed at 37^oC to facilitate detachment (**Note 16**).

3. Add 8 - 10 ml of growth medium to the cell suspension and wash any remaining cells from the bottom of the culture flask. Pipette the cell suspension up and down several times to ensure single cell dispersion.
4. Count the cells using a hemocytometer. Add 10 - 20 µl of medium containing cells to the hemocytometer, count the cells in four large corner squares (these are 1 mm x 1 mm in area) using a microscope at low magnification (10X) (**Note 17**). Take the average of the four counts and multiply that number times 1 x 10^4 to obtain the number of cells per ml. Take 50,000 cells and seed a new 75 cm^2 tissue culture flask containing 30 ml RPMI 1640 complete media.
5. Repeat steps 1 to 4 as the cells near confluence (2-3 days).

5.3.2.2 Preparation of compound solutions

1. The test compound stocks should be prepared the same way as described in 3.1.2. However, start with the original concentration of 20 mg/ml and based on the MIC of the test compound, make further dilutions.
2. Five separate serial dilutions of each test compound are prepared in complete medium, resulting in the final concentration ranging from 1X MIC to 25X MIC of the respective compound.

5.3.2.3 Cytotoxicity assay

1. Using a near confluent (75 – 95%) 75cm^2 tissue culture flask, pipette out the media and rinse the cells with 5 ml PBS buffer without disturbing the monolayer (**Note 14**).
2. To detach cells from the surface of the flask, add 5 ml trypsin and treat as described in 3.2.1.

3. Add 5 ml media and pipette up and down to form a single cell suspension.

4. Count 10 µl aliquot of the cells on a hemocytometer as described in 3.2.1.

5. Calculate and adjust cell suspension to 50,000 cells/ml by adding fresh RPMI 1640 complete media and dispense 100 µl/well in a sterile 96 well flat bottom plate in wells B2 to G11 (Figure. 5.3).

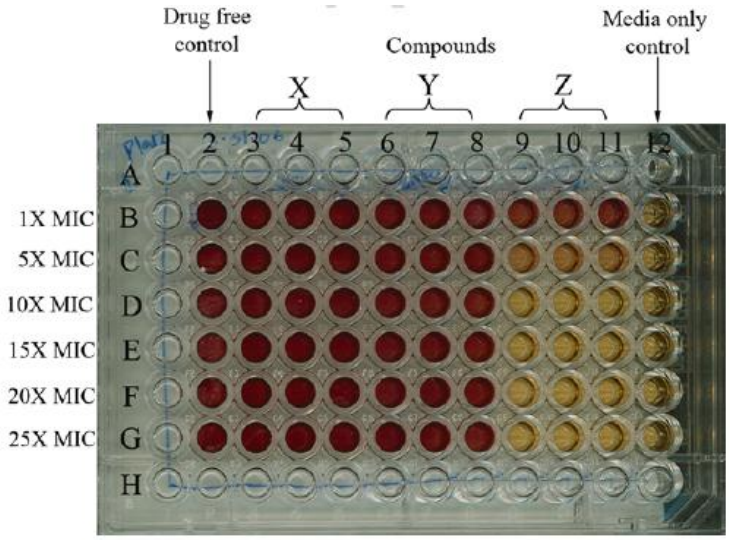

Figure 5.3 Representative 96 well plate format for screening compounds to determine their effect on the viability of a eukaryotic cell line.

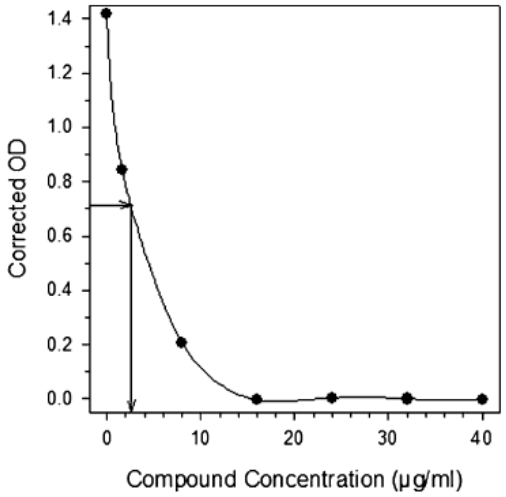

Figure 5.4 Representative graph showing cytotoxic effect of a compound and determination of its IC_{50} value (~ 2.5 µg/ml).

6. Add 200 µl sterile H_2O to wells A1 to A12, H1 to H12 and B1 to G1 on the outer perimeter of the 96 well plate to limit evaporation. Add 200 µl medium in wells from B12 to G12 as a media only (negative) control.
7. Incubate plate for 2 h in the CO_2 incubator to let the cells attach to the surface of the plate.
8. Add the test compounds to the wells B3 to G11 based on their MIC's starting at the 1X MIC and going up to 25X MIC (Figure. 5.3. Each concentration of the test compound should be done in triplicate. Therefore, three compounds can be tested in each 96 well plate (**Note 18**). Bring up the total volume of wells B2 to G11 to 200 µl by adding appropriate amount of fresh medium.
9. Incubate the plates for 72 h at 37ºC in the CO_2 incubator and visually inspect under the inverted microscope every 24 h to check for contamination or cell lysis.
10. After 72 h remove the media from all wells and wash the cells with PBS buffer. Add 100 µl of RPMI 1640 complete medium to each well from B2 to 12 (**Note19**).
11. Add 10 µl of thawed cell Titer 96 Aqueous One Solution Reagent to wells B2 to G12 and incubate at 37º C in CO_2 incubator for 4 h (17, 18, 19, 23) (**Note 20**).
12. Read the absorbance at 490 nm wavelength using a microplate (**Note 21**).
13. Calculate the IC_{50} value for each test compound. Background absorbance, due solely to the reaction of the reagents, is deducted from the absorbance values generated by the treated and untreated cells. The mean absorbance generated by the medium only control is denoted as $IC_{0.}$ The mean absorbance obtained from the cells only control is denoted as IC_{100} and for the test compounds as $IC_{100T.}$ To obtain the corrected absorbance, IC_0 is subtracted from the IC_{100} and IC_{100T}

absorbance values. To determine IC_{50} for each compound, plot the corrected absorbance at 490 nm (Y axis) versus concentration of the compound tested (X-axis), and calculate the IC_{50} value by determining the X-axis value corresponding to one-half the difference between the corrected IC_{100} and corrected IC_{100T} absorbance values(Promega, 1999) (Figure. 5.4).

5.3.3. Notes

1. Gently warm the oleic acid solution until it melts, do not microwave or heat above 55^{o}C. Albumin should be added gradually to avoid clumping. Store OADC at 4^{o}C, protected from light. The OADC supplement is extremely heat-labile and should not be added to hot media.

2. Mycobacteria, particularly Mtb, have a tendency to clump in culture because of the presence of a thick waxy outer cell wall. The addition of a non-ionic detergent to the media reduces the amount of clumping and provides a more homogenous suspension of cells. The 20% v/v working stock solution of Tween-80 should be filter sterilized through 0.2 µm membrane and stored at 4^{o}C.

3. Tryptic soy agar is mainly used as an initial growth medium to observe colony morphology and develop a pure culture. If the culture has contaminating bacteria in it, they will become apparent in 24-48 h.

4. The medium supplements are added along with 10% bovine calf serum. The pH of the complete media should be 7.0. The addition of non-essential amino acids may reduce the pH and this can be adjusted by adding potassium hydroxide (KOH) solution to the media.

5. The serum is always stored frozen. Before adding it to the RPMI 1640 media, remove the serum bottle from the freezer and allow it to acclimate to the room temperature for about 10 minutes and place in a 37^{o}C water bath. Excessive temperature can degrade the heat labile nutrients in the serum. Thawing of serum is crucial to its performance and, therefore, it is recommended to periodically swirl the serum container while thawing, otherwise cryoprecipitates are formed, which are often insoluble. Filtering serum to remove cryoprecipitates is not recommended as it could result in loss of nutrients.

6. It is always recommended to start cultures on a solid medium by taking a loopful of the thawed stock and streaking on an appropriate agar plate. After growth, pick a colony from the plate and add to liquid medium since it is sometimes difficult to start the bacterial growth in a liquid medium from the frozen state.

7. The purpose of having a staggered series of drop back cultures lagging behind the primary cultures is if the primary culture is contaminated there is no need to start a 10 ml culture again from the seed stock.

8. Passage number is important, the working stocks should be no greater than passage 6, the lower the better. Every time a culture is sub-cultured or plated onto a solid media, it is considered a passage.

9. To determine the cfu/ml, take one vial from each freezer box to plate out serial dilutions, keeping track of the boxes the vials come from. This is done in order to avoid any variations in the cfu/ml from cryovials filled at different times.

10. The concentration of the solvent carrier for the test compound in the medium with cells should not exceed to toxic levels. If a higher concentration of the compound is required, make dilutions using the tissue culture medium instead of the solvent.

11. The concentration of the test compounds used here are just representative values, and can be changed according to individual requirements and the nature of the compound being tested.

12. Alternately, the plates can be sealed in a ziplock bag and a damp paper towel placed on top of the plate inside the bag in order to prevent evaporation during incubation.

13. If the B11 well remains blue, the Alamar Blue reagent should be added to another control well C11 and reincubated for additional 24 h and checked for color change.

14. Wells may appear violet after 24 h incubation, but they invariably change to pink, after extended incubation at 37^{o}C, indicating growth. The MIC is defined as the lowest concentration of compound in which the dye remains blue. A standard scanner can be used to generate a permanent record of the plate (Figure.5.1).

15. Trypsin is the most common disassociating solution and its action is inhibited by serum. Residual amounts of serum are often responsible for the failure of the trypsin solution to detach the cells from the substrate. To avoid this, the cells are washed with PBS before treatment with trypsin.

16. After adding trypsin to the cells in the tissue culture flask and incubating for 10-15 minutes, a quick screening of the cell suspension under an inverted microscope is recommended in order to ensure complete detachment of cells from the surface of the tissue culture flask and also to get a suspension of at least 95% single cells.

17. It is easy to double count cells that lie on the lines between individual small squares. For cells that touch the lines defining the squares, only count those touching the top or left side of an individual square.

18. A separate plate should be used to determine that the solvent is at an acceptable (non-toxic) concentration.

19. PBS and RPMI 1640 complete media is stored at $4^{o}C$ and should not be used directly on the cells, bring to room temperature before use.

20. The Cell Titer 96 Aqueous Solution contains a tetrazolium compound [3-(4,5-dimethylthiazol-2-yl)-5-(3-carboxymethoxyphenyl)-2-(4-sulfophenyl)-2H-tetrazolium, inner salt; MTS] and an electron coupling reagent (phenazine ethosulfate; PES) which has an enhanced chemical stability and when combined with tetrazolium salt makes a stable solution. The tetrazolium compound is reduced by cells into a purple formazan product and thus the color change. The quantity of formazan is measured by a 96 well plate reader at 490 nm absorbance and is directly proportional to the number of viable cells in the culture medium (17).

21. Absorbance values lower than the control cells indicate a reduction in the rate of cell growth. Conversely, a higher absorbance indicates an increase in cell proliferation.

5.4 Acknowledgements

Research in the author's laboratories was supported by grants AI-057836, AI-37139, AI-18357, AI-46393, AI-49151 and U54 AI-06357 from the National Institute of Allergy and Infectious Diseases, National Institutes of Health, USA.

5.5 References

Ansar Ahmed, S., R.M. Gogal Jr, and J.E. Walsh. 1994. A new rapid and simple non-radioactive assay to monitor and determine the proliferation of lymphocytes: an alternative to [3H] thymidine incorporation assay. *J. Immunol. Methods*. 170:211-224.

Barltrop, J.A., T.C. Owen, A.H. Cory, and J.G. Cory. 1991. 5-(3-Carboxymethoxyphenyl)-2-(4, 5-dimethylthiazolyl)-3-(4-sulfophenyl) tetrazolium, inner salt (MTS) and related analogs of 3-(4, 5-dimethylthiazolyl)-2, 5-diphenyltetrazolium bromide (MTT) reducing to purple water-soluble formazans as cell-viability indicators. *Bioorg. Med. Chem. Lett.* 1:611-614.

Bassi, A., S. Piana, S. Penco, O. Bosco, S. Brenci, and M. Ferro. 1991. Use of an established cell line in the evaluation of the cytotoxic effects of various chemicals. *Boll Soc Ital Biol Sper. (Bollettino della Società italiana di biologia sperimentale)*. 67:809.

Canetti, G., W. Fox, A. Khomenko, H. Mahler, N. Menon, D. Mitchison, N. Rist, and N. Šmelev. 1969. Advances in techniques of testing mycobacterial drug sensitivity, and the use of sensitivity tests in tuberculosis control programmes. *Bull. World Health Organ.* 41:21.

Canetti, G., S. Froman, J. Grosset, P. Hauduroy, M. Langerová, H. Mahler, G. Meissner, D. Mitchison, and L. Šula. 1963. Mycobacteria: laboratory methods for testing drug sensitivity and resistance. *Bull. World Health Organ.* 29:565.

Collins, L., and S.G. Franzblau. 1997. Microplate alamar blue assay versus BACTEC 460 system for high-throughput screening of compounds against *Mycobacterium tuberculosis* and *Mycobacterium avium*. *Antimicrob. Agents Chemother.* 41:1004.

Cory, A., T. Owen, J. Barltrop, and J. Cory. 1991. Use of an aqueous soluble tetrazolium/formazan assay for cell growth assays in culture. *Cancer Commun.* 3:207.

Dhiman, R.K., S. Mahapatra, R.A. Slayden, M.E. Boyne, A. Lenaerts, J.C. Hinshaw, S.K. Angala, D. Chatterjee, K. Biswas, and P. Narayanasamy. 2009. Menaquinone synthesis is critical for maintaining mycobacterial viability during exponential growth and recovery from non replicating persistence. *Mol. Microbiol.* 72:85-97.

Espinal, M.A., S.J. Kim, P.G. Suarez, K.M. Kam, A.G. Khomenko, G.B. Migliori, J. Baez, A. Kochi, C. Dye, and M.C. Raviglione. 2000. Standard short-course

chemotherapy for drug-resistant tuberculosis: treatment outcomes in 6 countries. *JAMA*. 283:2537-2545.

Ferro, M., A. Bassi, and G. Nanni. 1988. Hepatoma cell cultures as in vitro models for the hepatotoxicity of xenobiotics. *ATLA*. 16:32-37.

Franzblau, S.G., R.S. Witzig, J.C. McLaughlin, P. Torres, G. Madico, A. Hernandez, M.T. Degnan, M.B. Cook, V.K. Quenzer, and R.M. Ferguson. 1998. Rapid, low-technology MIC determination with clinical *Mycobacterium tuberculosis* isolates by using the microplate Alamar Blue assay. *J. Clin. Microbiol.* 36:362.

Kritski, A.L., M.J. Marques, M.F. Rabahi, M.A. Vieira, E. Werneck-Barroso, C.E. Carvalho, N. Andrade Gde, R. Bravo-de-Souza, L.M. Andrade, P.P. Gontijo, and L.W. Riley. 1996. Transmission of tuberculosis to close contacts of patients with multidrug-resistant tuberculosis. *Am. J. Respir. Crit. Care Med.* 153:331-335.

Kurosu, M., P. Narayanasamy, K. Biswas, R. Dhiman, and D.C. Crick. 2007. Discovery of 1, 4-Didydroxy-2-naphthoate Prenyltransferase Inhibitors: New Drug Leads for Multidrug-Resistant Gram-Positive Pathogens. *J. Med. Chem.* 50:3973-3975.

Liav, A., S.K. Angala, P.J. Brennan, and M. Jackson. 2008. N-D-aldopentofuranosyl-N'-[p-(isoamyloxy)phenyl]-thiourea derivatives: potential anti-TB therapeutic agents. *Bioorg. Med. Chem. Lett.* 18:2649-2651.

Ma, Y., R.J. Stern, M.S. Scherman, V.D. Vissa, W. Yan, V.C. Jones, F. Zhang, S.G. Franzblau, W.H. Lewis, and M.R. McNeil. 2001. Drug targeting *Mycobacterium tuberculosis* cell wall synthesis: genetics of dTDP-rhamnose synthetic enzymes and development of a microtiter plate-based screen for inhibitors of conversion of dTDP-glucose to dTDP-rhamnose. *Antimicrob. Agents Chemother.* 45:1407.

Mosmann, T. 1983. Rapid colorimetric assay for cellular growth and survival: application to proliferation and cytotoxicity assays. *J. Immunol. Methods*. 65:55-63.

Musser, J.M. 1995. Antimicrobial agent resistance in mycobacteria: molecular genetic insights. *Clin. Microbiol. Rev.* 8:496.

Nachlas, M.M., S.I. Margulies, J.D. Goldberg, and A.M. Seligman. 1960. The determination of lactic dehydrogenase with a tetrazolium salt* 1. *Anal. Biochem.* 1:317-326.

Norden, M.A., T.A. Kurzynski, S.E. Bownds, S.M. Callister, and R.F. Schell. 1995. Rapid susceptibility testing of *Mycobacterium tuberculosis* (*H37Ra*) by flow cytometry. *J. Clin. Microbiol.* 33:1231.

Piatek, A.S., A. Telenti, M.R. Murray, H. El-Hajj, W.R. Jacobs Jr, F.R. Kramer, and D. Alland. 2000. Genotypic analysis of *Mycobacterium tuberculosis* in two distinct

populations using molecular beacons: implications for rapid susceptibility testing. *Antimicrob. Agents Chemother.* 44:103.

Promega, C. 1999. Cell-titer 96 aqueous one solution cell proliferation assay. *Promega Technical Bulletin*. 245:1-9.

Scherman, M.S., K.A. Winans, R.J. Stern, V. Jones, C.R. Bertozzi, and M.R. McNeil. 2003. Drug targeting *Mycobacterium tuberculosis* cell wall synthesis: development of a microtiter plate-based screen for UDP-galactopyranose mutase and identification of an inhibitor from a uridine-based library. *Antimicrob. Agents Chemother.* 47:378.

Stead, W. 1967. Pathogenesis of a first episode of chronic pulmonary tuberculosis in man: recrudescence of residuals of the primary infection or exogenous reinfection? *Am. Rev. Respir. Dis.* 95:729.

Stead, W.W., G.R. Kerby, D.P. Schlueter, and C.W. Jordahl. 1968. The clinical spectrum of primary tuberculosis in adults. *Ann. Intern. Med.* 68:731.

Wanger, A., and K. Mills. 1996. Testing of *Mycobacterium tuberculosis* susceptibility to ethambutol, isoniazid, rifampin, and streptomycin by using Etest. *J. Clin. Microbiol.* 34:1672.

Wilson, S.M., Z. Al-Suwaidi, R. McNerney, J. Porter, and F. Drobniewski. 1997. Evaluation of a new rapid bacteriophage-based method for the drug susceptibility testing of *Mycobacterium tuberculosis*. *Nat. Med.* 3:465.

Yajko, D.M., J.J. Madej, M.V. Lancaster, C.A. Sanders, V.L. Cawthon, B. Gee, A. Babst, and W.K. Hadley. 1995. Colorimetric method for determining MICs of antimicrobial agents for *Mycobacterium tuberculosis*. *J. Clin. Microbiol.* 33:2324.

Yasumura, Y., and Y. Kawakita. 1963. Vero cell line derived from the kidney of a normal adult, African green monkey (Cercopithecus) Nippon Rinsho. 21, 1209.

CHAPTER 6.0

SUMMARY AND FUTURE DIRECTIONS

Summary

D-arabinofuranose, a prominent component of the mycobacterial cell wall, is a constituent present in arabinogalactan (AG) and lipoarabinomannan (LAM) that are essential for the viability of Mtb (Bhamidi et al., 2009; Kaur et al., 2009). To date, seven arabinosyltransferases have been identified that are shown to be involved in the assembly of arabinan in AG and LAM. AftA transfers the first arabinose unit to the galactan chain (Alderwick et al., 2006), AftB terminates the arabinan biosynthesis by adding a terminal capping residue β-Ara*f*-(1→2) (Seidel et al., 2007), and AftC is responsible for internal α-1,3 branching in both AG an LAM (Birch et al.; Birch et al., 2008; Zhang et al., 2011). AftD has been shown to be involved in α-Ara*f*-(1→3) branching (Skovierova et al., 2009), EmbA and EmbB (arabinosyltransferases) are involved in the formation of a characteristic terminal Ara_6 motif, [β-D-Ara*f*-(1→2)-α-D-Ara*f*-(1→)]$_2$-(3,5)-α-D-Ara*f*-(1→5)-α-D-Ara*f*, of AG (Escuyer et al., 2001), and EmbC is involved in the elongation of arabinan in LAM pathway (Shi et al., 2006; Zhang et al., 2003). In mycobacteria, this small family of arabinosyltransferases is essential for the survival of the bacteria.

Ethambutol (EMB), a front-line anti-TB drug only targets the key arabinosyltransferases like EmbA, EmbB and EmbC proteins. The EMB insensitive arabinosyltransferases like AftB and AftC, that are not a target of EMB, thus require new compounds to prevent frequently encountered EMB resistance. As such, AftB and AftC arabinosyltransferases play a critical role in the arabinan biosynthesis (Birch et al.; Birch et al., 2008; Seidel et al., 2007). This work emphasizes, therefore, attempts to develop a robust cell free arabinosyltransferase assay for screening small molecule inhibitors against AftB and AftC activity. Hence, targeting these enzymes is an ideal choice in anti-tuberculosis drug development.

Summary of development of AftB arabinosyltransferase assay

When this project was initiated, the function of AftB was not reported, and my research was involved in the identification of D-Ara*f* transferases in *M. smegmatis* and their role in arabinan synthesis. In this direction, we developed a cell free arabinosyltransferase assay using a synthetic disaccharide as an acceptor and radioactive p[^{14}C]Rpp as an indirect arabinose donor in the presence of *M. smegmatis* crude membranes as enzyme source. Characterization of the enzymatic product revealed a trisaccharide (1→2) linked as shown in Figures 2.7 and 2.8. The formation of (1→2) linked enzymatic product was a characteristic feature of terminal capping residue β-Ara*f*-(1→2) present at the non-reducing end of AG and LAM in mycobacterial cell wall (Chatterjee, 1997). The overall goal of this work was then to move beyond chemical characterization of the enzymatic product and identify this linkage specific arabinosyltransferase by tagging benzophenone or biotinylated probes to the synthetic acceptors. At this point Seidel et al., 2007 reported AftB as a β-Araf-(1→2) capping enzyme. Our results using the disaccharide acceptor to

identify the AftB arabinosyltransferase activity in a cell free assay also showed (1→2) linkage. We decided to convert the radioactive cell free assay into a non-radioactive AftB specific arabinosyltransferase assay to identify inhibitors (novel compounds) against AftB activity.

It is evident from the literature that a monoclonal antibody (CS35-mAb) available at CSU recognizes glycans containing D-arabinofuranosides, in particular an arabinan segment composed of α-Araf-(1→5), α-Ara*f*-(1→3) and β-Ara*f*-(1→2) linked residues (Kaur et al., 2002; Rademacher et al., 2007). Based on this, we decided to probe AftB activity using CS35 since the enzymatic product was similar to recognition specificity of CS35. In this direction, we successfully biotinylated the aglycon of the disaccharide acceptor and developed a plate based ELISA for arabinosyltransferase assay using CS35-mAb. This method was laborious and time consuming as it required long incubation times and several washing steps. Moreover, there was sufficient background and the detection of enzymatic product was not as sensitive as the positive control reactions. Therefore, we decided to choose a more sensitive fluorescein labeling method for the AftB assay development. Unfortunately, we were not able to trace the fluorescein labeled substrate or its enzymatic product by TLC or mass spectrometry. In retrospect, this result was not surprising considering the number of parameters that had affected this method negatively. These parameters included 1) failure to detect a fluorescein labeled acceptor from the enzymatic mixture could be a structural modification of fluorescein by the enzymes of crude membranes from *M. smegmatis*, 2) absence of pure AftB enzyme, 3) fluorescein moiety could be interfering with CS35-mAb recognition.

A vision of the AftB future work

The following section describes the further development of AftB assay for screening small molecule inhibitors.

The two options for further development of AftB assay will be

i) Optimization of existing ELISA based assay developed in Chapter 3.

ii) Development of new assay method using commercially available AlphaLISA assay kit from Perkin elmer.

Optimization of existing AftB ELISA based assay developed in Chapter 3

In the AftB transferase assay, we already demonstrated that the enzymatic product formed is recognized by CS35-mAb, but this assay was not further optimized for screening compounds. The parameters which influenced the low signal detection of the enzymatic product by CS35-mAb are presumably substrate concentration, anitbody concentration, incubation times, and incubation temperatures. Optimization of these conditions may improve this assay into a robust and reproducible system for screening inhibitors for AftB activity and could be used in the future for other arabinosyltransferases as well.

AlphaLISA technology

This technology is non-radioactive, highly sensitive and will not involve any wash steps for measuring AftB activity. Further, AlphaLISA technology was well established for measuring enzymatic activities from crude cell lysates and culture supernatants (Szekeres et al., 2008). This technology was developed based on the use of different types of beads, AlphaLISA acceptor beads, and Alpha donor beads. Biotinylated antibody is conjugated to commercially available streptavidin donor beads while another anti-analyte antibody is

conjugated to AlphaLISA acceptor beads. The presence of the analyte in the reaction mixture brings both the beads in close proximity to each other. The excitation of the donor beads at 660 nm provokes the release of singlet oxygen molecules that triggers a series of chemical reactions in the acceptor beads, resulting in light emission at 615 nm as shown in Figure 6.1.

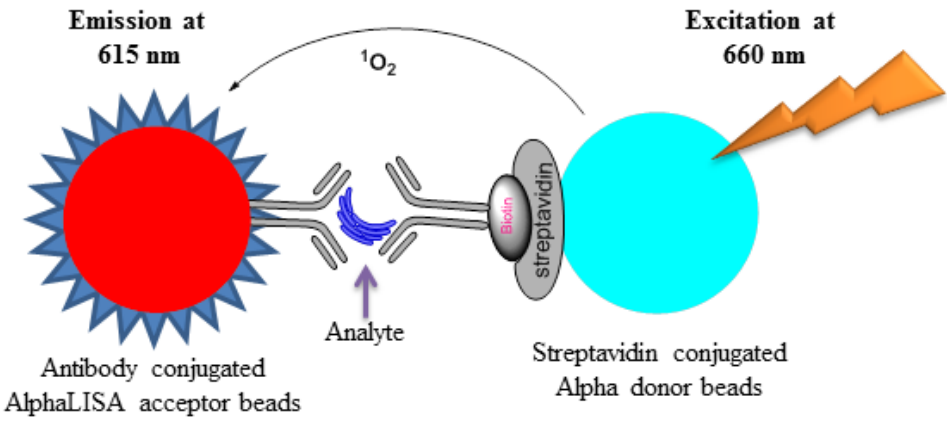

Figure 6.1 Principle of AlphaLISA technology. Antibodies conjugated both AlphaLISA acceptor beads and streptavidin Alpha donor beads bind specifically to the analyte molecule. This binding causes both beads to come in close proximity. Excitation of donor beads at 660 nm triggers generation of AlphaLISA signal in the form of oxygen singlet species resulting in emission of sharp peak at 615 nm (Ullman et al., 1996).

Development of AlphaLISA assay for AftB arabinosyltransferase

AlphaLISA technology is a versatile method and can be easily adapted to study AftB transferase activity based on the resources in hand. A hypothetical model is proposed in employing AlphaLISA technology for AftB specific arabinosyltransferase assay in Figure 6.2. The materials needed to develop this technology are; (i) biotinylated arabinose

disaccharide acceptor, (ii) arabinose donor, (iii) *M. smegmatis* membranes, (iv) acceptor beads conjugated with CS35-mAb, (v) streptavidin donor beads.

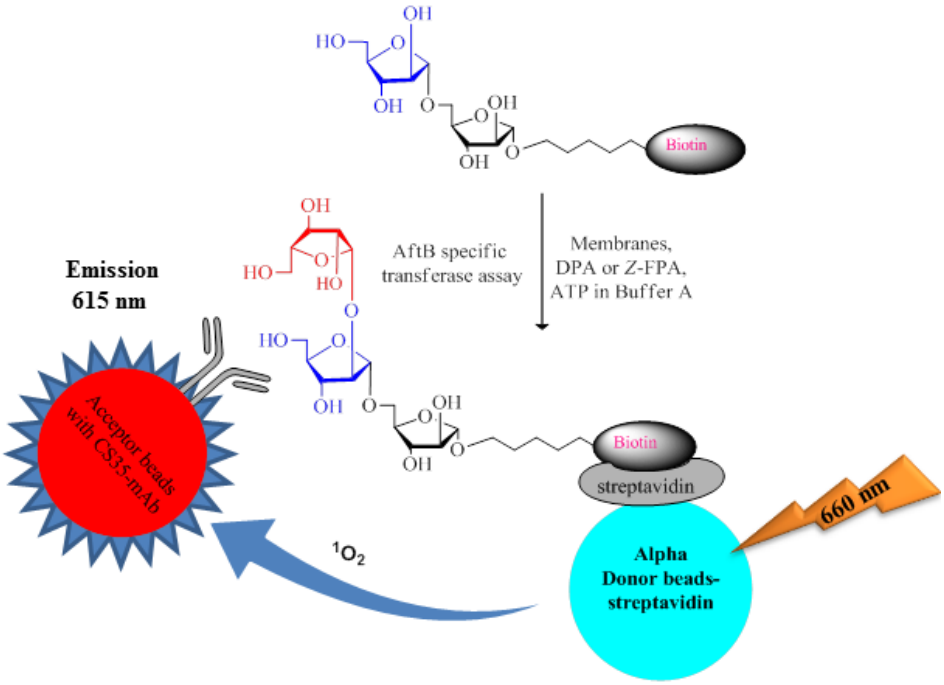

Figure 6.2 Hypothetical model for AftB specific AlphaLISA arabinosyltransferase assay. The CS35-mAb conjugated acceptor bead binds specifically to the AftB catalyzed enzymatic product, while the biotin group bound to it brings the streptavidin donor bead into its close proximity, allowing generation of AlphaLISA signal in the form of oxygen singlet species upon excitation at 660 nm (Ullman et al., 1996).

A typical AftB AlphaLISA assay includes biotinylated arabinose disaccharide acceptor, arabinose donor (DPA/Z-FPA) and crude membranes in BufferA incubated at 37^{o}C for 2 hr. AftB enzyme present in the crude membranes transfers arabinose from donor to the biotinylated acceptor. After 2 hr incubation, acceptor beads conjugated with CS35-mAb

will be added and incubated further for 30 min at 37^{o}C during which CS35-mAb will recognize and bind to the enzymatic product. Addition of streptavidin donor beads will bind to the biotinylated enzymatic product present in the crude reaction mixture. Excitation of donor beads at 660 nm generates flow of singlet oxygen species, activating a cascade of chemical events only in acceptor beads that are present in close proximity resulting in the emission of strong signal at 615 nm. This assay developed based on AlphaLISA technology may help in future for screening small molecule inhibitors for TB drug development.

Summary of AftC arabinosyltransferase

Expression of membrane bound arabinosyltransferases is a challenging task. In my study, we have been able to express, solubilize and purify Mtb AftC. We have developed an *in vitro* transferase assay using purified recombinant AftC and demonstrated that AftC retains transferase activity only when reconstituted into proteoliposomes.

In addition, we were also successful in synthesizing alternate arabinose donors *Z*-nerylphosphoryl-D-arabinose (*Z*-NPA), *Z,Z*-farnesylphosphoryl-D-arabinose (*Z*-FPA), *E,E*-farnesylphosphoryl-D-arabinose (*E*-FPA), and *Z,Z,Z,Z,E,E*-heptaprenylphosphoryl-D-arabinose (*Z*-HPA). Among these lipid donors, Z-FPA has shown better solubility in the assay buffer as compared to the native donor DPA. Reconstitution of AftC proteoliposomes is of particular interest given the fact that, AftC was functionally active only when proteoliposomes were made using mycobacterial total lipids and found inactive with commercial lipids. This led us to further identify the lipid specificity for AftC transferase activity which shows that AftC exhibits specificity for diacylated phosphatidylinositoldimannoside (Ac_2PIM_2).

A vision of AftC future work

In order to further explore the functions of AftC and characterize it a number of areas can be explored. As is evident from our earlier studies described in Chapter 5, acetamide inducible *aftC* overexpression system yields very low amounts of AftC. It is thus imperative to identify alternate *E. coli* expression systems to obtain a high yield of AftC protein. It will be worth trying to express this protein using commercially available *in vitro* coupled transcription and translation membrane protein expression kits. If any success is obtained from the *E. coli* expression, then it will open up new tools for the development of screening inhibitors for AftC.

To gain insight into the molecular mechanisms that govern arabinan biosynthesis, there is a need to explore the molecular and structural studies of AftC that will shed light on catalytic activities of arabinosyltransferases. Therefore, the additional objective will be mass spectrometry identification of AftC catalytic domains through well-established limited proteolysis technique (Gao et al., 2005). This approach reveals the catalytic domains of AftC that are located outside the AftC proteoliposomes. Digestion of AftC while enclosed in a liposome environment with trypsin, Lys-C (Roche), Glu-C (New England Biolabs) or Chymotrypsin (and other proteases if necessary) will allow one to identify the domains outside the lipid layer. Once the catalytic domains are identified, it will be worthwhile to express these domains and assess their catalytic activity in a cell free arabinosyltransferase assay. Crystallization of these catalytic domains with substrates (donor/acceptors) and the structural information obtained from these studies is key to understand their critical role in drug design and discovery.

References

Alderwick, L.J., M. Seidel, H. Sahm, G.S. Besra, and L. Eggeling. 2006. Identification of a novel arabinofuranosyltransferase (AftA) involved in cell wall arabinan biosynthesis in *Mycobacterium tuberculosis*. *J. Biol. Chem.* 281:15653-15661.

Bhamidi, S., M.S. Scherman, and M.R. McNeil. 2009. Mycobacterial Cell Wall Arabinogalactan: a Detailed. *Bacterial Polysaccharides: Curr. Innov. and Fut. Trends*:39.

Birch, H.L., L.J. Alderwick, B.J. Appelmelk, J. Maaskant, A. Bhatt, A. Singh, J. Nigou, L. Eggeling, J. Geurtsen, and G.S. Besra. A truncated lipoglycan from mycobacteria with altered immunological properties. *Proc. Natl. Acad. Sci. U. S. A.* 107:2634-2639.

Birch, H.L., L.J. Alderwick, A. Bhatt, D. Rittmann, K. Krumbach, A. Singh, Y. Bai, T.L. Lowary, L. Eggeling, and G.S. Besra. 2008. Biosynthesis of mycobacterial arabinogalactan: identification of a novel alpha(1-->3) arabinofuranosyltransferase. *Mol. Microbiol.* 69:1191-1206.

Chatterjee, D. 1997. The mycobacterial cell wall: structure, biosynthesis and sites of drug action. *Curr. Opin. Chem. Biol.* 1:579-588.

Escuyer, V.E., M.A. Lety, J.B. Torrelles, K.H. Khoo, J.B. Tang, C.D. Rithner, C. Frehel, M.R. McNeil, P.J. Brennan, and D. Chatterjee. 2001. The role of the *embA* and *embB* gene products in the biosynthesis of the terminal hexaarabinofuranosyl motif of *Mycobacterium smegmatis* arabinogalactan. *J. Biol. Chem*. 276:48854-48862.

Gao, X., K. Bain, J.B. Bonanno, M. Buchanan, D. Henderson, D. Lorimer, C. Marsh, J.A. Reynes, J.M. Sauder, and K. Schwinn. 2005. High-throughput limited proteolysis/mass spectrometry for protein domain elucidation. *J. Struct. Funct. Genomics*. 6:129-134.

Kaur, D., M.E. Guerin, H. Skovierová, P.J. Brennan, and M. Jackson. 2009. Biogenesis of the cell wall and other glycoconjugates of *Mycobacterium tuberculosis*. *Adv. Appl. Microbiol.* 69:23-78.

Kaur, D., T.L. Lowary, V.D. Vissa, D.C. Crick, and P.J. Brennan. 2002. Characterization of the epitope of anti-lipoarabinomannan antibodies as the terminal hexaarabinofuranosyl motif of mycobacterial arabinans. *Microbiology*. 148:3049-3057.

Rademacher, C., G.K. Shoemaker, H.S. Kim, R.B. Zheng, H. Taha, C. Liu, R.C. Nacario, D.C. Schriemer, J.S. Klassen, T. Peters, and T.L. Lowary. 2007. Ligand specificity of CS-35, a monoclonal antibody that recognizes mycobacterial lipoarabinomannan: a model system for oligofuranoside-protein recognition. *J. Am. Chem. Soc*. 129:10489-10502.

Seidel, M., L.J. Alderwick, H.L. Birch, H. Sahm, L. Eggeling, and G.S. Besra. 2007. Identification of a novel arabinofuranosyltransferase AftB involved in a terminal step of cell wall arabinan biosynthesis in Corynebacterianeae, such as *Corynebacterium glutamicum* and *Mycobacterium tuberculosis*. *J. Biol. Chem*. 282:14729-14740.

Shi, L., S. Berg, A. Lee, J.S. Spencer, J. Zhang, V. Vissa, M.R. McNeil, K.H. Khoo, and D. Chatterjee. 2006. The carboxy terminus of EmbC from *Mycobacterium smegmatis* mediates chain length extension of the arabinan in lipoarabinomannan. *J.Biol.Chem*. 281:19512-19526.

Skovierova, H., G. Larrouy-Maumus, J. Zhang, D. Kaur, N. Barilone, J. Kordulakova, M. Gilleron, S. Guadagnini, M. Belanova, M.C. Prevost, B. Gicquel, G. Puzo, D. Chatterjee, P.J. Brennan, J. Nigou, and M. Jackson. 2009. AftD, a novel essential arabinofuranosyltransferase from mycobacteria. *Glycobiology*. 19:1235-1247.

Szekeres, P.G., K. Leong, T.A. Day, A.E. Kingston, and E.H. Karran. 2008. Development of homogeneous 384-well high-throughput screening assays for Abeta1-40 and Abeta1-42 using AlphaScreen technology, *J.Biomol. Screen*. 13:101-111.

Ullman, E.F., H. Kirakossian, A. Switchenko, J. Ishkanian, M. Ericson, C. Wartchow, M. Pirio, J. Pease, B. Irvin, and S. Singh. 1996. Luminescent oxygen channeling assay (LOCI): sensitive, broadly applicable homogeneous immunoassay method. *Clin. Chem.* 42:1518.

Zhang, J., S.K. Angala, P.K. Pramanik, K. Li, D.C. Crick, A. Liav, A. Jozwiak, E. Swiezewska, M. Jackson, and D. Chatterjee. 2011. Reconstitution of Functional Mycobacterial Arabinosyltransferase AftC Proteoliposome and Assessment of Decaprenylphosphorylarabinose Analogues as Arabinofuranosyl Donors. *ACS chem. biol*. 6:819-828.

Zhang, N., J.B. Torrelles, M.R. McNeil, V.E. Escuyer, K.H. Khoo, P.J. Brennan, and D. Chatterjee. 2003. The Emb proteins of mycobacteria direct arabinosylation of lipoarabinomannan and arabinogalactan via an N-terminal recognition region and a C-terminal synthetic region. *Mol. Microbiol.* 50:69-76.